1999

Trace element fluxes from continental margin sediments : a comparison of three techniques for measuring flux

Eric S. Kingsley
San Jose State University

TRACE ELEMENT FLUXES FROM CONTINENTAL MARGIN SEDIMENTS:
A COMPARISON OF THREE TECHNIQUES FOR MEASURING FLUX

A Thesis

Presented to

The Faculty of Moss Landing Marine Laboratories

and San Jose State University

In Partial Fulfillment

Of the Requirements for the Degree

Master of Science

in Marine Sciences

By

Eric S. Kingsley

August 1999

UMI Number: 1396181

UMI
300 North Zeeb Road
Ann Arbor, MI 48103

APPROVED FOR THE DEPARTMENT OF BIOLOGICAL SCIENCES

Kenneth S. Johnson
____
Dr. Kenneth S. Johnson

Kenneth H. Coale
____
Dr. Kenneth H. Coale

William Broenkow
____
Dr. William W. Broenkow

APPROVED FOR THE UNIVERSITY

William Fish
____

Abstract

Trace Element Fluxes From Continental Margin Sediments: A Comparison of Three Techniques for Measuring Flux

by Eric S. Kingsley

Trace metal concentrations are elevated near the continental margins. Dissolved metal fluxes across the sediment-water interface are believed to be a major source that contributes to the elevated concentration in the water column. Deriving an accurate measurement of trace metal flux across the sediment-water interface in these areas is critical if we are to assess the importance of this source. Two cruises to the basins in the Southern California Borderlands in 1994 and 1995 and three cruises in Monterey Bay in 1993, 1994 and 1995 were conducted to compare different methods of estimating metal flux from sediments. The borderland basins provide chemically unique environments in which strong horizontal advection is minimized. This allows metal fluxes to be determined by measuring the vertical gradients of dissolved metal concentrations in the water column of the basins and then applying a vertical eddy diffusivity coefficient to this gradient to calculate diffusive metal transport. The fluxes determined by this method are compared with direct measurements from free vehicle benthic flux chambers and indirect measurements made by modeling the metal gradients in sediment porewaters. The results obtained by all three methods are compared to assess the accuracy of each method. Where methods differ hypotheses are presented to explain these differences.

Good agreement exists between these three methods of estimating flux in both high and low oxygenated basins for the metals studied. In most cases where

discrepancies between methods exist, the processes that create the differences can be explained through biogeochemical reactions.

ACKNOWLEDGMENTS

I would like to thank my advisors Drs. Ken Johnson and Kenneth Coale for helping me with this thesis project and inspiring me with their quest for knowledge in the area of research. Dr. William Berelson is thanked for his constant input and source of jokes during this project. Also special thanks goes to Dr. William Broenkow for challenging me in classes and always being encouraging. To Ginger Elrod, Jocelyn Nowicki Douglas, Debbie Colbert, Heidi Zamzow, Peter Von Langen, Teresa Coley, and members of the USC research group I would like to thank for the laughter and help during many long hours on board ship and in the lab during this project. The captains and crews of the R. V. Point Sur and R. V. New Horizon are thanked for their assistance during sample collection. Sheila Baldridge, Sandi O'Neill, and Joan Parker were of help in finding obscure references. Lynn McMasters is thanked for her amazing graphic skills. Gail Johnston, Sandy Yarborough, and Irene Chung are also thanked for their help in navigating the campus bureaucracy. This work was supported by NSF research grants awarded to Drs. Johnson and Coale at MLML and Dr. William Berelson at USC. Also the David and Lucille Packard Foundation awarded me a grant that allowed me to present this research at the AGU National Meeting in San Francisco, in December 1996. Lastly I want to thank my family for the love and support given to me during my education. This thesis is dedicated to the memory of my father who inspired me to do the best job I can in everything I undertake.

TABLE OF CONTENTS

LIST OF TABLES

LIST OF FIGURES

Introduction

Trace metals are important micronutrients (Brand and others, 1983) that may regulate ocean primary production (Coale and others, 1996). The horizontal distributions of most trace metals are not uniform, with concentrations near the coasts being generally higher than the open ocean (Chester, 1990). This is true for Cd, Cu, Ni, Zn (Bruland, 1980), Mn (Landing and Bruland, 1980; Landing and Bruland, 1987), and Fe (Martin and Gordon, 1988). Some exceptions to this trend include Al (Orians and Bruland, 1986), Ga (Orians and Bruland, 1988), and Pb (Flegal and Patterson, 1983). Concentrations of these metals are highest in the central gyres due to atmospheric deposition and decrease near the margins due to intense particle scavenging. One consequence of the generally higher metal concentrations in coastal waters is that oceanic and coastal species of phytoplankton have different trace metal requirements (Brand and others, 1983; Sunda and Huntsman, 1983; Sunda and others, 1991). As an example, many species of coastal phytoplankton require much larger amounts of Zn and Fe (Brand and others, 1983) than do oceanic species. Therefore, horizontal variations in metal concentration can have a strong impact on phytoplankton community structure.

Three significant sources for dissolved metals in the coastal zone are: 1) atmospheric deposition, 2) river input, and 3) flux from continental margin sediments. Chester (1990) summarizes various estimates of the global significance of diffusive sedimentary fluxes of Mn and Cu from the central Pacific and the fluvial and atmospheric fluxes of Mn, Fe, and Cu from the North Pacific. An estimate of the diffusive sedimentary flux of Fe in the central Pacific can be found in Sawlan and Murray (1983). The diffusive flux of Mn, Fe, and Cu from the sediments is between ~3-220 times greater than the fluvial flux and between ~45-270 times greater then the atmospheric flux for these metals. Fluxes of dissolved metal from margin sediments are a potentially important source that may regulate their horizontal distribution in the oceans (Martin and others 1985).

Many studies of inorganic carbon, radon, and nutrient flux across the sediment-water interface have been conducted in the nearshore environment (Archer and Devol, 1992; Bender and others, 1989; Berelson and Hammond, 1986; Berelson and others, 1987a; Berelson and others, 1987b; Berelson and others, 1989; Christensen and others, 1987; Devol, 1991; Devol and Christensen, 1993; Emerson and others, 1984; Hales and others, 1994; Ingall and Jahnke, 1994; Jahnke and others, 1990; McManus and others, 1994; Reimers and others, 1992; Rutgers van der Loeff, and others 1984; Smith and others, 1987; Sundby and others, 1986; Thamdrup and Canfield, 1996). Numerous studies of metal flux from coastal sediments have also been conducted (Alongi and others, 1996; Elderfiled and others, 1981; Emerson and others, 1984; Heggie and others, 1987; Hunt, 1983; Johnson and others, 1992; Lapp and Balzer, 1993; Sundby and others, 1986; Sawlan and Murray, 1983; Thamdrup and Canfield, 1996; Thamdrup and others, 1994; Westerlund and others, 1986; Widerlund, 1996; Uematsu and Tsunogai, 1983). Intercomparison of various methods used to generate estimates of dissolved metal flux are however very rare (Johnson and others, 1992; Murray, 1987; Thamdrup and others, 1994; Westerlund and others, 1986). Most estimates of metal flux have been derived from the gradient of dissolved metal concentrations in pore waters (Alongi and others, 1996; Elderfiled and others, 1981; Emerson and others, 1984; Heggie and others, 1987; Johnson and others, 1992; Lapp and Balzer, 1993; Sawlan and Murray, 1983; Thamdrup and Canfield, 1996; Widerlund, 1996). Metal concentrations may however, undergo large changes in the pore waters over small depth intervals, which make the gradients difficult to measure. These changes are particularly true for metals that undergo redox transformations such as Mn and Fe (Froehlich and others, 1979). To date there have been no systematic comparisons of various methods for estimating metal flux.

This thesis attempts to address this issue by examining metal fluxes derived from free vehicle benthic flux chambers, dissolved metal gradients in pore waters, and flux estimates derived from the accumulation of metals in the water column overlying submarine basins. This work focuses on the flux of Mn, Fe, Co. and Cu from the continental margin. A brief summary of the flux estimates that exist in the literature and how sediment geochemical processes effect metal flux estimates is given below. The next section summarizes the trace metal sampling including study area, collection and analysis methods, and discussion. Finally the last section describes how the fluxes were calculated, the results obtained, and gives recommendations for the best method of estimating the trace metal flux on continental margins.

Methods of Estimating Dissolved Metal Flux

Dissolved metal fluxes across the sediment-water interface can be estimated in three ways. First, direct measurements of the flux can be made with benthic flux chambers. These devices isolate water over the sediments and then collect samples of the overlying waters contained in the chambers. The rate of change in dissolved metal concentration per unit area of sediment gives a direct measurement of flux. Chambers may bias flux measurements if they alter the hydrodynamic characteristics of the benthic boundary layer (Santschi and others, 1991), alter the redox conditions of the overlying water (Sundby and others1986), or disturb the sediment during deployment (Berelson and others, 1989). Second metal gradients measured in sediment pore waters can be used to estimate metal flux. However, large changes in concentration due to variable redox conditions may make gradients difficult to measure near the interface. Bioirrigation of sediments may also add a component to the flux that cannot be measured by this method. Finally, in areas where horizontal advection is restricted, such as a submarine basin, the metal flux can be estimated from the accumulation of dissolved metal in the near-bottom portion of the water column.

Flux Comparison Studies

Methods of determining the benthic fluxes of oxygen, inorganic carbon, alkalinity, or nutrients have often been compared in several studies (Archer and Devol, 1992;

Berelson and Hammond, 1986; Berelson and others, 1987a; Berelson and others, 1987b; Berelson and others, 1989; Berelson and others, 1990; Devol and Christensen, 1993; Reimers and others, 1996; Sundby and others, 1986). In the Southern California Borderlands nutrient fluxes were estimated using a free vehicle benthic flux chamber or lander, gradients in the water column, and gradients in the sediment pore waters (Berelson and others, 1987b). It was found that in San Pedro Basin, a low bottom water oxygen; high sedimentation rate environment, flux estimates agreed for all three procedures (Berelson and others, 1987b). However in San Nicholas Basin, which has a higher bottom water oxygen and a lower sedimentation rate than San Pedro Basin, the TCO_2 and radon estimates from the pore water gradients did not match those obtained from the lander. This difference was attributed to the bioirrigation of the sediments (Berelson and others, 1987b). Also, to address concerns about sediment disturbance during lander deployment Berelson and others (1989) deployed both free vehicle benthic flux chambers and flux chambers placed using the submersible ALVIN. In this study no difference in flux estimate from either type of chamber was observed. Lastly if oxygen content in the chambers is maintained at ambient bottom water values the redox conditions of the overlying water will not effect the flux measured (Sundby and others 1986).

Very few comparisons of flux estimation methods for trace metals exist in the literature (Johnson and others, 1992; Murray, 1987; Thamdrup and others, 1994; and Westerlund and others, 1986). Manganese fluxes have been determined from flux chambers and pore water gradients on the continental margin (Johnson and others, 1992; Thamdrup and others, 1994) and in lakes (Murray, 1987). In a shallow 6 m station in a coastal bay Cd, Cu, Ni, and Zn fluxes were also determined using both flux chambers and pore water gradients (Westerlund and others, 1986). On the continental margin Johnson and others (1992) found that the Mn flux derived from gradients in pore waters underestimated lander derived fluxes by factors of 5 to 25 on the shelf but were comparable in deeper water. This suggests irrigation of the sediments by benthic macro fauna was the cause of the bias (Johnson and others, 1992). In the coastal bay no correlation between pore water and chamber measured fluxes was observed, but the chambers did show significant seasonal differences (Westerlund and others, 1986).

Although no synthesis of the three methods of estimating flux has been attempted for metals, general reviews of pore water sampling techniques can be found in Hong and others (1995), Krivkov and Manheim (1982), and Murdroch and Azcue (1995), but trace metal studies of the extraction techniques for pore water do exist (Carignan and others, 1985; Jahnke, 1988; Schults and others, 1992; Teasdale and others, 1995). Porewater sampling using centrifugation has been compared with dialysis or sediment peepers (Carignan and others, 1985; Schults and others, 1992; Teasdale and others, 1995). Centrifuging at 11,000 rpm gave trace metal concentrations equivalent to dialysis (Carignan and others, 1985) but concentrations were variable at lower centrifuge speeds (Carignan and others, 1985; Schults and others, 1992). Whole core pressurization gave results similar to centrifuged core pore water for both nutrients and metals (Jahnke, 1988). In this thesis the advantages and limitations of each method are examined for trace metal fluxes from continental margin sediments.

Sediment Geochemistry

Manganese and iron are both redox sensitive elements. As electron acceptors in respiration, they are important in the breakdown of organic carbon (Froelich and others, 1979). Manganese is present as oxides of Mn^{4+} in oxic seawater (Bruland, 1983) and in oxygenated porewater (Sawlan and Murray, 1983). It can also be found as Mn^{2+} in oxic water due to its slow oxidation kinetics (Johnson and others 1996). Iron exists as Fe(III) oxy-hydroxides in oxic environments (Balzer, 1982 and Millero and others, 1987). In anoxic pore waters Mn(IV) and Fe(III) hydroxides can be reduced during the oxidation of organic carbon to Mn^{2+} and Fe^{2+}. The depth at which they are first used to breakdown organic carbon and are hence reduced, has a large influence on the Mn or Fe flux from the sediments. The oxidation of organic carbon and the release of the more soluble Mn^{2+} and Fe^{2+} to the pore waters occurs in distinct regions of the sediment (Froelich and others, 1979). The distinct zones of the Froelich and others (1979) model have been found to be compressed or even overlapped due to differing bottom water O_2 concentrations and organic carbon flux (Shaw and others, 1990). If reduction of the Mn(IV) and Fe(III) occurs near the sediment-water interface, then fluxes may be large. If reduction occurs deep in the sediments, then fluxes are typically small.

In oxygenated seawater and pore water, cobalt is present in the Co^{2+} oxygenation state (Bruland, 1983). In sediments, Co^{2+} has a strong affinity for MnO_2 particles (Heggie and Lewis, 1984; Shaw and others, 1990; Sundby and others, 1986). Upon absorption onto the MnO_2 particles Co^{2+} is oxidized to Co^{3+}, which is insoluble (Heggie and Lewis, 1984; Murray and Dillard, 1979). Shaw and others (1990) found that the retention of Co in sediments by Mn oxides decreased in the low bottom water oxygen environments of the nearshore Borderland basins. This was attributed to a compression of the redox boundaries allowing Co to be released to bottom waters (Shaw and others, 1990).

Copper is present as Cu^{2+} in oxygenated seawater and porewater (Bruland, 1983). Copper is often associated with organic carbon (Johnson and others, 1988; Klinkhammer, 1980; Klinkhammer and others, 1982; Coale and Bruland, 1990; Shaw and others, 1990; Zamzow, 1997). Organically bound Cu accounts for up to 99.88% of surface seawater Cu and for up to 91.50% of mid-depth seawater Cu present (Coale and Bruland, 1990; Zamzow, 1997). This large fraction of organically bound Cu should be released during sediment diagensis. The calculated ratios of Cu/C flux measured in the Guatemala Basin and Baja California (Hong and others, 1995; Sawlan and Murray, 1983) support this trend. In the California Borderlands, Shaw and others (1990) found that the release of copper to the bottom water was lower in the shallower basins possibly due to a greater preservation of biogenic material (Johnson and others, 1988) and organically bound copper associated with this material.

Trace Metal Sampling

Study Area

Samples were collected from the basins in the Southern California Borderland (Figure 1) and in Monterey Bay (Figure 2) as part of our trace element flux on continental margins (Teflon) study. The Southern California Borderlands consist of a series of basins. The environment of the basins ranges from low bottom water O_2 in San Pedro and Santa Monica (Berelson, 1985) to deep, oxygenated basins such as Tanner Basin and the open ocean site, Patton Escarpment. Besides being unique redox environments (Berelson, 1985) the restricted horizontal flow in the basins allows chemical flux to be estimated from the change in water column concentration. The Borderland basins have been used for studies of nutrient, inorganic carbon, and radon fluxes from sediments (Bender and others, 1989; Berelson and Hammond, 1986; Berelson and others, 1987b; Berelson and others, 1989; Berelson and others, 1996; Hammond and others, 1990; Ingall and Jahnke, 1994; Jahnke, 1988; Jahnke, 1990; and Smith and others, 1987). Trace metal flux studies are less extensive in the Borderlands with flux estimates from the water column data for Co (Johnson and others, 1988) being the only one conducted in this environment. Although metal flux studies are lacking, the pore waters in several basins have been examined for Mn (Shaw and others, 1990), Co (Heggie and Lewis, 1984), and Fe (Jahnke, 1988; Leslie and others, 1990; Reimers and others, 1996; and Shaw and others, 1990).

Monterey Bay (Figure 2) is an area known to have high bio-irrigation (Berelson, 1996 personal communication). Due to insufficient oxygen to support macro faunal communities, bioirrigation does not occur in all of the basins. However, rapid exchange of water in the Monterey Bay precludes estimates of flux from vertical water column gradients. Monterey Bay has been studied for fluxes of both nutrients (Berelson and others, 1996) and Mn (Johnson and others, 1992) as derived from benthic flux chamber and pore water measurements. Monterey Bay was sampled in 1993, 1994, and 1995, whereas the Southern California Borderland was sampled only in 1994 and 1995 (Table 1).

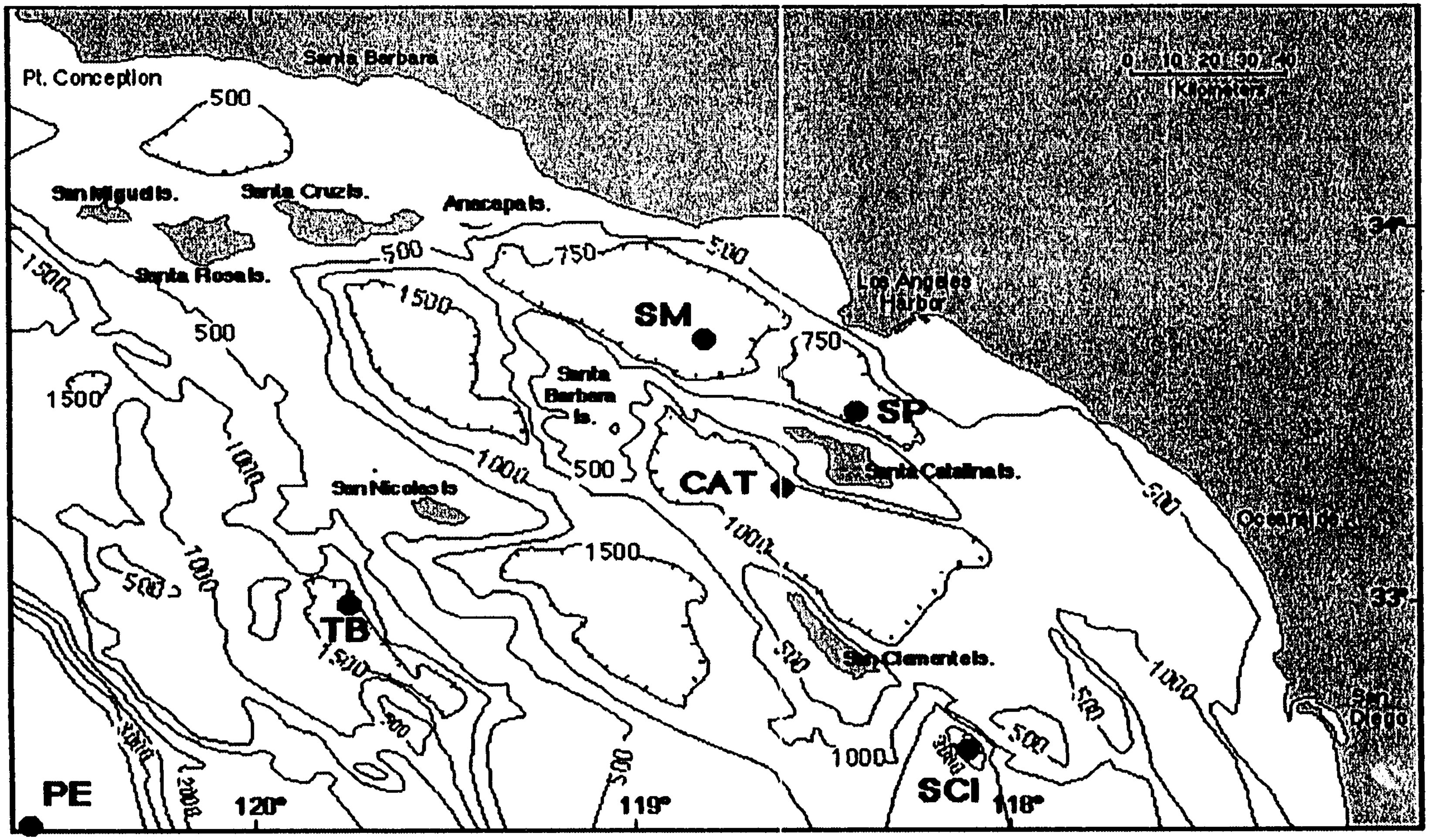

Figure 1. Map of the Southern California Borderlands showing station locations.

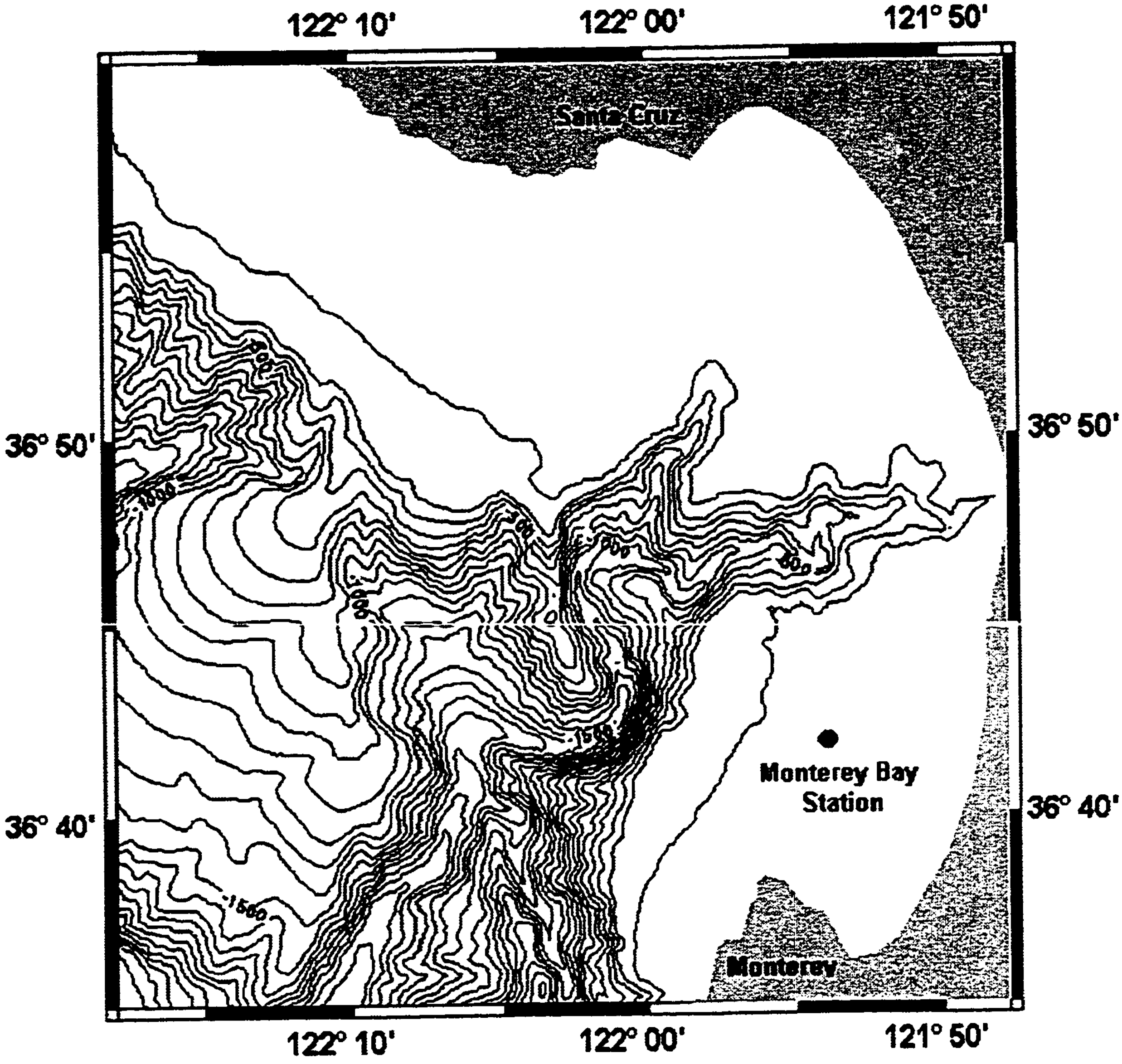

Figure 2. A standard bathymetry map of the Monterey Bay showing station location. The contour interval is 100 meters. Modified from a map on the Monterey Bay Aquarium Research Institute's world wide web page (MBARI, 1997) which was created using SeaBeam data from the USGS.

Table 1. Sample collection by date, station depth, and sill depth. Sill depths for Borderland stations are from Emery (1960). Also included are station locations from an earlier study in Monterey Bay in 1991 and 1992, station T1-11 and T2-7 respectively (Johnson and others 1992).

Cruise	Station Name or Date	Station ID	Latitude (°N)	Longitude (°W)	Station depth, z (m)	Sill Depth, (m)
Teflon '94	San Pedro Basin	SP	33.5	118.4	896	737
	Santa Monica Basin	SM	33.7	118.8	905	737
	Santa Catalina Basin	CAT	33.3	118.6	1300	982
	Tanner Basin	TB	33.0	119.7	1514	1165
	San Clemente Basin	SCl	32.6	118.1	2062	1816
	Patton Escarpment	PE	32.4	120.6	3709	–
Teflon '95	Santa Monica Basin	SM	33.7	118.8	905	737
	Tanner Basin	TB	33.0	119.7	1514	1165
	San Clemente Basin	SCl	32.6	118.1	2062	1816
	Patton Escarpment	PE	32.4	120.6	3709	–
Monterey Bay	6/13/91	T1-11	36.7	121.9	99	–
	5/19/92	T2-7	36.7	121.9	99	–
	6/15/93	TS1	36.7	121.9	99	–
	9/8/93	TS2	36.7	121.9	99	–
	12/14/93	TS3	36.7	121.9	99	–
	3/4/94	TS4	36.7	121.9	99	–
	11/1/95	TS5	36.7	121.9	99	–

Sample Collection

Water samples were collected at each basin station (Table 1) from the water column, the water overlying the sediment, and the pore water. The Monterey Bay station (Table 1) was sampled only for the water overlying the sediment in the chambers and the pore water. The water column was sampled with a 12-bottle CTD rosette. The CTD rosette was equipped with 10 L Niskin sampling bottles triggered remotely from onboard the ship. At each station either 12 or 24 bottles were collected, from depths chosen to cover the entire water column.

The water overlying the sediment, within the first few centimeters of the sediment-water interface, was sampled by deploying benthic flux chambers (Berelson and Hammond, 1986) at each site. Each benthic chamber was deployed with three separate chambers to isolate sediment and overlying water. Each chamber had a stir bar attached to the lid to provide mixing at a rate near ambient conditions. The lander was programmed to draw water samples from the chambers at predetermined intervals through a series of sampling tubes. At the end of each deployment weights were released and the lander returned to the surface. To determine the flux, the volume of water isolated by the chambers was determined from the dilution of a CsCl spike injected into the chambers (Berelson, 1985; Berelson and others, 1987b).

A multi-corer (Barnet and others, 1984) was deployed at each station to collect sediment. Immediately upon recovery the cores were placed in a cold van to minimize temperature effects (Fanning and Pilson, 1971) with the lids of the core tubes still attached to reduce the exchange of oxygen with the water overlying the sediments. Once recovered, the cores were sectioned into known depth intervals (0.5 - 2.5 cm) under a N_2 atmosphere to eliminate any oxidation artifacts (Lyons and others, 1979). Sediment from the center of each section was transferred under the N_2 atmosphere into centrifuge tubes, capped, and centrifuged at 6,000 rpm for 15 min in the cold room to separate sediments from the pore water. The pore water was then filtered under a N_2 atmosphere prior to analysis.

Sample Analysis

Before trace metal analysis, all water from landers and cores was filtered through acid washed 0.5 μm Millex-LCR filters (Millipore Corporation). Water from hydrocasts was filtered for the 1995 cruise only. Samples were analyzed for the trace metals Mn, Co, Cu, and Fe using flow injection analysis with chemiluminescence detection. The Mn analysis is based on the oxidation of 7,7,8,8-tetracyanoquinodimethane in an alkaline solution (Chapin and others, 1991). Cobalt analysis was based on the Co-enhanced chemiluminescent oxidation of gallic acid in alkaline hydrogen peroxide (Sakamoto-Arnold and Johnson, 1987). The Cu analysis is based on the oxidation by hydrogen peroxide of a complex formed between Cu and 1,10-phenanthroline (Coale and others, 1992). Iron analysis is based on the reaction of luminol with hydrogen peroxide and Fe(III) in a basic environment (Obata and others, 1993; Obata and others, 1997) as adapted for flow injection analysis. A cation exchange column of immobilized 8-hydroxyquinoline was used to help separate interferences and to preconcentrate the samples for all trace metal analysis (Sakamoto-Arnold and Johnson, 1987). Lander and pore water samples typically required dilutions of ~1:20 to ~1:3400 to bring the concentrations into the working range of the methods. Water column samples were also analyzed for dissolved oxygen using the Winkler method with an automated oxygen titrator (Friederich and others, 1991).

Results

Bottom water dissolved oxygen has been shown to affect many trace metals during early diagenesis (Shaw and others, 1990). In the Southern California Borderlands bottom water oxygen (Table 2) was low (~<10 μM) in San Pedro and Santa Monica Basins and increases with depth reaching a maximum at the offshore station, Patton Escarpment (~135 μM). This data is similar to that found by others (Berelson, 1991; Johnson and others, 1988; Shaw and others, 1990) for these same stations. The bottom water oxygen in Monterey Bay shows some variation over the years (~101-185 μM) but its range brackets the 126 μM bottom water oxygen reported by Chapin (1990) at a nearby location in Monterey Bay.

The metal concentrations and supplementary data from hydrocasts, centrifuged core pore waters, and dilution corrected landers are presented in Appendix 1. Vertical profiles of the water column for the Teflon '94 and Teflon '95 cruises are reported. In addition, a Mn hydrocast from a 1990 cruise to Santa Monica Basin (Coale and others, 1990) is included. Pore water metal data are reported for the Teflon '94, Teflon '95, and Monterey Bay cruises. The lander metal data for the Teflon '94, Teflon '95, and the Monterey Bay cruises are also shown. Lander data from cruises in the Monterey Bay in 1991 and 1992 (Johnson and others, 1992) are also included.

Table 2. Bottom water dissolved oxygen values from this study. Also included are bottom water oxygen values taken in earlier studies in Monterey Bay in 1991 and 1992, stations T1-11 and T2-7 respectively (Johnson and others, 1992).

Cruise	Station Name or Date	Bottom Water O_2 (μM)
Teflon '94	San Pedro Basin	8.5
	Santa Monica Basin	10.4
	Santa Catalina Basin	19.2
	Tanner Basin	26.6
	San Clemente Basin	58.6
	Patton Escarpment	131.3
Teflon '95	Santa Monica Basin	8.9
	Tanner Basin	26.3
	San Clemente Basin	65.3
	Patton Escarpment	137.2
Monterey Bay	T1-11	132.0
	T2-7	142.0
	TS1	101.2
	TS2	136.1
	TS3	184.9
	TS4	132.8
	TS5	152.6

Trace Metal Hydrocast Data

The hydrocast profiles for Mn in the borderland basins (Figure 3) are between 1 - 8 nM in the surface waters and decrease with depth. They generally follow the offshore station (Patton Escarpment) profile with the exception of the shallow, low oxygenated basins of San Pedro and Santa Monica. In both of these basins Mn concentrations increase near the sediment interface, with Santa Monica exhibiting some temporal variability. Manganese concentrations near the bottom reached ~8 nM in 1990, ~15 nM in 1994, and ~12 nM in 1995 (Figure 3). This variation in bottom water may be due to flushing of sub-sill waters in the basin with water from outside the basin (Berelson, 1991), resuspension of sediments during hydrocast sampling, or analytical methodology (unfiltered hydrocast samples in 1994).

The hydrocast profiles of Fe show much variability between stations and years (Figure 4). Surface concentrations range between 1 - 10 nM and generally increase with depth for the basin stations. The offshore station (Patton Escarpment, Figure 4) is fairly uniform with depth with a slight increase in the surface waters. The sediment-water interface values increase to between ~26 - 30 nM in the nearshore basins of San Pedro and Santa Monica (Figure 4). These elevated deep concentrations are most likely resulting from resuspension of sediments at the sill depth and greater dust input in the nearshore stations. Variability between years is apparent in the Patton Escarpment station with the profiles centering around 4 nM in 1994 (Figure 4) and 1.8 nM in 1995 (Figure 4). Using a similar analytical method, Obata and others (1997) found that unfiltered samples gave elevated iron concentrations. The difference in concentrations can be explained since the 1994 profiles were unfiltered and the 1995 profiles were filtered.

Dissolved cobalt concentrations in the borderland basins hydrocasts (Figure 5) range between 100 - 250 pM in the surface waters and generally decrease with depth. An exception to this decrease in Co concentration with depth, again is found in San Pedro and Santa Monica basins where dissolved Co increases near the sediment interface to ~250 pM. In a previous study of Santa Monica Basin, Johnson and others (1988) reported surface concentrations of Co to be between ~40 - 100 pM near the surface and reached ~120 pM near the sediment interface. While the absolute concentrations are different, the overall trends in the data are similar indicating strong temporal variability can occur in Santa Monica Basin.

Copper was only measured for hydrocasts in 1994 and ranges between 1 - 4 nM in surface waters (Figure 6). Copper profiles are fairly uniform or slightly increasing with depth, with the exception again being Santa Monica Basin (Figure 6) which reaches ~5 nM near the sediment-water interface. Although the elevated deep water Cu concentration is different, the surface value of ~3 nM (Figure 6) agrees with what has been reported previously (Johnson and others, 1988) lending credence to this data.

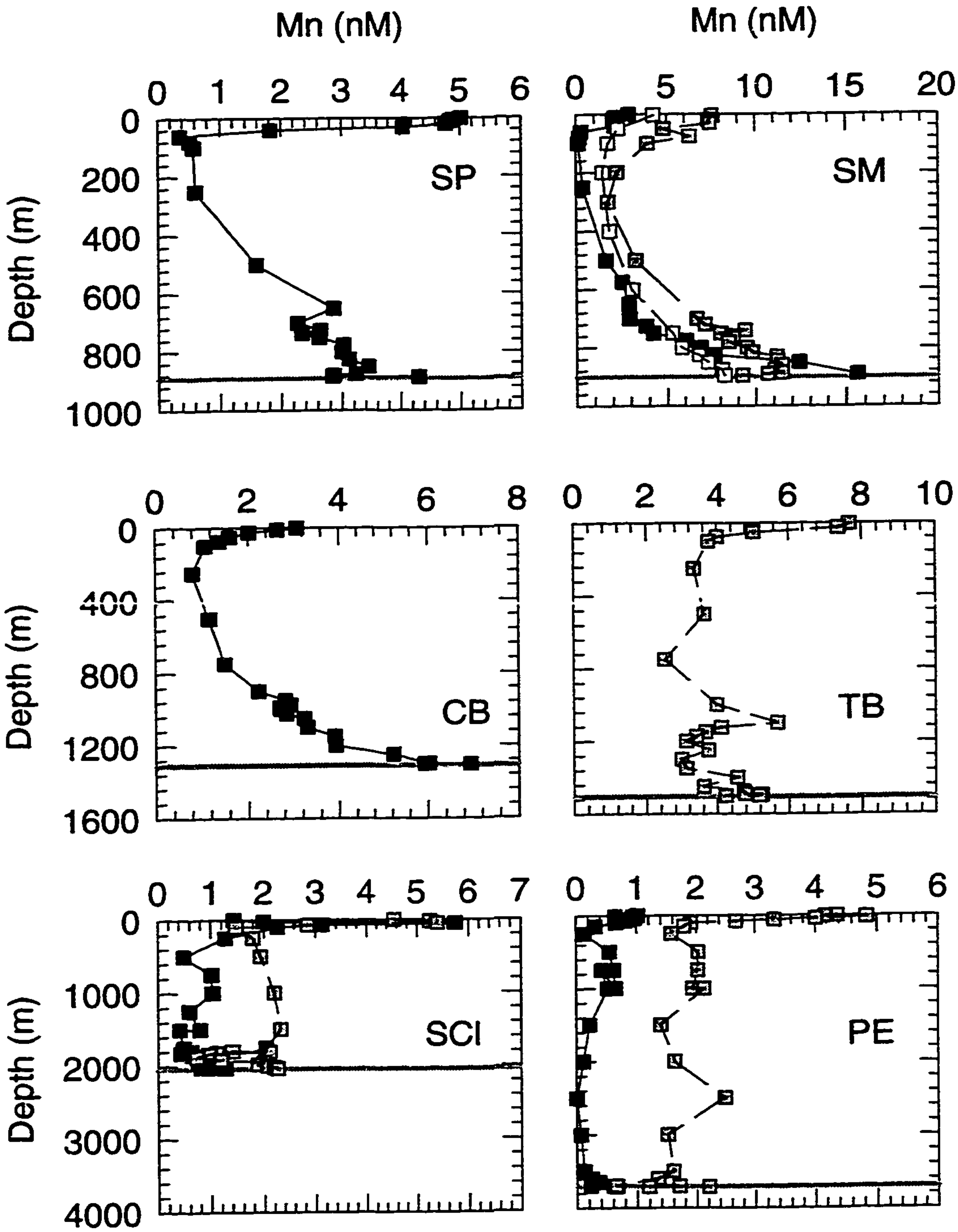

Figure 3. Pt Sur '90 (Coale and others, 1990) and Teflon '94 and '95 trace metal hydrocast Mn data. The horizontal line represents the bottom depth at each station (Table 1). Station abbreviations are as in Table 1. White symbols are Pt Sur '90, black symbols are Teflon '94, and grey symbols are Teflon '95 data.

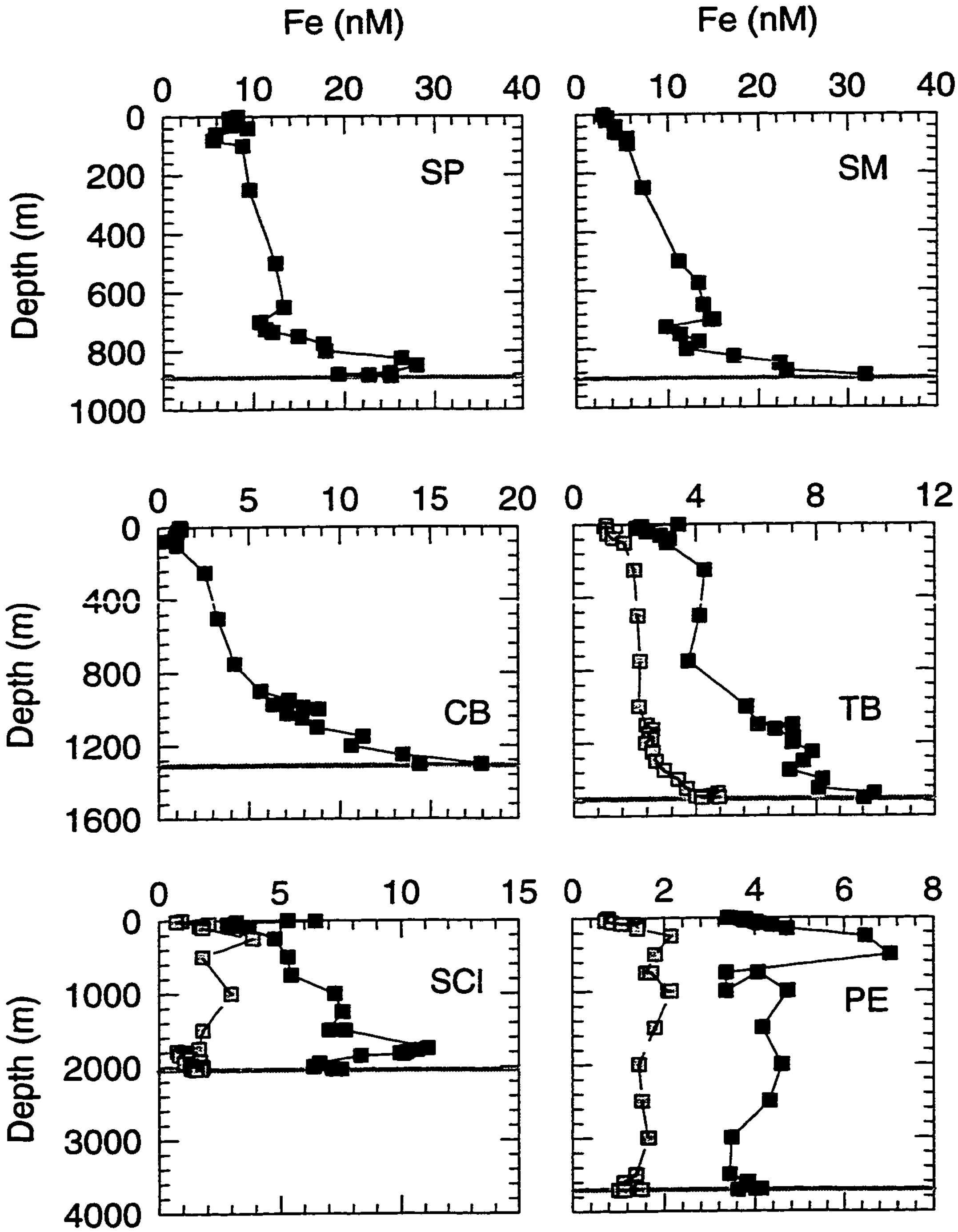

Figure 4. Teflon '94 and '95 trace metal hydrocast Fe data. The horizontal line represents the bottom depth at each station (Table 1). Station abbreviations are as in Table 1. Black symbols are Teflon '94 and grey symbols are Teflon '95 data. Hydrocast samples were filtered as described in the text for Teflon '95 samples only.

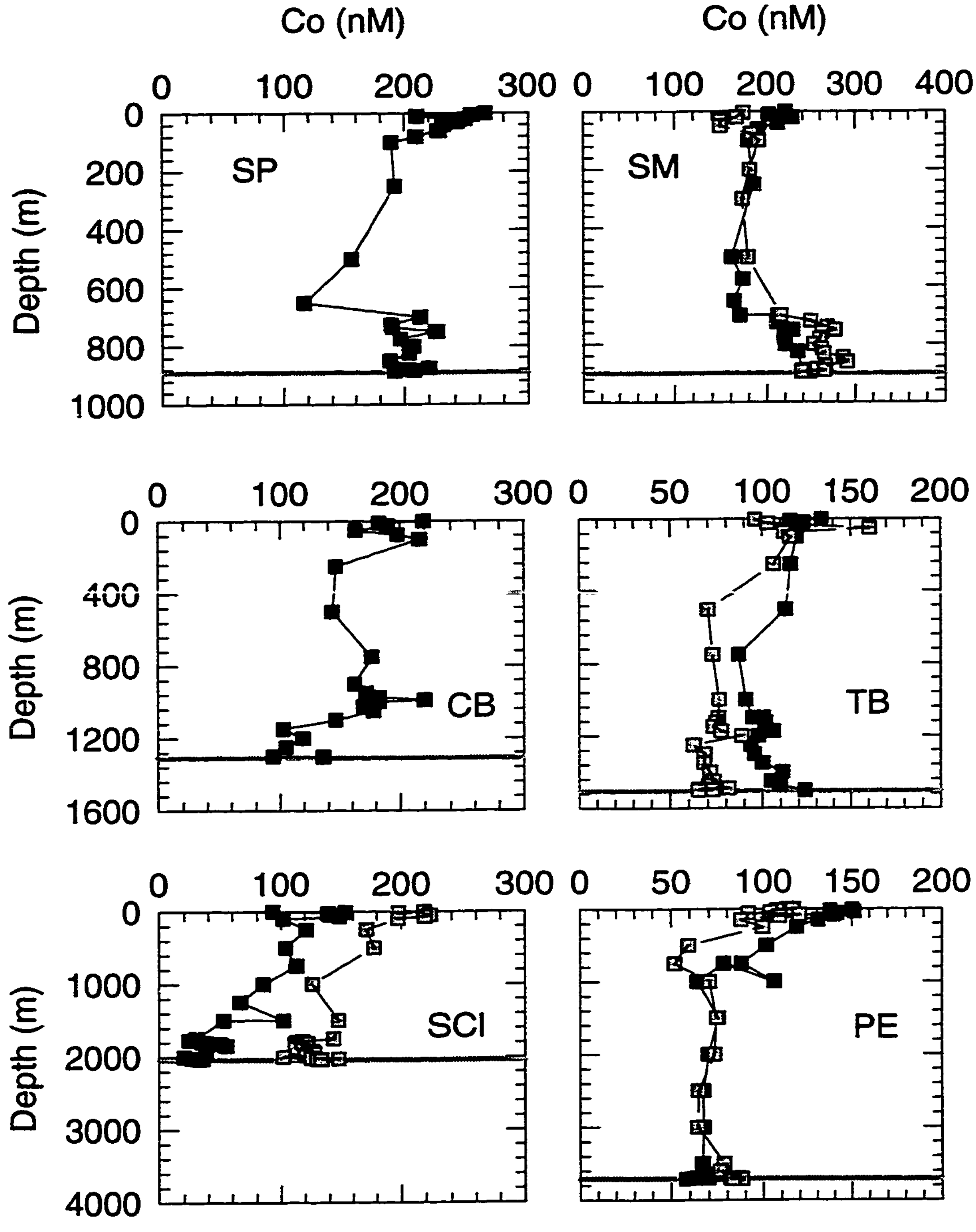

Figure 5. Teflon '94 and '95 trace metal hydrocast Co data. The horizontal line represents the bottom depth at each station (Table 1). Station abbreviations are as in Table 1. Black symbols are Teflon '94 and grey symbols are Teflon '95 data.

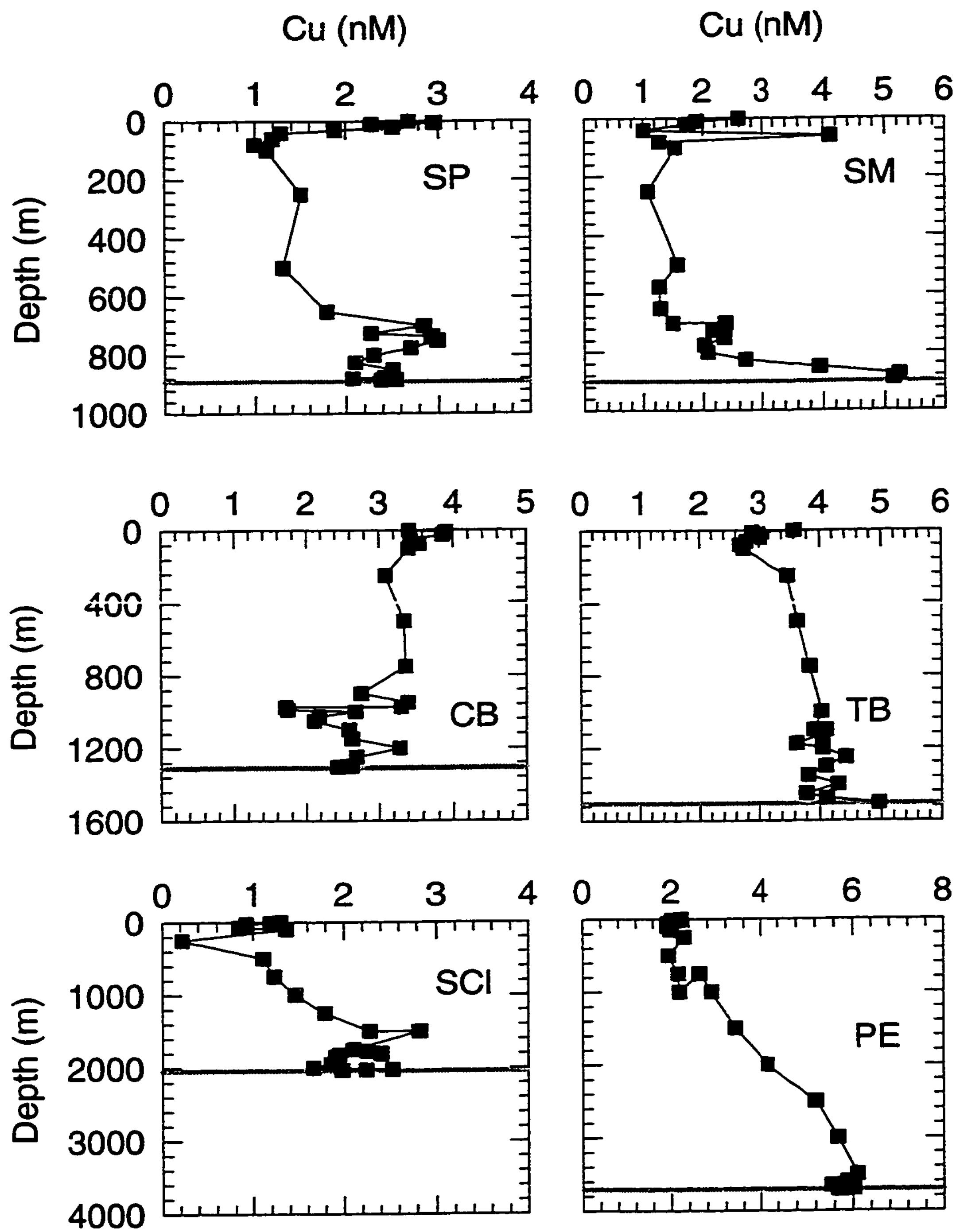

Figure 6. Teflon '94 hydrocast Cu data. The horizontal line represents the bottom depth at each station (Table 1). Station abbreviations are as in Table 1.

<u>Trace Metal Pore Water Data</u>

The Mn pore water profiles in the basins are similar for both years studied (Figure 7) except for elevated levels near the surface of the Santa Monica Basin core in 1994 (Figure 7). Examination of the Santa Monica Basin 1994 and 1995 data, along with literature values (Shaw and others, 1990) suggest that the surface values > ~25 μM that were measured are in error. These values are not used in the analysis of the profile for Santa Monica Basin (Figure 7). Most stations' profiles are relatively smooth, increase with depth, and show a maximum value near 10 cm depth in the core. This is similar to profiles reported in the literature for this area (Shaw and others, 1990). The Mn concentration in pore waters of sediments in the basins with low bottom water O_2, Santa Monica and San Pedro Basins (Table 2), are relatively low. This may indicate that Mn oxides are reduced before they are buried in the sediment. The Mn profiles in Monterey Bay (Figure 11) exhibit uniform surface concentrations of ~0 - 1 μM similar to that found by Fairey (1992) at a nearby location.

Iron pore water profiles exhibit elevated concentrations in the low oxygenated basins of San Pedro and Santa Monica (Figure 8) in contrast to Mn (Figure 7). The high Fe concentrations must reflect its tendency to be reduced at a higher redox potential than Mn (Froelich and others, 1979). San Pedro surface pore water iron concentrations reach ~150 μM similar to that reported elsewhere for San Pedro Basin (Leslie and others, 1990). In San Pedro Basin Fe reaches ~200 μM by 2 cm down into the sediments as was found by Shaw and others (1990). Iron concentrations reach smaller maximum values (Figure 8) at greater depths in the sediments in the other basins, reflecting their more oxic conditions. In Monterey Bay surface pore water concentrations of Fe are ≤ 1 μM (Figure 11) and of similar magnitude as reported for nearby stations (Fairey, 1992).

Cobalt pore water profiles generally show a maximum value in the upper 10 cm (Figure 9). Similar Co pore water profiles have been reported in San Clemente Basin (Johnson and others, 1988) and at Patton Escarpment (Shaw and others, 1990). Monterey Bay, Co surface pore water concentrations are uniform (Figure 11) ranging up to ~10 nM as also reported by Fairey (1992) for nearby stations.

Copper pore water values in the borderland basins are only reported for Patton Escarpment (Figure 10) because the high Fe values (Figure 8) in the other basins appear to interfere with the chemiluminescent Cu measurements. The Patton Escarpment profile shows similar trends to that found in the literature (Shaw and others, 1990). In Monterey Bay only two years of pore water data are available (Figure 11). The surface pore water concentrations of Cu are uniform (Figure 11) and similar to those reported for nearby stations (Fairey, 1992).

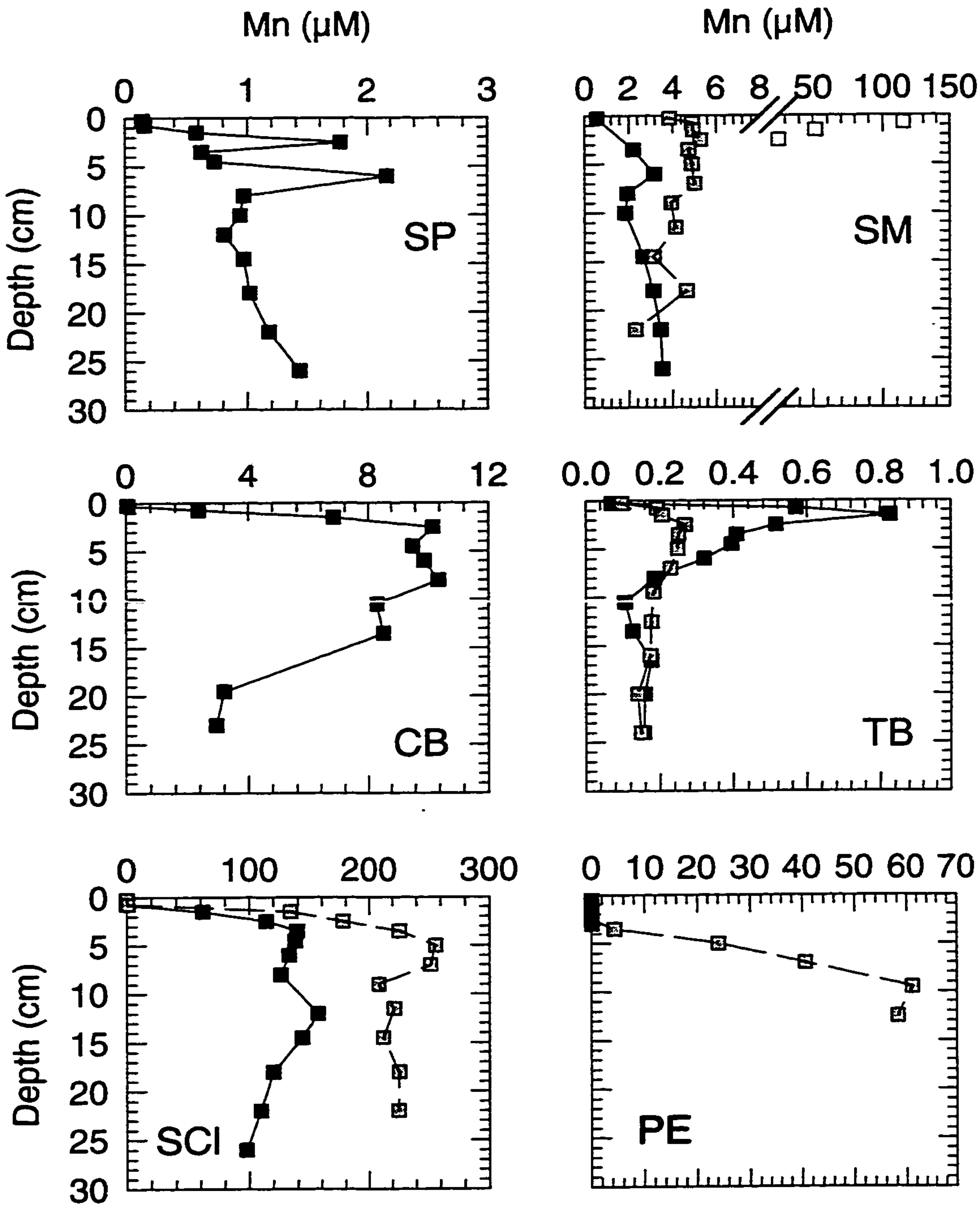

Figure 7. Teflon '94 and '95 pore water Mn data. Black symbols are Teflon '94 data and grey symbols are Teflon '95 data. White symbols are three points believed to be in error. Station abbreviations in the legend are as in Table 1.

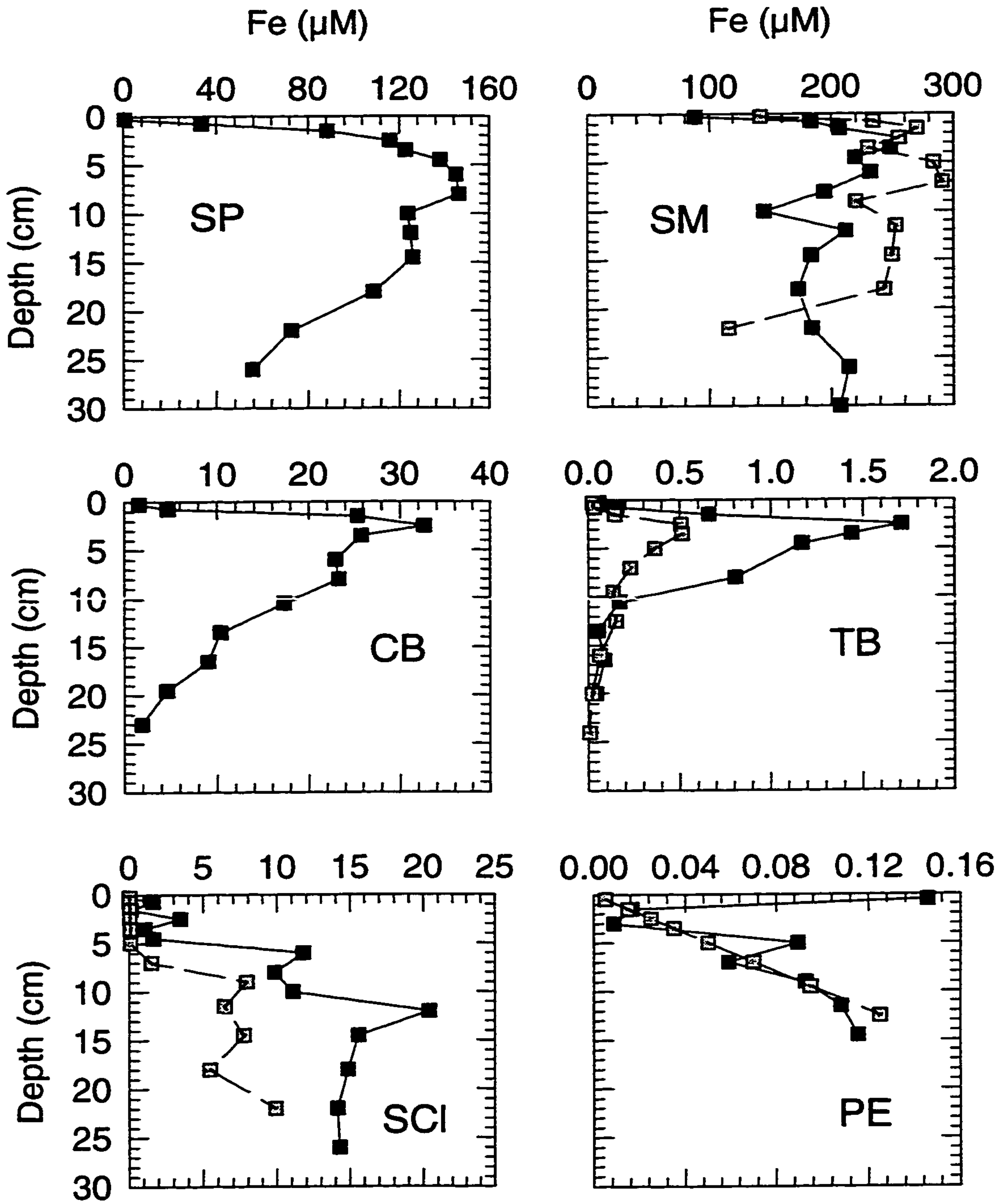

Figure 8. Teflon '94 and '95 pore water Fe trace metal data. Black symbols are Teflon '94 data and grey symbols are Teflon '95 data. Station abbreviations in the legend are as in Table 1.

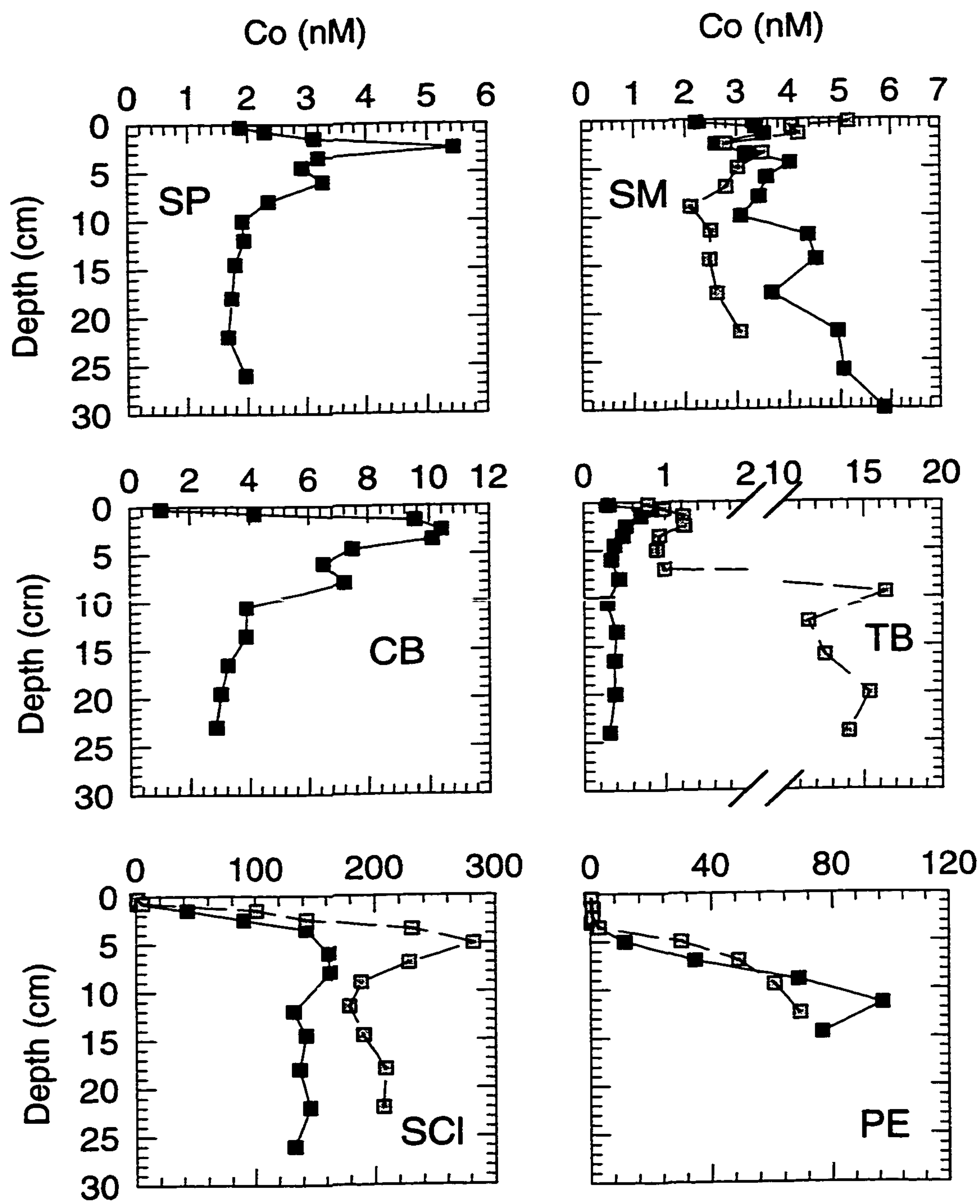

Figure 9. Teflon '94 and '95 pore water Co trace metal data. Black symbols are Teflon '94 data and grey symbols are Teflon '95 data. Station abbreviations in the legend are as in Table 1.

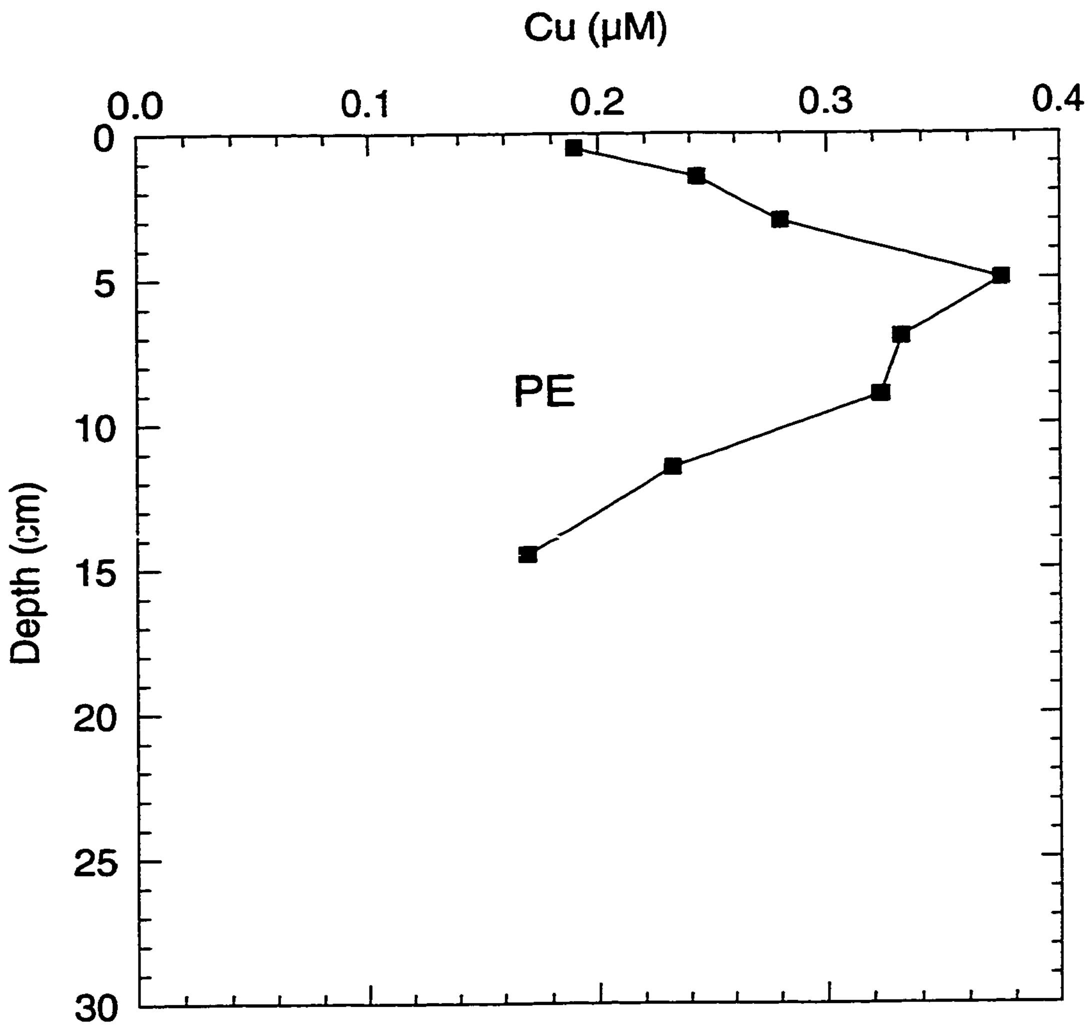

Figure 10. Teflon '94 pore water Cu trace metal data for Patton Escarpment. Station abbreviations in the legend are as in Table 1.

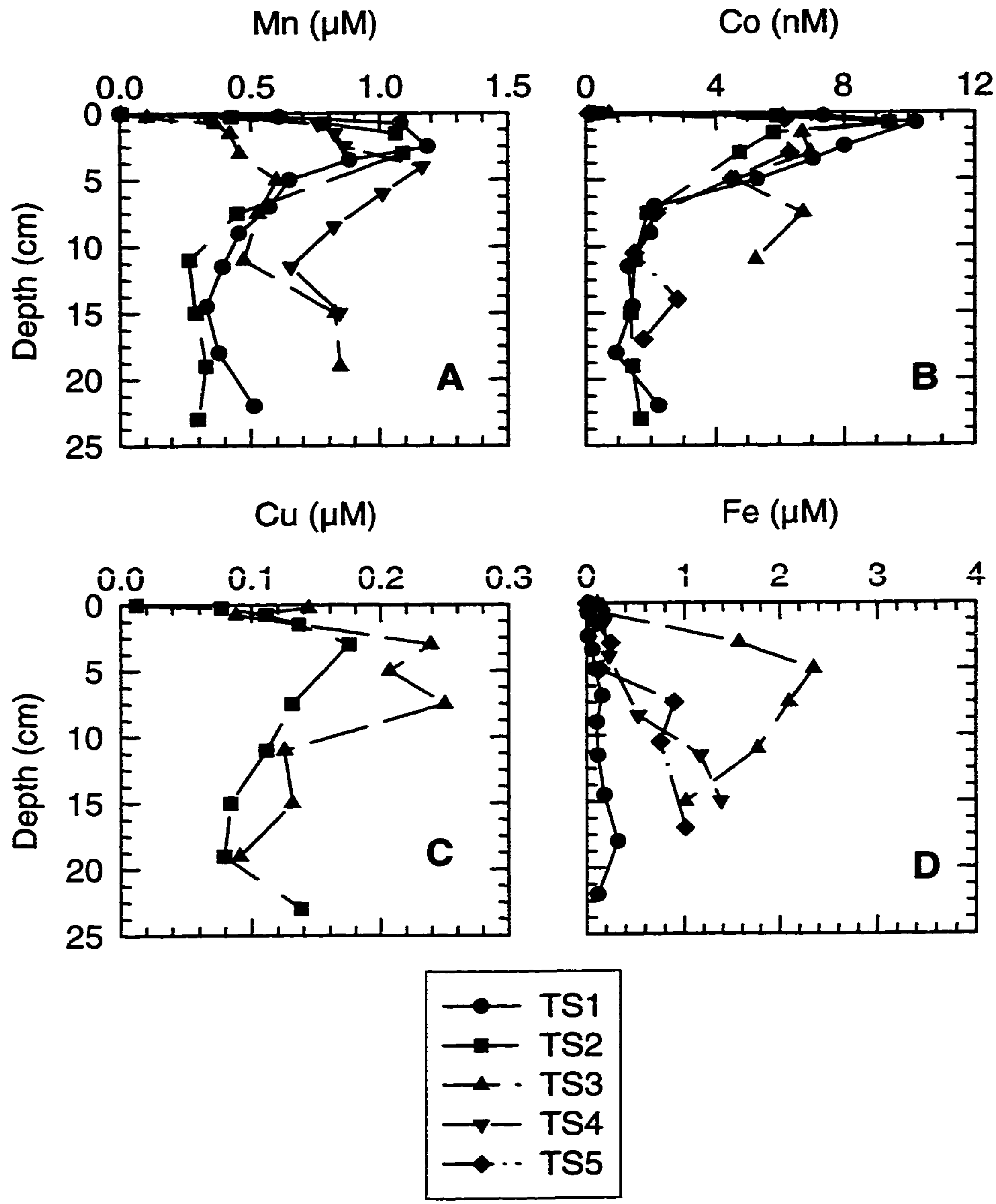

Figure 11. Monterey Bay pore water trace metals data for Mn (A), Co (B), Cu (C), and Fe (D). Station abbreviations in the legend are as in Table.

Trace Metal Lander Data

While the magnitude of the metal concentrations in the samples, collected from the benthic flux chambers, shows some temporal variation (Figures 12-17), the individual chambers on a lander have generally consistent trends for the rates of change of Mn, Cu, or Fe over time. As will be discussed later, these rates of change in metal concentration are proportional to the flux determined by the lander. An example of this variability can be found in the Santa Monica Basin lander Mn data (Figure 12). In 1994 initial Mn concentrations were ~30 nM while in 1995 they were ~70nM. In spite of this apparent temporal variability, the individual chambers show consistent trends in the flux of Mn over the time of deployment. Cobalt data is not shown due to apparent contamination of the chamber water from the blue paint on the stainless steel housing on the thermistors in each of the lander chambers.

In the basins, the rate of change of the Mn concentration in chamber waters with time is smallest at Patton Escarpment and generally increases toward shore (Figure 12). This increase in the rate of change, or flux, is similar to that reported by Johnson and others (1992) for the open continental margin. The Monterey Bay values observed in this study (Figure 15) were also consistent with those of Johnson and others (1992) at a similar station in Monterey Bay (Figure 15).

While the magnitude of the Cu lander sample concentrations shows some temporal variability in the basins (Figure 13), the rate of change generally increases nearshore as organic carbon inputs increase (Berelson and others, 1996). This lends support to the argument for Cu remobilization during organic carbon oxidation (Hong and others, 1995; Sawlan and Murray, 1983). The Monterey Bay, Cu values observed in this study (Figure 16) are generally similar, reaching no more than ~50 nM. This is consistent with those measured earlier in Monterey Bay (Figure 15) and with the organic carbon production found in Monterey Bay (Pilskaln and others, 1996).

In the basins, the highest Fe values in the chambers are found in the low oxygenated basins San Pedro and Santa Monica (Figure 14). While in Monterey Bay the concentrations observed in this study are fairly uniform (Figure 17) and of similar magnitude to those observed by Johnson and others (1992) at a similar station in Monterrey Bay (Figure 17). This trend of high chamber Fe concentrations in low oxygenated waters, holds with the geochemistry of iron, since Fe^{2+} is not stable in oxygenated seawater (Balzer, 1982; Millero and others, 1987; von Langen and others, 1997).

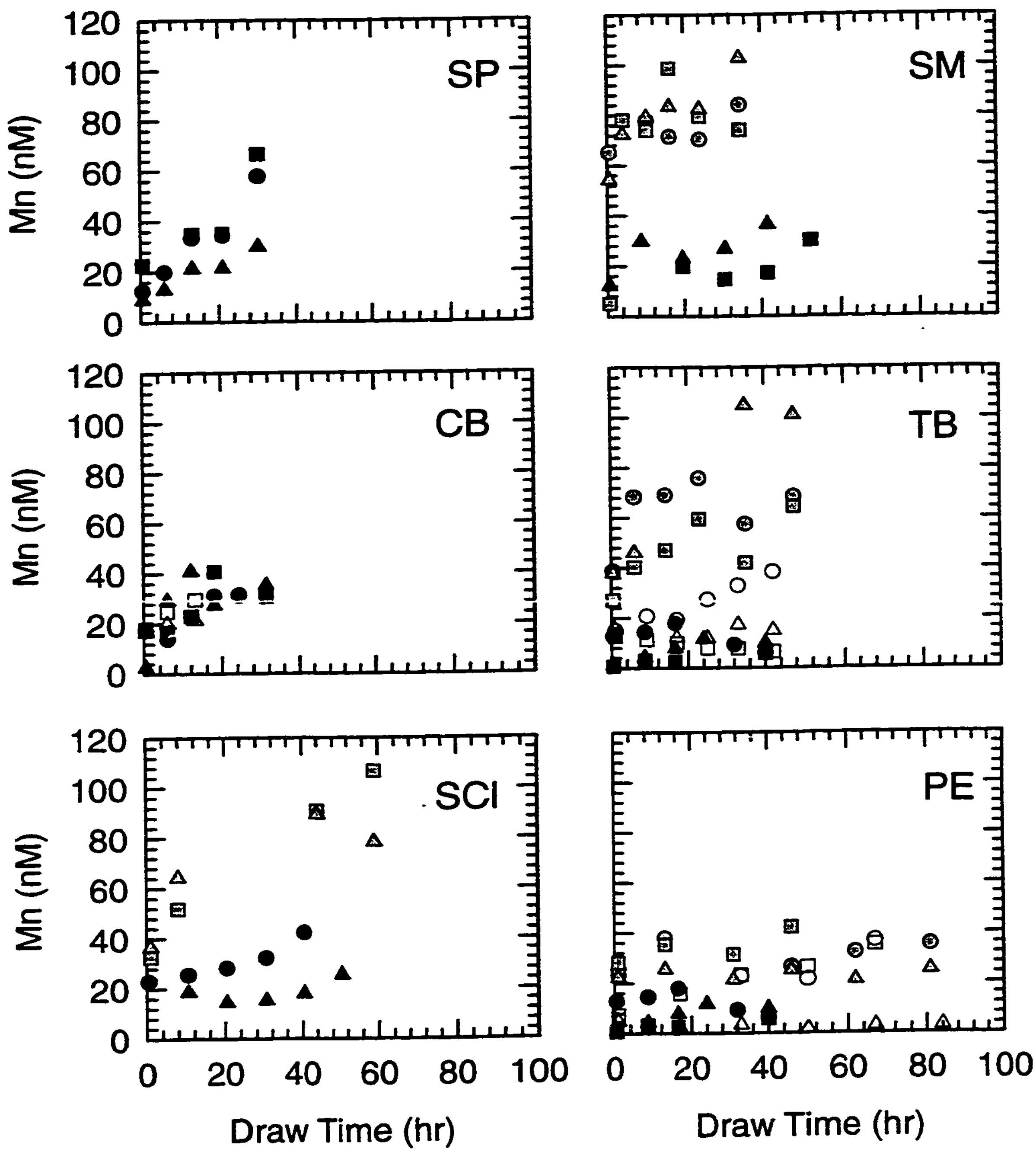

Figure 12. Lander overlying water Mn data for the Teflon '94 and '95 cruises. Black and white symbols are data from two different landers deployed during the Teflon '94 cruise at some stations. Grey symbols are data from the Teflon '95 cruise. Each lander contains three chambers which are represented by the circles, squares, and triangles respectively. Station abbreviations are as in Table 1.

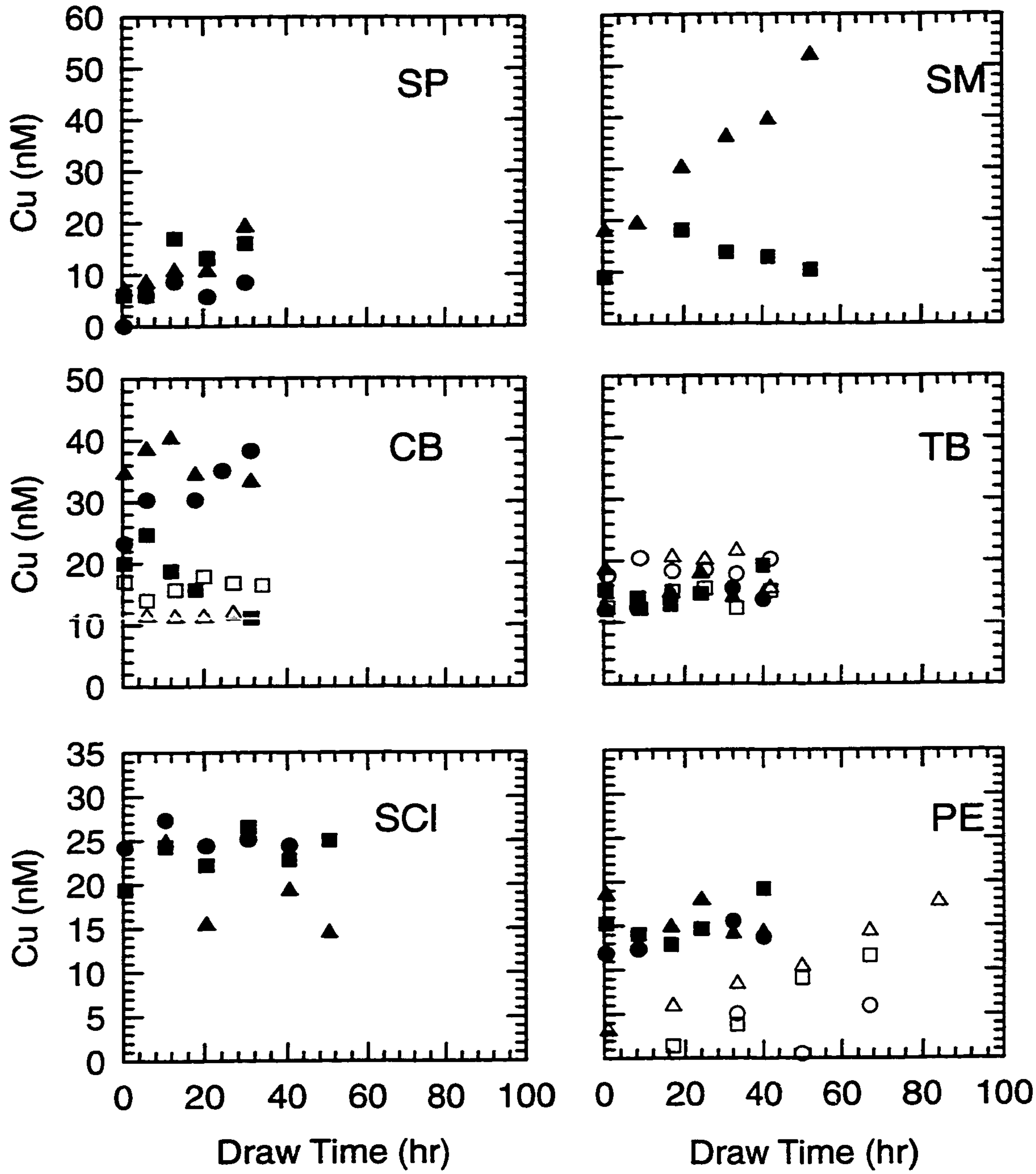

Figure 13. Lander overlying water Cu data for the Teflon '94 and '95 cruises. Black and white symbols are data from two different landers deployed during the Teflon '94 cruise at some stations. Grey symbols are data from the Teflon '95 cruise. Each lander contains three chambers which are represented by the circles, squares, and triangles respectively. Station abbreviations are as in Table 1.

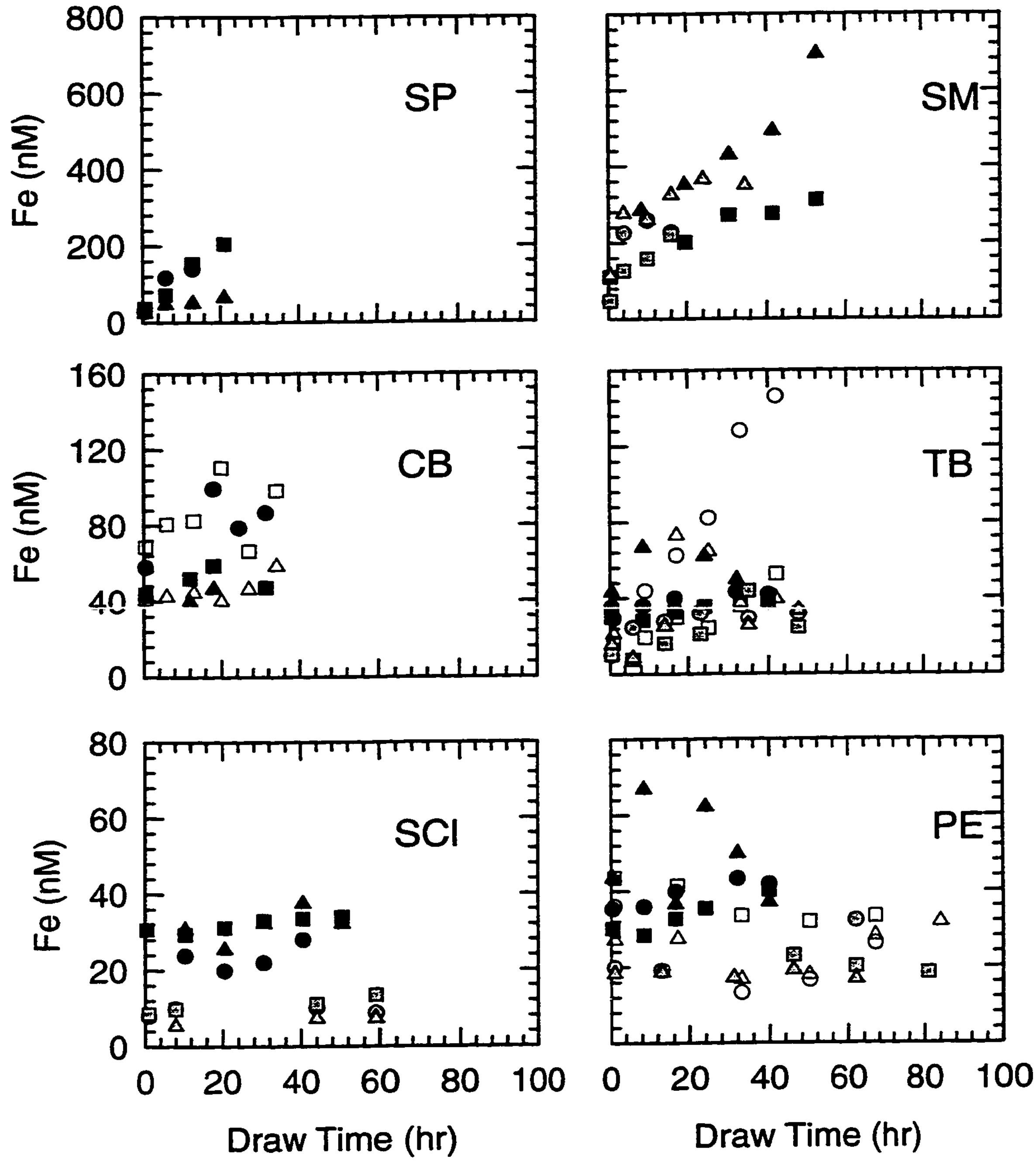

Figure 14. Lander overlying water Fe data for the Teflon '94 and '95 cruises. Black and white symbols are data from two different landers deployed during the Teflon '94 cruise at some stations. Grey symbols are data from the Teflon '95 cruise. Each lander contains three chambers which are represented by the circles, squares, and triangles respectively. Station abbreviations are as in Table 1.

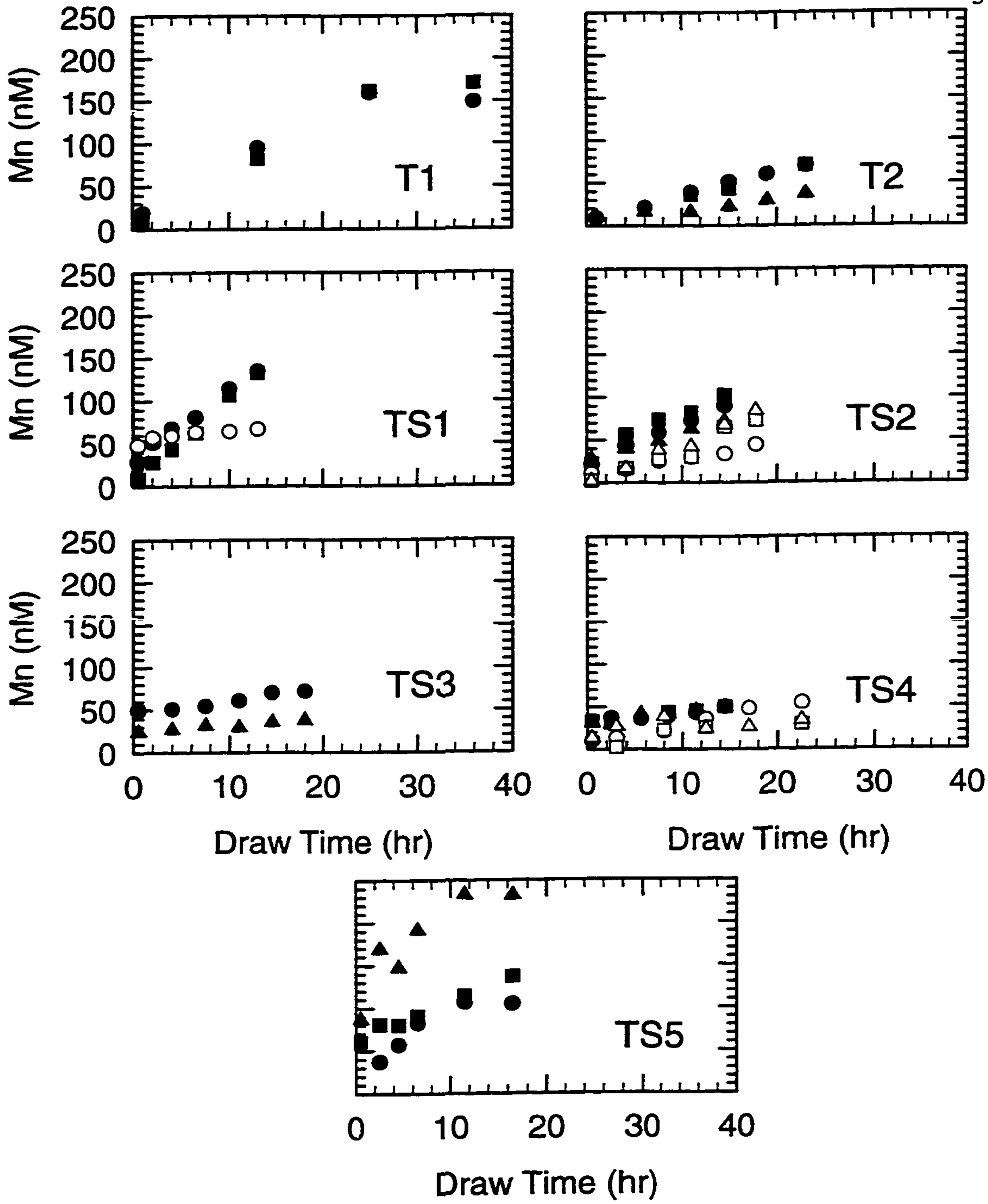

Figure 15. Lander overlying water Mn data for the Monterey Bay cruises. Black and white symbols are data from two different landers deployed during some cruises. Each lander contains three chambers which are represented by the circles, squares, and triangles respectively. Station abbreviations are as in Table 1, except T1 and T2 are the data from the 1991 and 1992 samples respectively taken from Johnson and others (1992).

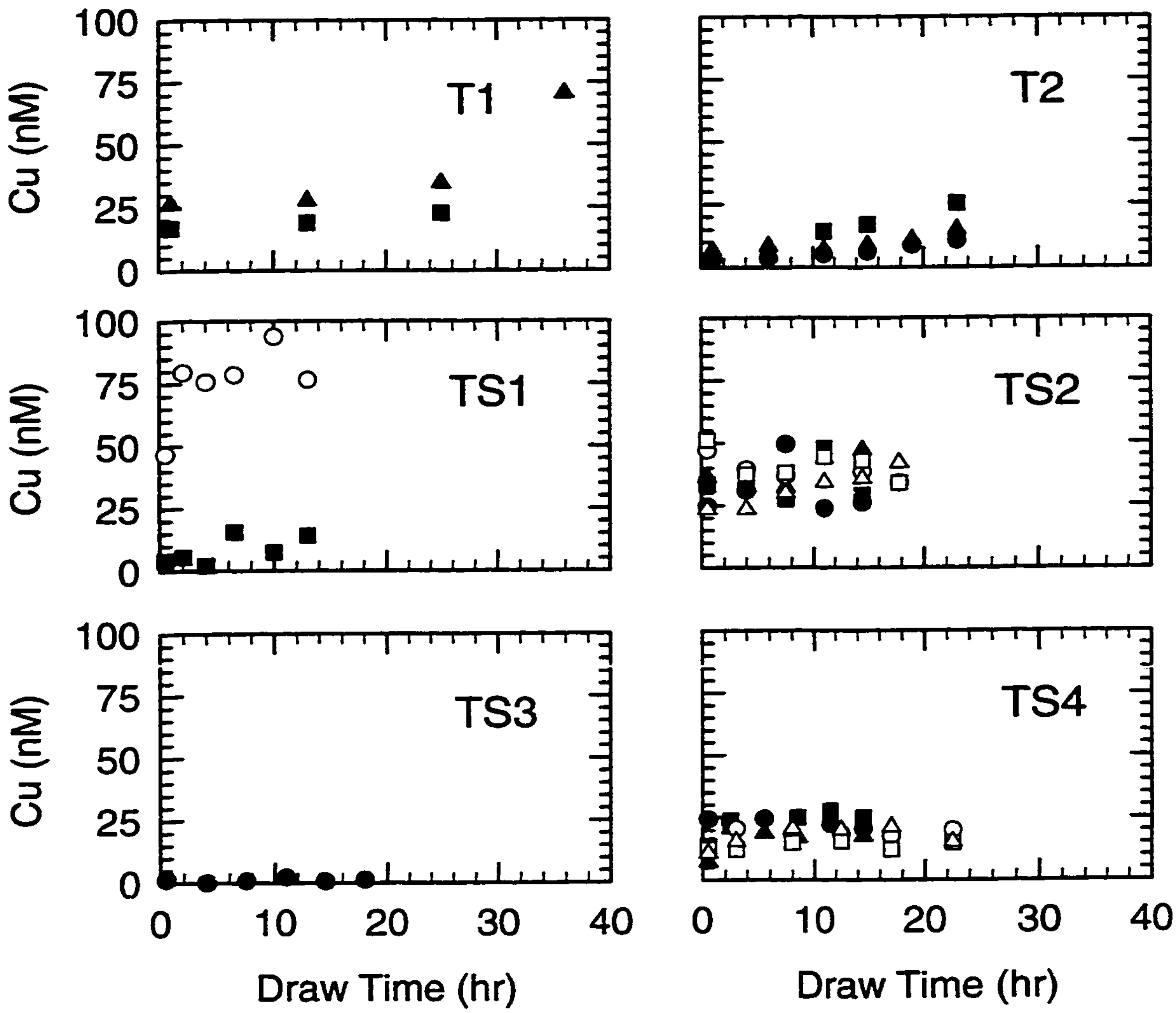

Figure 16. Lander overlying water Cu data for the Monterey Bay cruises. Since no Cu was measured for the TS5 cruise it is not shown. Black and white symbols are data from two different landers deployed during some cruises. Each lander contains three chambers which are represented by the circles, squares, and triangles respectively. Station abbreviations are as in Table 1, except T1 and T2 are the data from 1991 and 1992 .

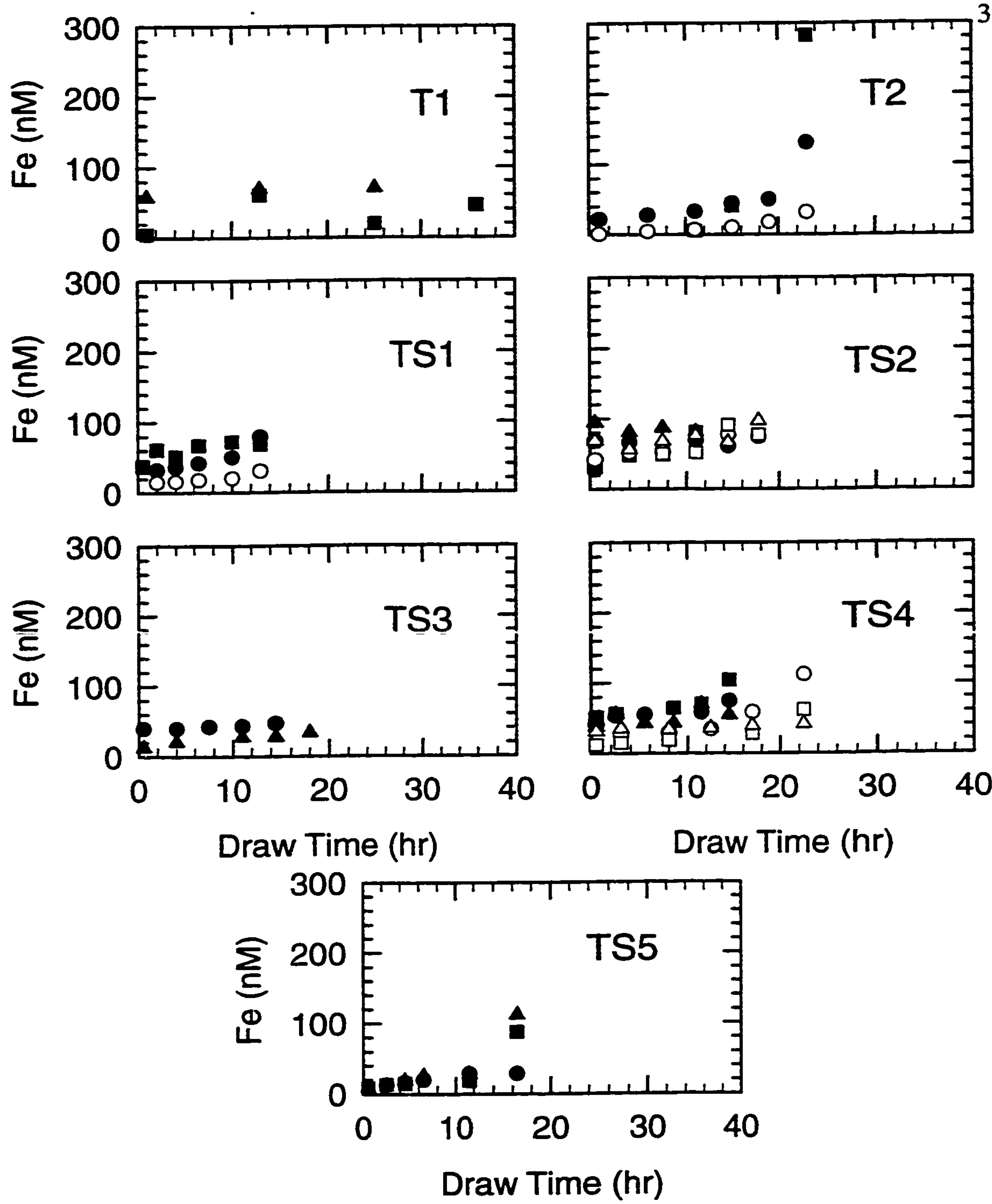

Figure 17. Lander overlying water Fe data for the Monterey Bay cruises. Black and white symbols are data from two different landers deployed during some cruises. Each lander contains three chambers which are represented by the circles, squares, and triangles respectively. Station abbreviations are as in Table 1, except T1 and T2 are the data from 1991 and 1992 samples.

Trace Metal Fluxes

Flux Calculations

Benthic Flux Chamber Estimate

After a lander is recovered, the samples are analyzed for trace metal concentrations. These concentrations are then corrected for dilution of the chamber water with bottom water that flows in to replace each sample that is removed (Berelson and Hammond, 1986). The dilution corrected concentrations of a typical lander chamber were plotted against the chamber incubation time (Figure 18). A linear regression of the data (Figure 18) gives the rate of change, dc/dt, with units of nmol/L/hr. The flux, in units of μmol/cm^2/day, can then be calculated from the rate of change in the concentration and the chamber height, h, which has units of cm:

$$\text{Flux} = \frac{dc}{dt}h \tag{1}$$

By convention, flux out of the sediments is taken as positive. During deployment each cylinder shaped chamber on the lander sinks into the sediments to a different height. To determine the chamber height, a precisely known concentration and volume of CsCl was injected into each chamber. The CsCl in the water contained in the chamber was determined by measuring the concentration in the subsequent sample drawn. Chamber volume and height can be calculated from the dilution of the CsCl. The standard error of an individual chamber flux value is obtained by combining the standard error of the height with the standard error of the gradient. Flux is reported as the mean ± standard error for each individual lander (Appendix 1) or for each station (Appendix 2). The mean is obtained from the average of the fluxes of all functional chambers either on an individual lander (Appendix 1) or for all landers deployed at that station (Appendix 2). The variability in the flux obtained from the replicate values determined with each functional chamber, either on an individual lander (Appendix 1) or for all landers deployed at that station (Appendix 2), was used to calculate the standard error in the flux.

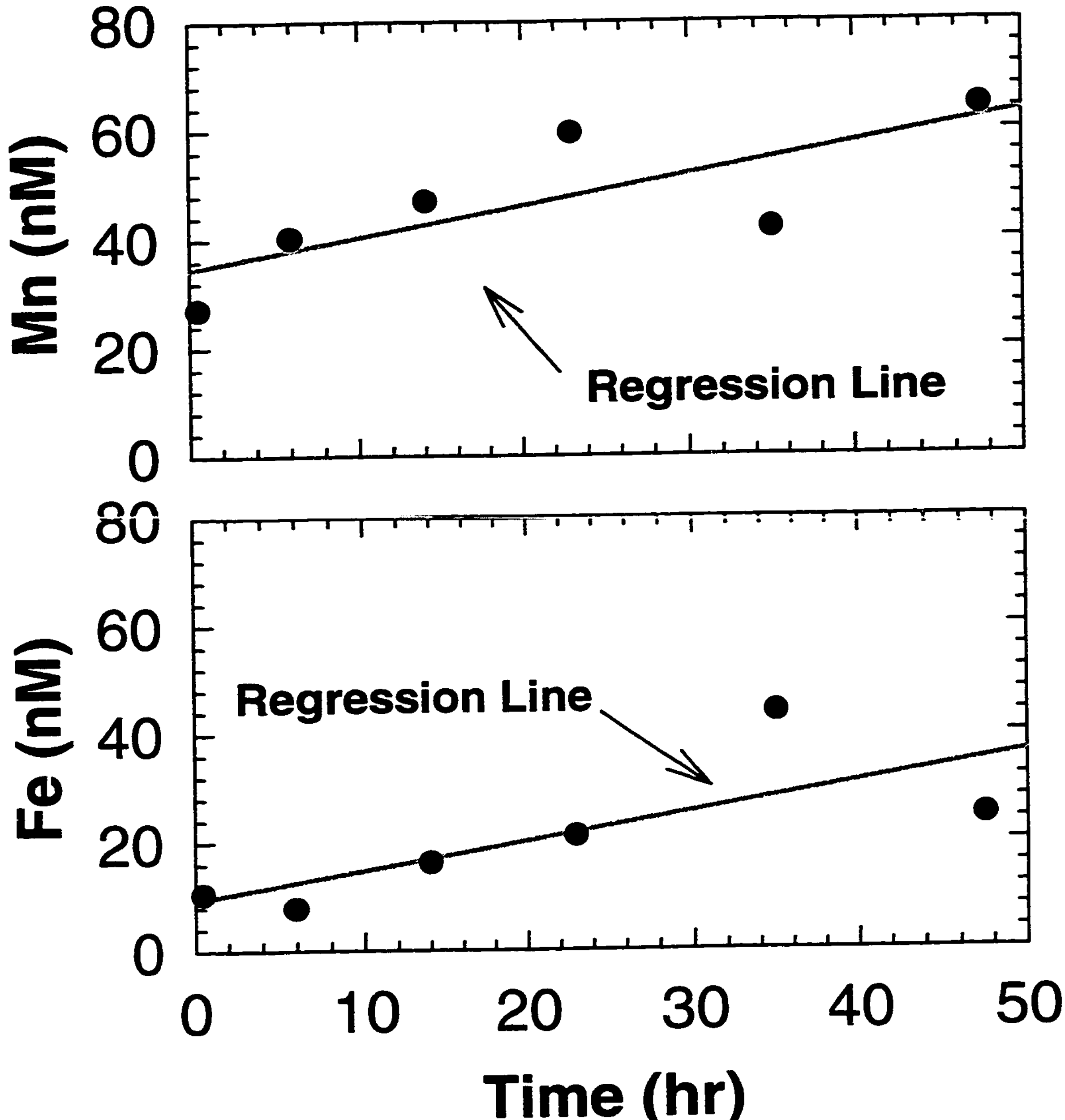

Figure 18. Typical lander chamber data for Mn and Fe from the Teflon '95 cruise in Tanner Basin (Figure 1 and Table 1). Top panel: change in concentration of Mn over time. Bottom panel: change in concentration of Fe over time. The regression of the data to obtain the slope of concentration vs. time that is used with the chamber height to calculate flux (Equation 1) is shown.

Pore Water Gradient Flux Estimate

The benthic flux of dissolved metal can also be estimated from the depth dependent gradient in concentrations measured within the pore waters (Figure 19). This gradient should merge smoothly with the dissolved metal concentrations at the bottom of the water column. The overlying water concentration was obtained from the bottom hydrocast bottle (Appendix 1, Figures 3-6). The gradient of each metal within the sediment may change rapidly due to reduction of oxides, remineralization of organic carbon, and sorption onto solid phases. Developing a simple model of metal diagenesis that can be curve fitted to all the data to estimate the gradient, as is done for Si (Berelson and others, 1987b), is therefore not possible. Selection of the proper depth interval to use for the gradient estimate is subjective. A straight line was fitted to the upper portion of each profile over the range that appeared linear as in Figure 19. This generally produces a minimum estimate of the gradient.

The depth intervals used for each of the gradient estimates of each metal are given in Table 3 and were estimated independently for different cores. The depth intervals estimated from cores taken at different times at the same site, were generally in good agreement (Table 3) for the same metal. However, the linear ranges for metals with dissimilar geochemical properties were often quite different. Using the depth gradient in concentration, dc/dz, the porosity, Φ, and the sediment diffusion coefficient, D_s, Berner's (1980) diffusion model gives the flux:

$$\text{Flux} = -\phi D_s \frac{dC}{dz} \quad (2)$$

The porosity is the percent water in the sediment in each sample interval. This is obtained by weighing a sample of sediment wet, drying the sediment, and weighing it dry. Since the porosity never varies more than 10% (Appendix 1) over the depth intervals used for the gradient estimates (Table 3), the average porosity was used for all flux calculations. This should result in errors of 4% or less in flux calculations (Klump and Martens, 1989). Free solution diffusion coefficients, D_o, are available (Li and Gregory, 1974) which can be related to the sediment diffusion coefficient, D_s, using the tortuosity, Θ:

$$D_s = \frac{D_o}{\Theta^2} \quad (3a)$$

Tortuosity is the actual distance around all the sediment grains that an ion travels per length of sediment (Berner, 1980, Ullman and Aller, 1981). In practice measuring the tortuosity is impossible, but it can be related to the electrical resistance of the sediment (Berner, 1980, Ullman and Aller, 1981), or the formation factor, F and the porosity, Φ:

$$\Theta^2 = \Phi F \quad (3b)$$

An empirical relationship (Equation 3c) has been developed (Berner, 1980, Ullman and Aller, 1981) relating the formation factor, F, to the porosity,Φ, where m is a constant depending on the type of sediment:

$$F = \frac{1}{\Phi^m} \qquad (3c)$$

When m = 2, Equation 3c is known as Archie's Law (Berner, 1980). The Archie relationship has been used in past studies in the Borderland basins (Berelson and others, 1987b) and in the Monterey Bay (Fairey, 1992). Using the Archie relationship Equations 3c and 3b can be substituted into Equation 3a to give the final form relating the sediment diffusion coefficient, D_s, to the free solution diffusion coefficient, D_o:

$$D_s = D_o \phi \qquad (3d)$$

Free solution diffusion coefficients were corrected for temperature (Table 4) only. This results in at most an 8% error in the sediment diffusion coefficient due to the effects of pressure that are not taken into account (Li and Gregory, 1974). Changing the coordinate system to agree with the lander estimated fluxes (multiplying Equation 2 by -1) and substituting Equation 3d into Equation 2 gives the final equation used for estimating flux:

$$\text{Flux} = \phi^2 D_o \frac{dC}{dz} \qquad (4)$$

The standard error of the gradient calculated from the linear regression was used in place of the gradient, dc/dz, in Equation 4 to give the standard error of the flux estimate.

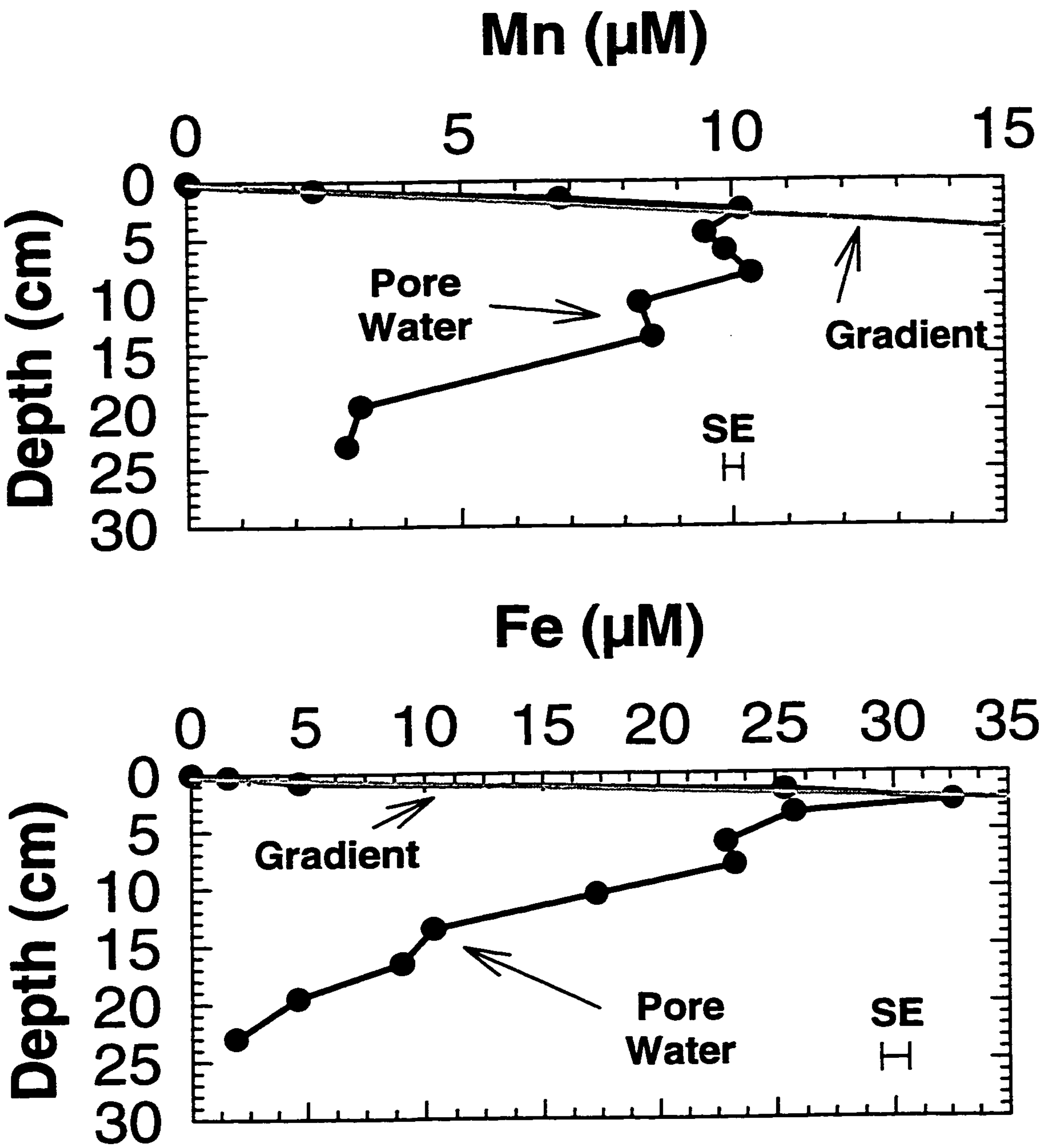

Figure 19. Typical pore water profile for Mn and Fe from the Teflon '94 cruise in the Santa Catalina Basin (Figure 1 and Table 1). Top panel: Mn pore water profile. Bottom panel: Fe pore water profile. On both plots a regression of the surface data has been preformed to obtain the gradient used in flux calculations (Equation 4). The maximum standard error, SE, of the data is shown on both plots as an index of analytical precision.

Table 3. Depth intervals in centrifuged cores over which the gradient was estimated for pore water flux calculations (Equation 4). Dashes indicate no data was available.

		Depth interval (cm)			
Cruise	Station Name or Date	Mn	Co	Fe	Cu
Teflon '94	San Pedro Basin	2.50	6.00	2.50	2.50
	Santa Monica Basin	3.50	2.50	3.50	3.50
	Santa Catalina Basin	0.75	2.50	2.50	2.50
	Tanner Basin	1.50	1.50	2.50	3.50
	San Clemente Basin	0.75	0.75	5.00	1.50
	Patton Escarpment	3.00	3.00	14.50	5.00
Teflon '95	Santa Monica Basin	2.50	1.50	1.50	–
	Tanner Basin	0.75	1.50	3.50	–
	San Clemente Basin	0.75	0.25	5.00	–
	Patton Escarpment	2.50	2.50	12.50	–
Monterey Bay	TS1	3.50	0.75	2.50	–
	TS2	3.00	0.75	–	3.00
	TS3	1.50	0.75	–	3.00
	TS4	0.75	0.75	8.50	8.50
	TS5	–	0.50	–	–

Table 4. Temperature corrected free solution diffusion coefficients, D_o (Li and Gregory, 1974) used for pore water flux calculations (Equation 4).

	D_o (x 10^{-6} cm^2/sec)			
Station Name	Mn	Co	Fe	Cu
San Pedro Basin	3.81	4.06	4.09	4.10
Santa Monica Basin	3.81	4.06	4.09	4.10
Santa Catalina Basin	3.66	3.93	3.95	3.96
Tanner Basin	3.63	3.90	3.93	3.94
San Clemente Basin	3.44	3.74	3.76	3.77
Patton Escarpment	3.28	3.61	3.61	3.62
Monterey Bay	4.6	4.53	4.58	4.61

Water Column Flux Estimate

The flux across the sediment-water interface can be estimated in the basins when a gradient in concentration develops relative to water at the sill depth in the basin (Figure 20) if we assume that each profile is in steady state. The bathymetry in the Southern California Borderlands Basins restricts horizontal flow (Berelson and others, 1987b) below the sill depth (Table 1). The flux is given by the product of the concentration gradient, dCz/dz at the interface and the vertical eddy diffusivity, K_z:

$$\text{Flux} = -K_z \frac{dC_z}{dz} \qquad (5)$$

where C_z is the concentration at depth, z. Berelson (1985) measured the concentrations of ^{222}Rn and ^{226}Ra in the water column and the sediments to arrive at the vertical eddy diffusivity in San Pedro, Tanner, and San Clemente basins (Table 5). Johnson and others (1988) report a K_z value for Santa Monica Basin (Table 5). The vertical eddy diffusivity for Santa Catalina Basin has not been reported. It has a similar bottom depth and sill depth (Table 1) to that in Tanner Basin and its vertical eddy diffusivity was assumed to be equal to that for Tanner Basin (Table 5). The concentration gradient at the sediment-water interface can be estimated most accurately if data from the entire sub-sill water column is used. However, dissolved metals may be removed in the water column by scavenging and the gradient should be determined using a model that incorporates this possibility. If a steady state is assumed then diffusion can be balanced by the chemical reaction occurring in the water column. Here we assume k is the first order scavenging rate constant:

$$K_z \frac{d^2C}{dz^2} - kC = 0 \tag{6}$$

Solving Equation 6 gives a relationship between the concentration at depth, C_z and the concentration at the sediment surface, C_o:

$$C_z = C_o e^{-\sqrt{\frac{k}{K_z}}\, z} \tag{7}$$

Taking the natural logarithm of Equation 7 results in:

$$\ln C_z = \ln C_o - \sqrt{\frac{k}{K_z}}\, z \tag{8}$$

A linear fit of ln C_z, observed in each basin, vs. z should result (Figure 20). Equation 7 is substituted into Equation 5 to give:

$$\text{Flux} = -K_z C_o \left(-\sqrt{\frac{k}{K_z}}\right) e^{-\sqrt{\frac{k}{K_z}}\, z} \qquad (9)$$

Using a coordinate system with the depth set to 0 m at the sediment-water interface and increasing upwards gives the final form of flux in the water column occurring at the sediment-water interface:

$$\text{Flux} = -K_z C_o \left(-\sqrt{\frac{k}{K_z}}\right) \qquad (10)$$

The standard errors of the y-intercept and slope of the linear fit (Equation 8) are used in Equation 10 to give the standard error of the estimated flux.

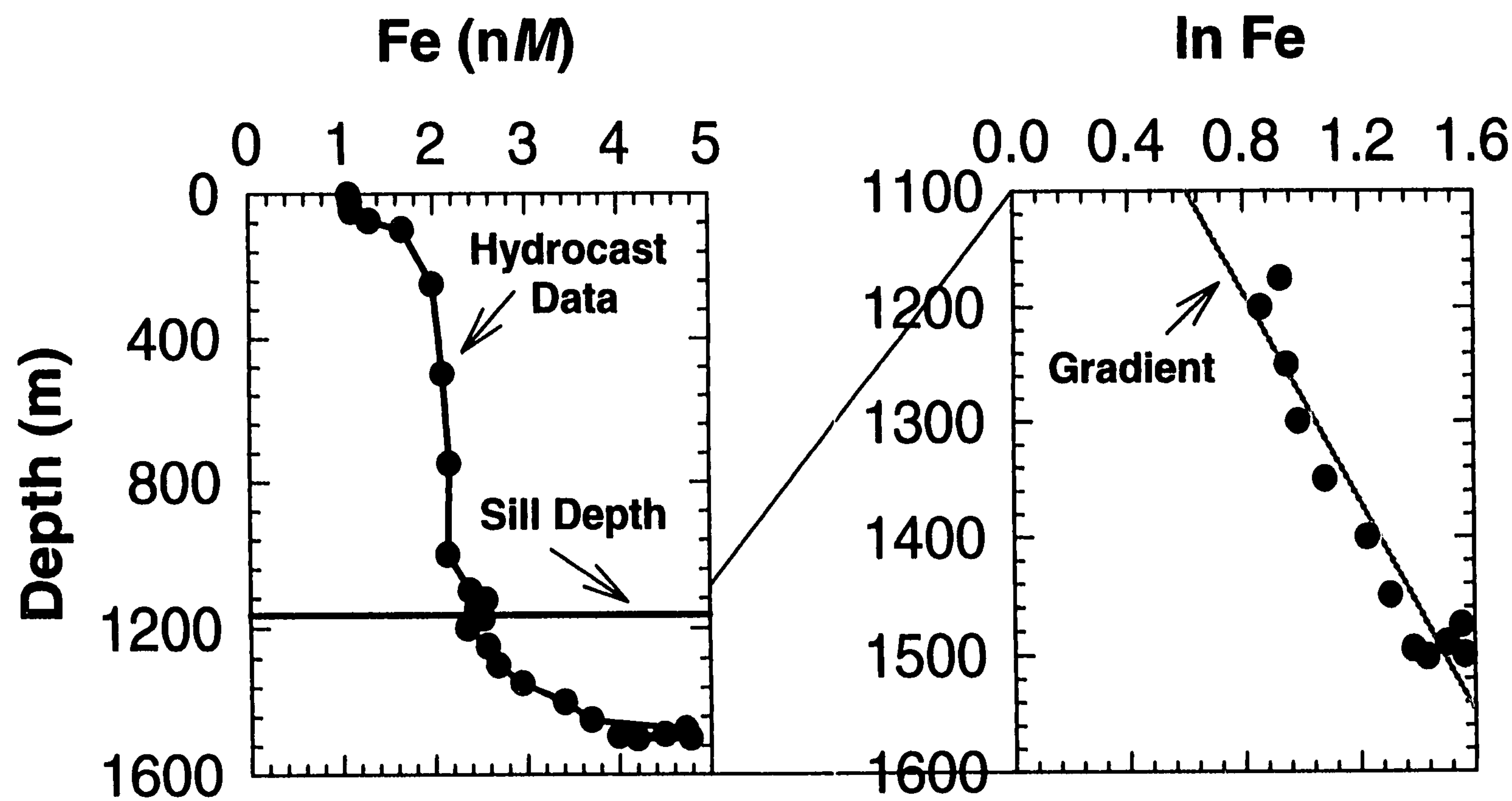

Figure 20. Typical hydrocast data for Fe from the Teflon '95 cruise in Tanner Basin (Figure 1 and Table 1). Top panel: Fe hydrocast data and the sill depth (horizontal line). Bottom panel: the Fe data has been transformed with the natural logarithm to regress the data and obtain the gradient (Equation 8). Hydrocast data from a rosette typically can be contaminated by 1-2 nM Fe but it appears relatively constant and does not affect the gradient.

Table 5. Vertical eddy diffusivity values used in this study. San Pedro, Tanner, and San Clemente Basins are from Berelson (1985). Santa Monica is from Johnson and others (1988). No value exists for Santa Catalina Basin in the literature, but with its similar bottom depth and sill depth (Table 1) its vertical eddy diffusivity was assumed to be equal to that for Tanner Basin.

Station Name	Station ID	Kz ± SE (cm^2/sec)
San Pedro Basin	SP	4.6 ±1.2
Santa Monica Basin	SM	3
Santa Catalina Basin	CAT	9.8
Tanner Basin	TB	9.8±3.9
San Clemente Basin	SCl	24±9

Flux Averages

Chemical fluxes from sediments are affected by temperature in shallow water environments (Klump and Martens, 1989) or organic carbon input in constant temperature environments (Sugai, 1987). Temperature changes in any of the basins are small. The temperature range at the 100 m Monterey Bay station, where variability in flux is the largest, was 8.7 - 11.3 °C. However, Monterey Bay is known to have large episodic inputs of organic carbon (Pilskaln and others, 1996). Due to these variations, the fluxes from the sediments in Monterey Bay may not be in a steady state. The basins are also known to undergo periodic flushing (Berelson, 1991) and water column profiles may not reflect the steady state assumed in Equation 6. All flux estimates from multiple years were averaged together (Table 6), therefore, before comparing the flux derived by each method. The Mn flux derived from the 1990 Santa Monica Basin hydrocast data (Coale and others, 1990) and the lander data from Johnson and others (1992) were also included in the averaging (Table 6). The standard error (Table 6) was derived from the variability in each independent calculated flux.

Table 6. The flux estimates derived from landers, centrifuged core pore water, and hydrocast values. The fluxes are reported as the mean ± the standard error of multiple year measurements. The standard error was derived from the variability in independent observations. Units for Mn, Fe and Cu are µmol/m^2/day and for Co are nmol/m^2/day. Station abbreviations are as in Table 1, except MB is the Monterey Bay station. Flux types are landers, core - centrifuged core pore waters, and hydros - hydrocasts. Fluxes with a * are believed to be biased due to contamination from the lander. The number of measurements, N, used for the mean and standard deviation calculations are shown.

Station ID	Flux Type	Mn	Mn SE	N	Co	Co SE	N	Fe	Fe SE	N	Cu	Cu SE	N
MB	Landers	9.57	1.38	25	*	*	*	5.64	0.94	24	1.26	0.34	20
	Core	0.63	0.29	4	18.41	2.69	5	0.085	0.051	3	0.075	0.024	2
	Hydros	---	---	---	---	---	---	---	---	---	---	---	---
SP	Landers	2.62	0.53	3	*	*	*	14.40	5.18	3	0.71	0.12	3
	Core	1.74	0.33	1	0.94	0.64	1	140.31	15.53	1	—	—	—
	Hydros	0.41	0.16	1	-0.10	2.98	1	4.30	1.12	1	-0.13	0.08	1
SM	Landers	1.51	0.44	5	*	*	*	15.77	2.53	5	0.64	0.64	2
	Core	2.86	1.27	2	3.35	1.32	2	275.90	13.58	2	—	—	—
	Hydros	2.03	0.95	3	3.26	0.29	2	5.65	1.07	1	1.36	0.35	1
CAT	Landers	1.73	0.21	5	*	*	*	1.06	0.37	5	-0.03	0.35	5
	Core	8.09	2.64	1	11.39	1.99	1	36.79	5.41	1	—	—	—
	Hydros	1.61	0.26	1	—	—	—	4.03	0.54	1	—	—	—
TB	Landers	0.71	0.38	9	*	*	*	1.37	0.71	9	0.10	0.08	6
	Core	1.06	0.43	2	1.45	0.34	2	1.16	0.70	2	—	—	—
	Hydros	0.55	0.18	1	3.56	1.30	2	0.75	0.08	2	0.13	0.10	1
SCI	Landers	1.35	0.45	4	*	*	*	0.19	0.06	6	-0.10	0.17	3
	Core	1.69	0.91	2	6.98	3.15	2	0.48	0.43	2	—	—	—
	Hydros	1.04	0.06	2	20.46	9.99	1	0.80	0.56	1	—	—	—
PE	Landers	0.32	0.13	9	*	*	*	-0.10	0.12	9	0.24	0.10	6
	Core	0.08	0.06	2	0.46	0.28	2	0.020	0.002	2	—	—	—
	Hydros	—	—	—	—	—	—	—	—	—	—	—	—

Discussion

An initial examination of the average fluxes determined by each of the three methods in the Southern California Borderland Basins shows that the results for each metal are generally comparable (Table 6). Even so, examination of the variability of the average fluxes (Table 6) indicates some significant differences in some cases (e.g. Monterey Bay data). Since the variances were not similar a non-parametric Mann-Whitney U statistical test must be employed to test for significant differences between methods. All three of the methods of estimating flux are not significantly different (Mann-Whitney U, $P<0.10$) in 10 of the 13 cases where there is enough data to allow for a statistical comparison (Table 7). In the cases where only a single flux measurement or estimate is available for a particular method (e.g. San Pedro Basin), the values generally agree to within the estimated error of the flux measurement. However, clear examples of disagreement exist as well. In this discussion, examples where the fluxes agree are first presented to establish that the methods can yield comparable estimates of metal flux from continental margin sediments in certain environments. The cases where a significant disagreement exists are then examined to show that most of these differences can be explained by fundamental biogeochemical processes. Review of the data suggests that these exceptions are driven by 4 factors: temporal variability in the flux, difficulty in estimating pore water gradients, rapid changes in redox potential, and bioirrigation. Each of these processes will be considered in turn.

Table 7. Results of single factor Mann-Whitney U tests comparing different methods of estimating flux. Station abbreviations are as in Table 1. The null hypothesis, H_o, and the calculated probability, P, for each Mann-Whitney U conducted is shown where L - average lander estimated flux, CC - average centrifuged core estimated flux, and H - average hydrocast estimated flux as described in the text. **Bolded** cells signify stations where the methods are significantly different (Mann-Whitney U, P<0.10). Those cells with dashes are stations where a calculation could not be made because the measurements were not replicated or because of measurement error (Cu in pore waters or Co in the benthic flux chambers).

Station	Mn		Co		Fe		Cu	
ID(s)	H_o	P	H_o	P	H_o	P	H_o	P
SP	—	—	—	—	—	—	—	—
SM	L=H=CC	0.31	H=CC	1.00	L=CC	**0.053**	—	—
CAT	—	—	—	—	—	—	—	—
TB	L=CC	0.24	H=CC	0.121	L=H=CC	0.98	—	—
SCI	L=H=CC	0.92	—	—	L=CC	0.74	—	—
PE	L=CC	0.64	—	—	L=CC	0.48	—	—
MB	**L=CC**	**0.002**	—	—	**L=CC**	**0.003**	L=CC	0.25

Flux Agreement

The fluxes of dissolved Mn, Fe, Co, and Cu from Santa Monica and San Clemente Basins sediments for each method are compared in Figures 21 and 22. Santa Monica Basin has low bottom water O_2 (~10 μM, Table 2) with no macro-fauna present (Berelson, 1985; Christensen and others, 1994; Gorsline, 1992). These sediments are anoxic or reducing up to the bottom water interface (Jahnke, 1990). Consequently, this basin should not be influenced by bio-irrigation. Conversely, San Clemente has a much higher O_2 concentration (62.0 µM, Table 2) and it may be somewhat influenced by macro fauna (Townsend and others, 1996). Using the distribution of Mn (Froelich and others, 1979) or NO_3^- (Heggie and Lewis, 1984) as a proxy for oxygen penetration depth, it is apparent that the sediments in San Clemente Basin (Figure 7, Appendix 1) become oxygen deficient at ~1.5 cm and Fe reduction to a form detectable by the analytical method does not begin until a depth >5cm (Figure 8).

The Mn fluxes that were estimated from the landers, the pore water gradients, and the water column gradients were not significantly different (Table 7, Mann-Whitney U $P<0.10$) in either Santa Monica or San Clemente Basins. It appears that all three methods of estimating flux can give comparable results in each of these basins. Further, it is interesting that the Mn flux is relatively similar for all three methods in both low and high oxygen conditions (Mann-Whitney U, $P<0.10$). The Mn flux in Santa Monica Basin is only moderately higher (~1 - 2.5 times greater) than in San Clemente Basin. This confirms the results of Johnson and others (1992) that the Mn flux is not dramatically elevated under low oxygen conditions as was previously proposed by others (Martin and others 1985).

The three methods of estimating Fe flux also appear to agree in the oxygenated waters of San Clemente Basin. The lander and the centrifuged core derived estimates of the Fe flux are not significantly different (Table 7, Mann-Whitney U $P<0.10$). There is only one replicate for the flux derived from the gradients in the water column, but the mean ± standard error of this estimate lies within the mean ± standard error interval of the other two methods (Figure 21, Table 6). However, the lander and centrifuged core methods for estimating Fe flux in Santa Monica Basin are significantly different from each other (Table 7, Mann-Whitney U $P<0.10$). Again there is only one replicate of the flux derived from the water column, which precludes statistical comparison. It is much lower than the other values, however. The pore water metal gradient gives the highest flux, the benthic lander gives a value 17.5 times lower and the water column gradient yields a value 37 times lower. Further, the Fe fluxes observed by all three methods in the low oxygenated water of Santa Monica Basin are at least 9 times greater than any of the Fe fluxes estimated in San Clemente Basin (Figure 21, Table 6). The cause of these differences is probably related to the strongly reducing conditions in this basin. Iron is stable as Fe(II) in the porewater (Millero and others, 1987) which is oxidized and scavenged as Fe(III) as it leaves the sediments. This removal of Fe is discussed further below.

Cobalt lander flux estimates (Figure 22, Table 6) were not presented because the samples appear to be contaminated. There is no regular pattern in the lander fluxes when stations are plotted versus depth and the fluxes are not repeatable. The contamination may be related to the blue paint coating the stainless steel housing for the temperature sensors on the O_2 electrode in the flux chambers. Only fluxes based on water column and pore water gradients are compared. The Co fluxes in Santa Monica Basin are averages of multi-year data. The two methods are not significantly different (Table 7, Mann-Whitney U $P<0.10$). In San Clemente Basin only one year of hydrocast data is available (Figure 22, Table 6). The statistical comparison of the two methods is not justified, therefore.

Copper fluxes are only available for one year of data (Figure 22, Table 6). The estimates of flux determined by the lander and the hydrocast in Santa Monica Basin are not significantly different although the measurements are not replicated. Pore water values are not reported for Cu because high Fe values appear to interfere with the chemiluminescent Cu measurements.

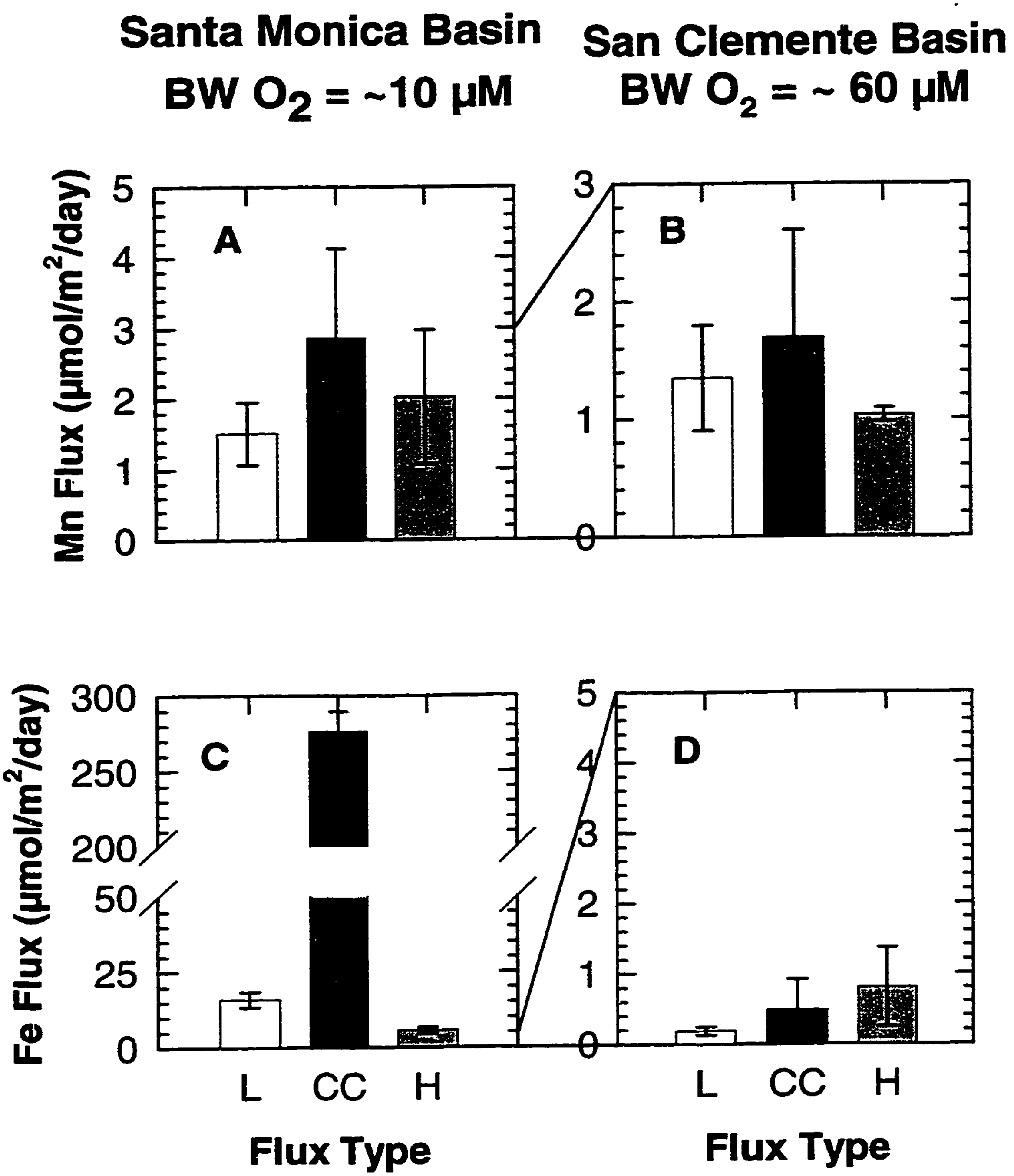

Figure 21. A comparison of flux estimates of Mn (A, B) and Fe (C, D) in Santa Monica (SM) and San Clemente (SCl) Basins. In the plots, L is the lander calculated flux, CC is the centrifuged core estimated flux, and H is the hydrocast estimated flux. The standard error of multiple year averages or the standard error of the analytical estimate for a single year is shown. The fluxes shown are the average of multiple year data where available, or of a single year data where not (Table 6).

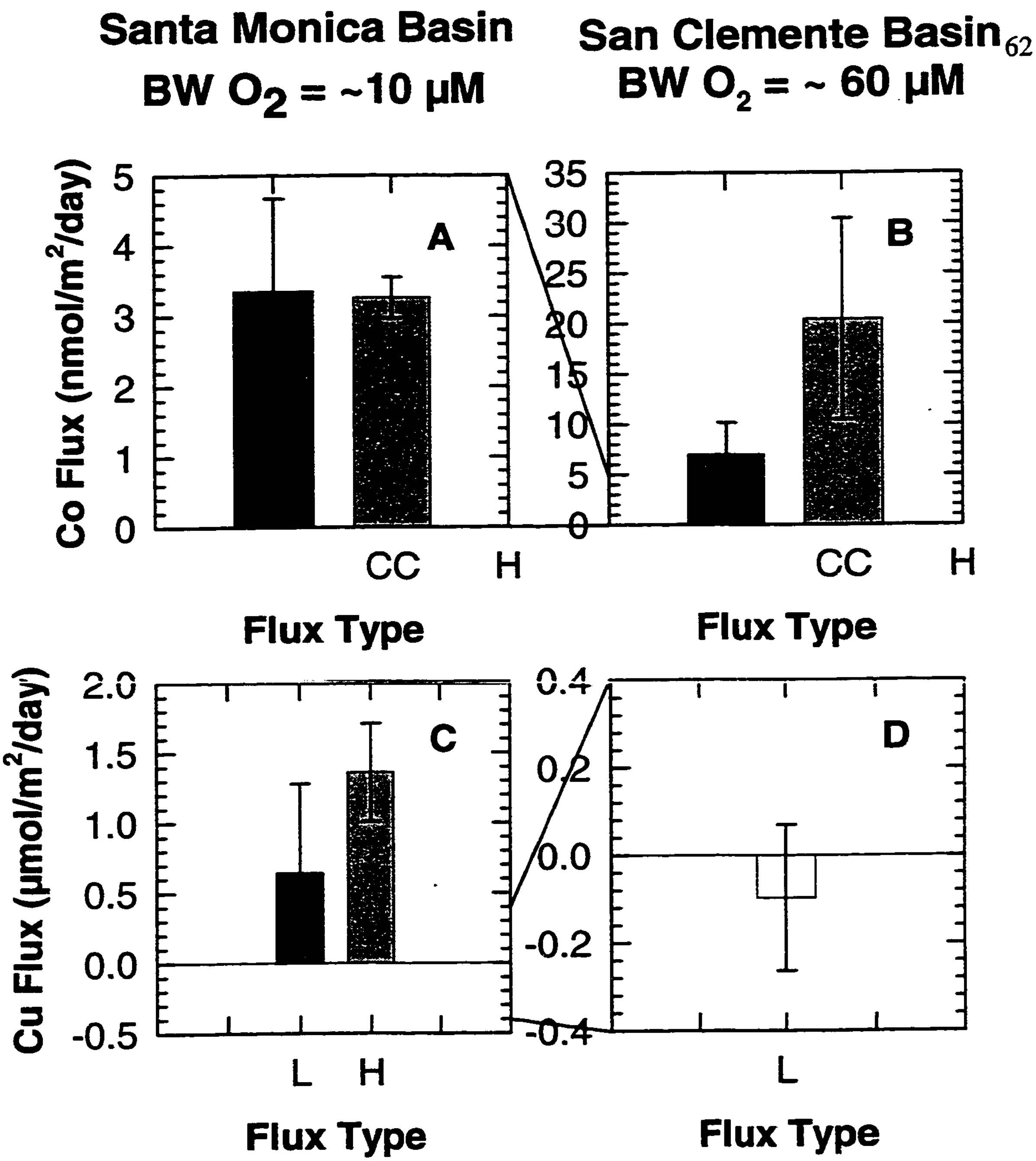

Figure 22. A comparison of flux estimates of Co (A, B) and Cu (C, D) in Santa Monica (SM) and San Clemente (SCl) Basins. Flux types are as in Figure 21. The standard error of multiple year averages or the standard error of the analytical estimate for a single year is shown. Co lander flux is not shown due to sample contamination (Table 6). Copper values are not available from the hydrocasts in the SCl basin or the centrifuged cores in either basin. Only one year of lander data was available for the Cu fluxes. Co fluxes are averages of mult-year data for CC and H estimates in the SM basin, while only one year was available for the H estimate in the SCl basin.

Biogeochemical Processes Effecting Flux

Temporal Variability

Temporal variability in metal flux can account for some of the differences observed. This can be seen in basins where there are several years of data. In this respect, Santa Monica Basin is the best studied (Figure 23). This basin has low bottom water oxygen (Table 2) with no macro-fauna present (Berelson, 1985) and temporal variations due to bio-irrigation can be ignored. Even so, all three estimates of flux show that there is significant temporal variation between years. Lander and centrifuged core flux estimates in 1995 are ~2.5 times the 1994 estimates. Hydrocast flux estimates differ in that the 1994 values, are ~2.9 times the 1995 values and ~4.6 times those measured in 1990. The elevated hydrocast flux estimate could be due to a flushing period occurring during 1994 and 1995 as described by Berelson (1991), to resuspension of sediments during hydrocast sampling, or that the 1994 hydrocast samples were not filtered before analysis. Since the 1995 hydrocast estimate is only moderately higher (~1.6 times) then the 1990 estimate, resuspension of sediments or particles in the unfiltered samples are the most likely causes of the elevated 1994 estimate.

The temporal variability in Mn flux in Santa Monica Basin demonstrates that these systems are not at a steady state. Multiple measurements of flux over time are required to accurately estimate metal fluxes. Differences between years can range from two (lander) to five times (hydrocast). Care must be taken when interpreting the results if relying only on a limited data set.

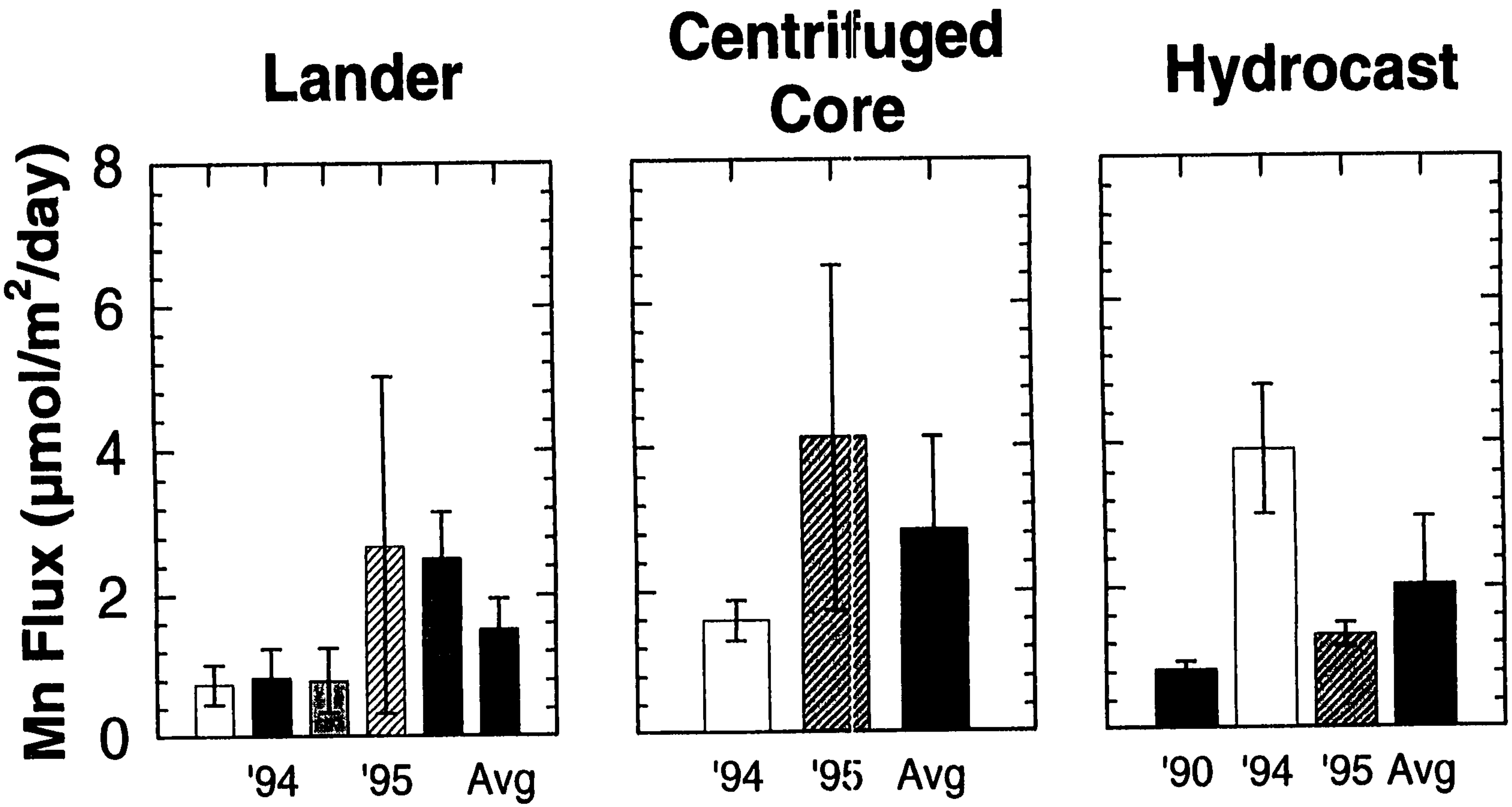

Figure 23. The temporal variation that can occur in a lander, centrifuged core, and hydrocast estimated flux is shown from the Santa Monica Basin (Figure 1, Table 1). Data from cruises conducted in 1990, 1994, and 1995 are shown along with the multiple year average ± standard error. The individual year's standard errors result from experimental error, including regression line uncertainty. The average lander calculated flux contains the data from the 3 individual chambers of the 1994 lander and the 2 chambers that functioned in the 1995 lander.

Choice of Pore Water Gradient

The choice of the correct pore water gradient for flux calculations can present difficulties with trace metals because of the sharp changes in their profiles (Froelich and others, 1979; Shaw and others, 1990). As an example, consider the pore water Mn profile in the San Clemente Basin, Teflon '94 data (Figure 7). Examination of the surface sediments reveals a sharp change in Mn concentrations that occurs after the first two sediment samples (Figure 24). Either the first 3 points at 0, 0.25, and 0.75 cm, or the first 5 points can be chosen to estimate the gradient. The 3-point gradient agrees best with the independent lander and hydrocast estimated fluxes. Apparently there is a sharp increase in the Mn gradient beyond the first 1 cm of sediment. Oxygen must penetrate into the sediment and oxidize Mn^{2+} in the upper 1 cm, which reduces the concentration gradient at the sediment-water interface. However, few investigators would rely on three points without corroborating evidence. As a result, metal flux estimates based on pore water gradients can have a large bias.

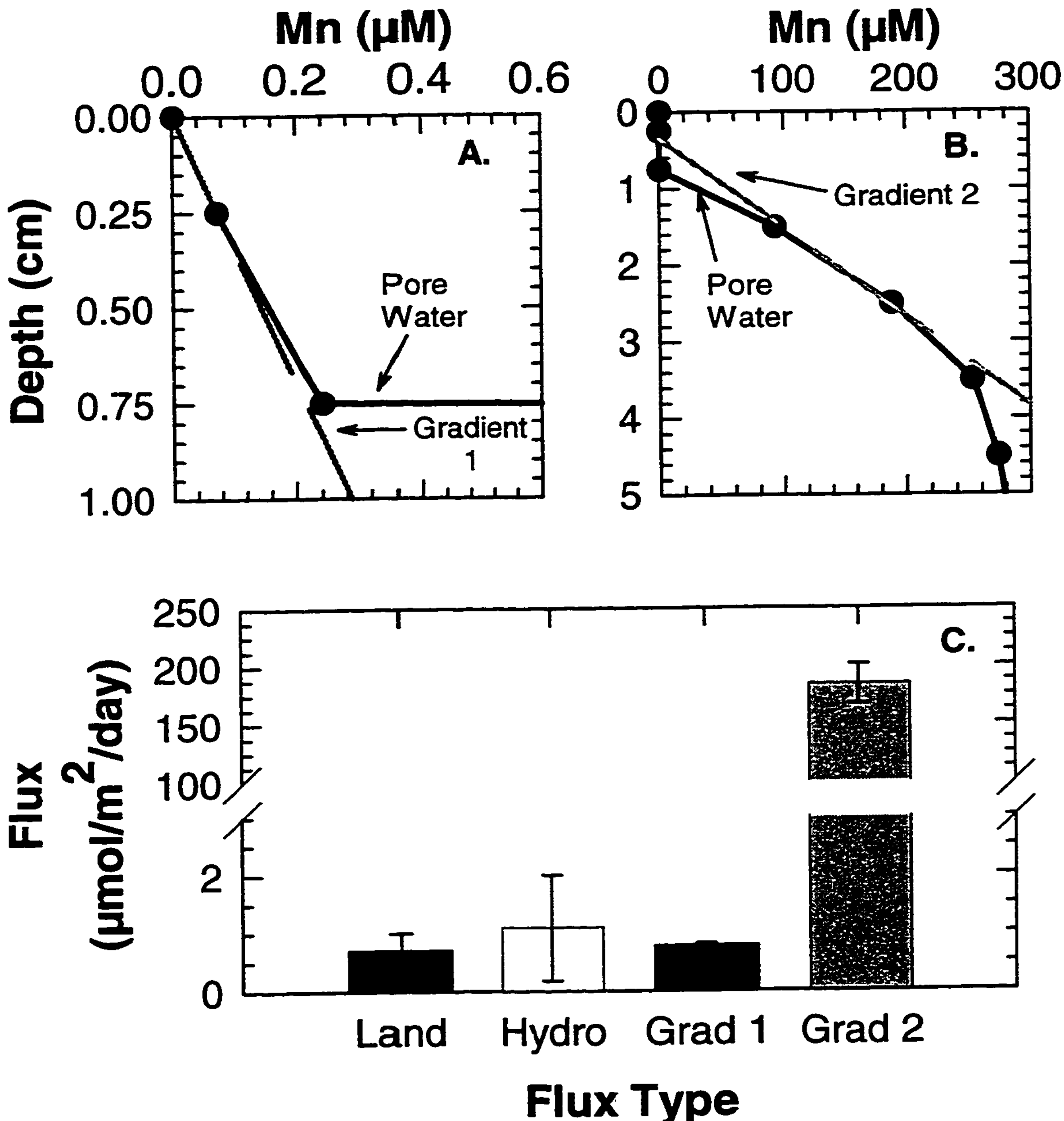

Figure 24. Pore water flux estimate resulting from the choice of two different gradients to use in the calculations. Looking at the surface sediments (A, B) of the Mn pore water profile from San Clemente Basin (Figure 7), during the Teflon '94 cruise (Figure 1, Table 1), two gradients' one of two points (A) and one of five points (B) are possible. The flux estimates from the lander (Land), the hydrocast (Hydro), the 3-point gradient (Grad 1), and the 5-point gradient (Grad 2) at the same station (C).

Changes in Redox Potential

The depths in the sediment column that trace metals are remobilized are governed in part by the penetration depth of oxygen into the redox reactive sediments. Under low bottom water oxygen conditions oxygen is depleted at the sediment-water interface. This leads to large redox gradients in a few millimeters distance. The compression of redox zones in low bottom water oxygen environments (Shaw and others, 1990) creates a very large gradient and leads to a high metal flux at the sediment-water interface. However, if the metal undergoes rapid changes in oxidation state, then little of it may actually escape the sediments. For example, Fe (III) is poorly soluble in the presence of O_2 (Millero and others, 1987), while Fe(II) is much more soluble under reducing conditions. Fe(II) can oxidize to Fe(III) quite rapidly (Millero and others1987) which will trap the Fe within the sediments.

The low O_2 environment of Santa Monica Basin is an area where Fe oxidation states may change rapidly at the sediment-water interface. The Fe concentrations in water above the sediment-water interface (23.1 nM) are much lower than in the pore waters (88-142 μM), therefore the gradients in the pore waters are large (Figure 25). The Fe flux predicted from this gradient is much larger than observed with the benthic flux chamber (Figure 25). The expected flux based on the pore water gradient is not realized because iron is trapped upon oxidation within the upper few millimeters of the sediments. The sampling interval fails to resolve the small gradients over which redox transitions occur. Thus these pore water estimates of flux results are high. In turn, the benthic lander based flux estimate is larger than that based on accumulation of Fe in the water column (Figure 25). Evidently, Fe oxidation and scavenging are continuing in the water column above the lander, but below the depths resolved by the hydrocasts. In this case the best flux estimate may be that based on the water column accumulation rate of Fe.

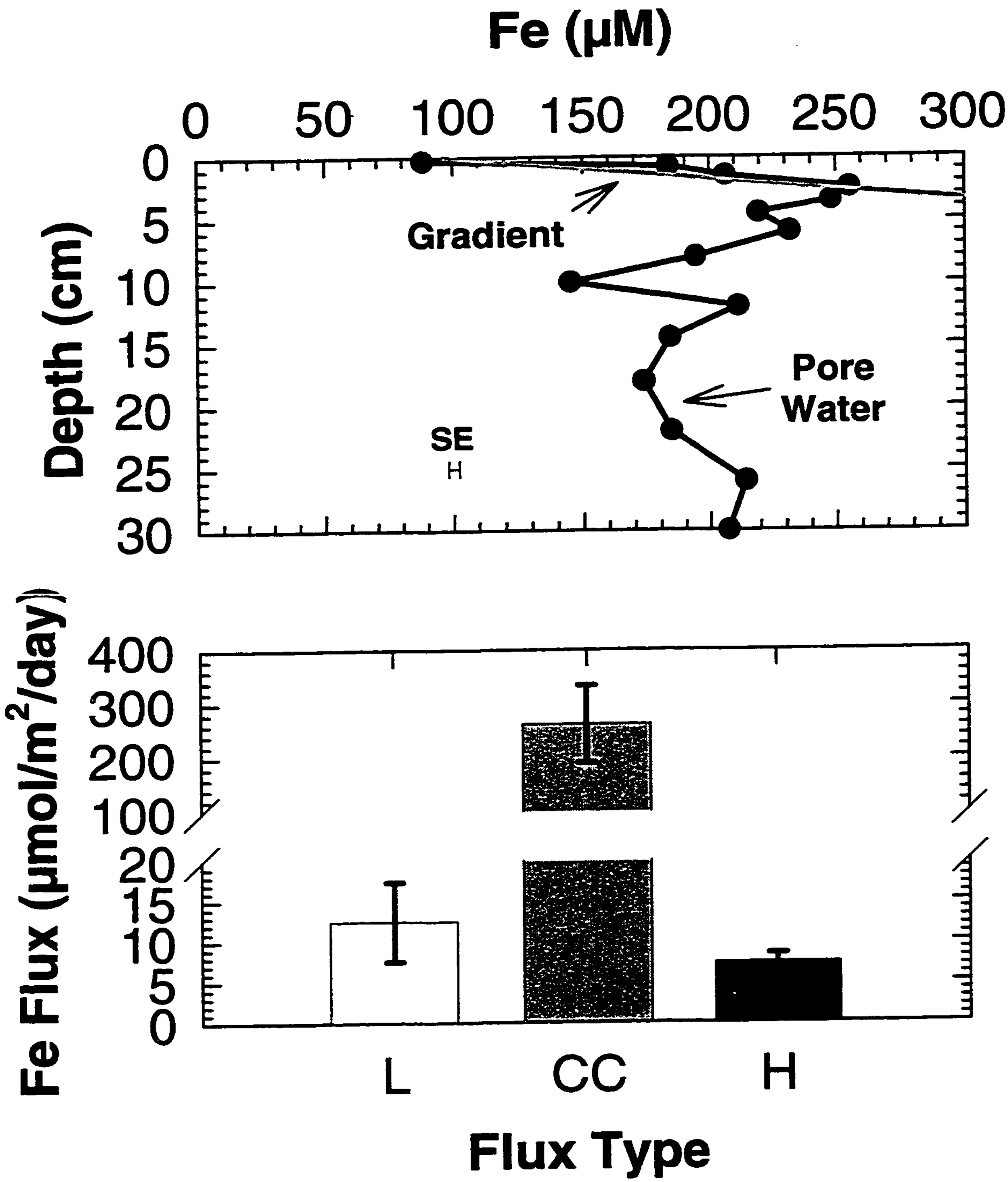

Figure 25. The effect of changes in redox potential due to low bottom water O_2 concentrations in the Santa Monica Basin, Teflon '94 pore water profile of Fe (top panel). The top panel shows the gradient of the surface pore water values. The fluxes measured from the lander (L), calculated from the centrifuged core (CC), and the hydrocast (H) are shown in the bottom panel.

Bio-irrigation Effects

The solute transport model based on the gradient in pore water concentrations of metals is premised on the assumption that molcular diffusion accounts for all the transport of solutes (Berner, 1980). The model does not take into account the advection of pore waters due to bio-irrigation of sediments nor does it account for chemical reactions in the sediments. Advection will increase the flux and fluxes based on pore water gradients will underestimate the correct value (Archer and Devol, 1992; Berner, 1980). On the other hand, the lander integrates the flux due to both diffusion and bio-irrigation and provides a more realistic estimate of flux in sediments of high biological activity. Monterey Bay is known to be highly bio-irrigated (Berelson, 1996 personal communication) and this effect should be apparent in a comparison of the lander and centrifuged core derived fluxes (Figure 26). The lander calculated fluxes of Mn, Fe, and Cu are 15 to 85 times greater than the centrifuged core fluxes. It is apparent that bioirrigation plays a major role in controlling metal flux from shallow sediments where there is a well developed infaunal population. Bioirrigation has even been found to have a significant effect across the continental shelf to a depth of 200 - 600 m (Archer and Devol, 1992; Devol and Christensen, 1993; Johnson and others, 1992).

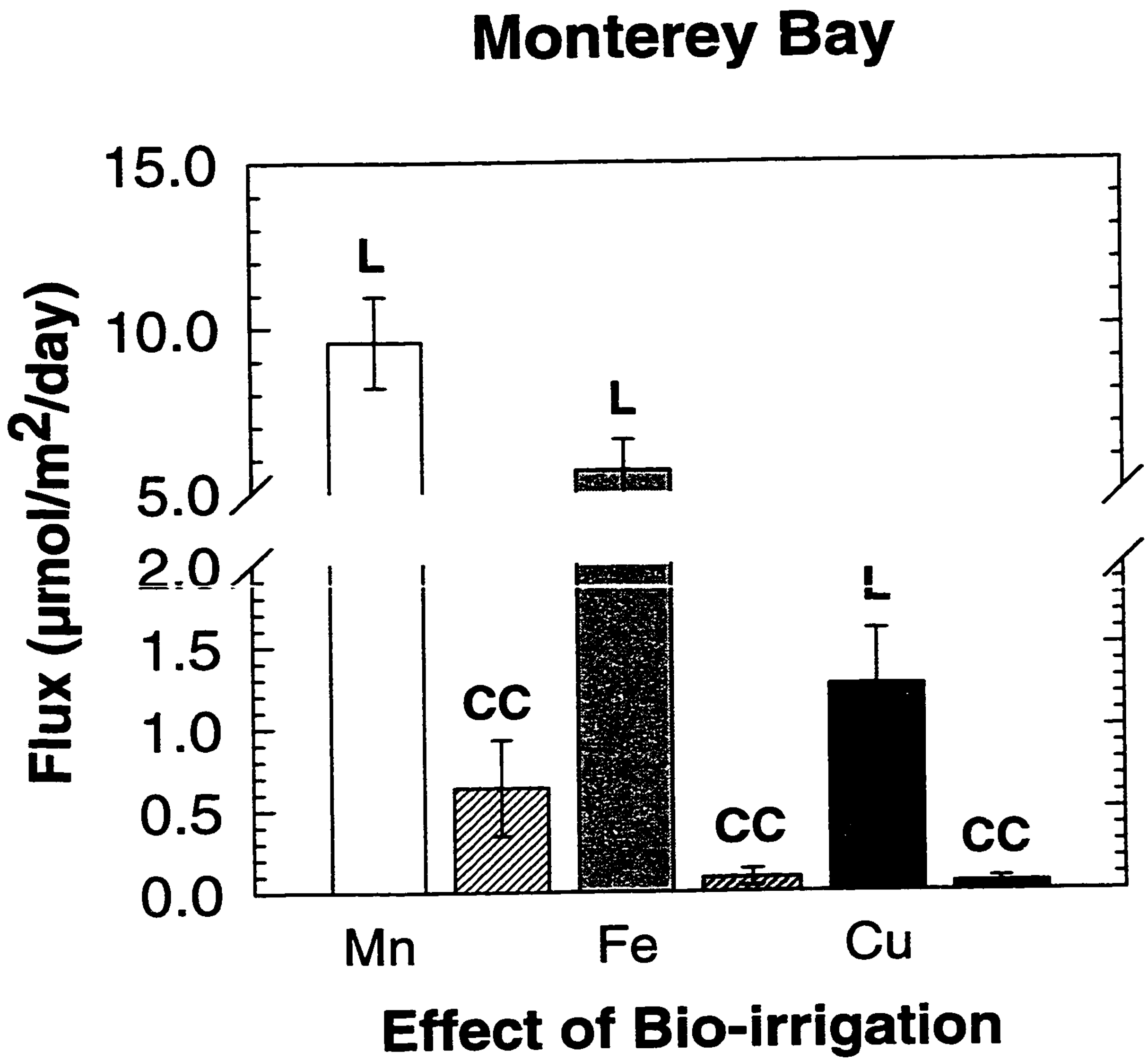

Figure 26. The effect of bio-irrigation on pore water estimated fluxes (CC) of Mn, Fe, and Cu are compared with the lander measured fluxes (L) from the Monterey Bay station (Figure 2, Table 1).

Conclusions

Estimates of flux from landers and modeled hydrocast or pore water data generally agree (Figures 21 and 22). Where they do not agree, differences can be attributed to: temporal variability in the environment (Figure 23), inability to resolve the correct pore water gradients (Figure 24), precipitation reactions occuring within the first few millimeters of sediment (Figure 25), and increased flux due to bio-irrigation (Figure 26).

So what is the most useful method of estimating flux? Pore water derived fluxes, underestimate the actual flux if there is high bioirrigation (Figure 26). They can also overestimate the flux of redox reactive metals if the redox gradient is near the sediment-water interface as occurs in low bottom water O_2 conditions (Figures 24 and 25). Flux estimates based on water column profiles can only be calculated in basins where horizontal advection is minimized. Therefore, benthic flux chambers (landers) provide the most useful and direct measurement of flux over a variety of sediment environments where the above-mentioned processes may occur.

Literature Cited

Alongi, D. M.; Boyle, S. G.; Tirendi, F.; Payn, C.. 1996. Composition and behaviour of trace metals in post-oxic sediments of the Gulf of Papua, Papua New Guinea. Estuarine, Coastal, and Shelf Science 42: 197-211.

Archer, D.; Devol, A. 1992. Benthic oxygen fluxes on the Washington shelf and slope: a comparison of in situ microelectrode and chamber flux measurements. Limnology and Oceangraphy 37(3): 614-629.

Balzer, W. 1982. On the distribution of iron and manganese at the sediment/water interface: thermodynamic versus kinetic control. Geochimica et Cosmochimica Acta 46: 1153-1161.

Barnet, PRO; Watson, J.; Conelly, D.. 1984. A multiple corer for taking virtually undisturbed samples from shelf, bathyal, and abyssal sediments. Oceanology Acta, 4:399-408.

Bender, M.; Jahnke, R.; Weiss, R. 1989. Organic carbon oxidation and benthic nitrogen and silica dynamics in San Clemente Basin, a continental borderland site. Geochimica et Cosmochimica Acta 53: 685-697.

Berelson, W. M. 1985. Studies of water column mixing and benthic exchange of nutrients, carbon and radon in the southern California borderland. Ph. D. Dissertation, University of Southern California, 219 p.

Berelson, W. M. 1991. The flushing of two deep-sea basins, southern California borderland. Limnology and Oceanography 36(6): 1150-1166.

Berelson, W. M.; Hammond, D. E. 1986. The calibration of a new free-vehicle benthic flux chamber for use in the deep sea. Deep-Sea Research 33(10):1436-1454.

Berelson, W. M.; Hammond, M. R.; Buchholtz, D. E.; Santschi, P. H. 1987a. Radon fluxes measured with the MANOP Bottom Lander. Deep-Sea Research 34(7): 1209-1228.

Berelson, W. M.; Hammond, D. E.; Giordani, P. 1989. Effect of sea-floor disturbance on benthic flux measurements in the continental margin off Southern California (Catalina Basin). Giornale di Geologia 51/2: 143-150.

Berelson, W. M.; Hammond, D. E.; Johnson, K. S. 1987b. Benthic fluxes and the cycling of biogenic silica and carbon in two southern California borderland basins. Geochimica et Cosmochimica Acta, 51: 1345-1363.

Berelson, W. M.; Hammond, D. E.; O'Neill, D.; Xu, X. M.; Chin, C.; Zukin, J. 1990. Benthic fluxes and pore water studies from sediments of the central equatorial north Pacific: nutrient diagensis. Geochimica et Cosmochimica Acta 54: 3001-3012.

Berelson, W. M.; McManus, J.; Coale, K.; Johnson, K. S.; Kilgore, T.; Burdige, D.; Pilskaln, C. 1996. Biogenic matter diagenesis on the sea floor: a comparison between two continental margin transects. Journal of Marine Research 54: 731-762.

Berner, R. A. 1980. Early Diagenesis. A Theoretical Approach. Princeton, Princeton University Press. 241 p.

Brand, L. E.; Sunda, W. G.; Guillard, R. R. L. 1983. Limitation of marine phyoplankton reproductive rates by zinc, manganese, and iron. Limnology and Oceanography 28(6): 1182-1198.

Bruland, K. W. 1980. Oceanographic distribution of cadmium, zinc, nickel, and copper in the North Pacific. Earth and Planetary Science Letters 47: 176-198.

Bruland, K. W. 1983. Trace Elements in Seawater. Riley, J. P.; Chester,R. eds. In: Chemical Oceanography, Volume 8. London, Academic Press. 398 p.

Carignan, R.; Rapin, F.; Tessier, A. 1985. Sediment porewater sampling for metal analysis: A comparison of techniques. Geochimica et Cosmochimica Acta 49:2493-2497.

Chapin, T. P. 1990. Determination of manganese in seawater by flow injection analysis with Chemiluminescence Detection. Master's Thesis, San Jose State University 71 p.

Chapin, T. P.; Johnson, K. S.; Coale, K. H. 1991. Rapid determination of manganese in seawater by flow injection analysis with chemiluminescence detection. Analytica Chimica Acta, 249: 469-478.

Chester, R. 1990. Marine Geochemistry. London, Unwin Hyman Ltd. 698 p.

Christensen, C. J.; Gorsline, D. S.; Hammond, D. E.; Lund; S. P. 1994. Non-annual lamination and expansion of anoxic basin-floor condition in Santa Monica Basin, California Borderland, over the past four centuries. Marine Geology 116: 399-418.

Christensen, J. P.; Smethie Jr., W. M.; Devol, A. H. 1987. Benthic nutrient regeneration and denitrification on the Washington continental shelf. Deep-Sea Research 34(5/6): 1027-1047.

Coale, K. H.; Bruland, K. W. 1990. Spatial and temporal variability in copper complexation in the North Pacific. Deep-Sea Research 37(2):317-336.

Coale, K. H.; Johnson, K. S.; Chapin, T.; Stout, P. M. 1990. The constrasting behavior of Mn and Co in seawater from the southern California borderlands and the Equatorial Pacific. EOS, Transactions, American Geophysical Union. 904 p.

Coale, K. H.; Johnson, K. S.; Fitzwater, S. E.; Gordon, R. M.; Tanner, S.; Chavez, F. P.; Ferioli, L.; Sakamoto, C.; Rogers, P.; Millero, F.; Steinberg, P.; Nightingale, P.; Cooper, D.; Cochlan, W. P.; Landry, M. R.; Constantinou, J.; Rollwagen, G.; Trasvina, A.; Kudela, R. 1996. A massive phytoplankton bloom induced by an ecosystem-scale iron fertilization experiment in the equatorial Pacific Ocean. Nature 383:495-501.

Coale, K. H.; Johnson, K. S.; Stout, P. M.; Sakamoto, C. M. 1992. Determination of copper in sea water using a flow-injection method with chemiluminescence detection. Analytica Chimica Acta, 266(2): 345-351.

Devol, A. H. 1991. Direct measurement of nitrogen gas fluxes from continental shelf sediments. Nature 349: 319-321.

Devol, A. H.; Christensen, J. P. 1993. Benthic fluxes and nitrogen cycling in sediments of the continental margin of the eastern North Pacific. Journal of Marine Research 51: 345-372.

Elderfield, H.; McCaffrey, R. J.; Luedtke, N.; Bender, M.; Truesdale, V. W. 1981. Chemical diagenesis in Narragansett Bay sediments. American Journal of Science 281: 1021-1055.

Emerson, S.; Jahnke, R.; Heggie, D. 1984. Sediment-water exchange in shallow water estuarine sediments. Journal of Marine Research 42: 709-730.

Emery, K. O. 1960. The Sea Off Southern California. New York, John Wiley & Sons, Inc. 365 p.

Fairey, R. 1992. Sampling and Analysis of Trace Metals in Sediment Interstitial Waters. Master's Thesis, San Jose State University. 99 p.

Fanning, K. A.; Pilson, M. E. Q. 1971. Interstitial silica and pH in marine sediments: some effects of sampling procedures. Science 173: 1228-1230.

Flegal, A. R.; Patterson, C. C. 1983. Vertical concentration profiles of lead in the Central Pacific at 15°N and 20°S. Earth and Planetary Science Letters 4: 19-32.

Friederich, G.; Codispoti, L.; Sakamoto, C. 1991. An easy to construct, automated Winkler titration system. MBARI Technical Report 91-6. Monterey Bay Aquarium Research Institute, Moss Landing, CA

Froelich, P. N.; Klinkhammer, G. P.; Bender, M. L.; Luedtke, N. A.; Heath, G. R.; Cullen, D.; Dauphin, P.; Hammond, D.; Hartman, B.; Maynard, V. 1979. Early oxidation of organic matter in pelagic sediments of the eastern equatorial Atlantic: suboxic diagenesis. Geochimica et Cosmochimica Acta 43: 1075-1090.

Gorsline, D. S. 1992. The geological setting of Santa Monica and San Pedro Basins, California Continental Borderland. Progress in Oceanography 30: 1-36.

Hales, B.; Emerson, S.; Archer, D. 1994. Respiration and dissolution in the sediments of the western North Atlantic: estimates from models of in situ microelectrode measurements of porewater oxygen and pH. Deep-Sea Research 41(4): 695-719.

Hammond, D. E.; Marton, R. A.; Berelson, W. M.; Ku, T. 1990. Radium 228 distribution and mixing in San Nicolas and San Pedro Basins, Southern California Borderland. Journal of Geophysical Research 95(C3): 3321-3335.

Heggie, D.; Klinkhammer, G.; Cullen, D. 1987. Manganese and copper fluxes from continental margin sediments. Geochimica et Cosmoshimica Acta 51: 1059-1070.

Heggie, D.; Lewis, T. 1984. Cobalt in pore waters in marine sediment. Nature 311: 453-455.

Hong, J.; Calmano, W.; Forstner, U. 1995. Interstitial Waters. Salbu, B.; Steinnes, E. eds. In: Trace Elements in Natural Waters. Boca Raton, CRC Press. 301 p.

Hunt, C. D. 1983. Variability in the benthic Mn flux in coastal marine ecosystems resulting from temperature and primary production. Limnology and Oceanography 28(5): 913-923.

Ingall, E.; Jahnke, R. 1994. Evidence for enhanced phosphorus regeneration from marine sediments overlain by oxygen depleted waters. Geochimica et Cosmochimica Acta 58(11): 2571-2575.

Jahnke, R. A. 1988. A simple, reliable, and inexpensive pore- water sampler. Limnology and Oceanography 33(3): 483-487.

Jahnke, R. A. 1990. Early diagensis and recycling of biogenic debris at the seafloor, Santa Monica Basin, California. Journal of Marine Research 48: 413-436.

Jahnke, R. A.; Reimers, C. E.; Craven, D. B. 1990. Intensification of recycling of organic matter at the sea floor near ocean margins. Nature 348: 50-54.

Johnson, K. S.; Berelson, W. M.; Coale, K. H.; Coley, T. L.; Elrod, V. A.; Fairey, W. R.; Iams, H. D.; Kilgore, T. E.; Nowicki, J. L. 1992. Manganese flux from continental margin sediments in a transect through the oxygen minimum. Science 257: 1242- 1245.

Johnson, K. S.; Coale, K. H.; Berelson, W. M.; Gordon, R. M. 1996. On the formation of the manganese maximum in the oxygen minimum. Geochimica et Cosmochimica Acta 60(8): 1291-1299.

Johnson, K. S.; Stout, P. M.; Berelson, W. M.; Sakamoto- Arnold, C. M. 1988. Cobalt and copper distributions in the waters of Santa Monica basin, California. Nature 332(6164): 527-530.

Klinkhammer, G. P. 1980. Early diagenesis in sediments from the eastern equatorial Pacific. II. Pore water metal results. Earth and Planetary Science Letters 49: 81-101

Klinkhammer, G.; Heggie, D. T.; Graham, D. W. 1982. Metal diagenesis in oxic marine sediments. Earth and Planetary Science Letters 61: 211-219.

Klump, J. V.; Martens, C. S. 1989. The seasonality of nutrient regeneration in an organic-rich metal sediment: kinetic modeling of changing pore-water nutrient and sulfate distributions. Limnology and Oceanography 34(3): 559-577.

Kriukov, P. A.; Manheim, F. T. 1982. Extraction and investigative techniques for study of interstitial waters of unconsolidated sediments: a review. In: The Dynamic Environment of the Ocean Floor. Fanning, K. A.; Manheim, F. T. eds. Lexington, MA, Lexington Books. 502 p.

Landing, W. M.; Bruland, K. W. 1980. Manganese in the North Pacific. Earth and Planetary Science Letters 49: 45-56.

Landing, W. M.; Bruland, K. W. 1987. The constrasting biogeochemistry or iron and manganese in the Pacific Ocean. Geochimica et Cosmochimica Acta 51: 29-43.

Lapp, B.; Balzer, W. 1993. Early diagensis of trace metals used as an indicator of past productivity changes in coastal sediments. Geochimica et Cosmochimica Acta 57: 4639-4652.

Leslie, B. W.; Hammond, D. E.; Berelson, W. M.; Lund, S. P. 1990. Diagenesis in anoxic sediments from the California continental borderland and its influence on iron, sulfur, and magnetite behavior. Journal of Geophysical Research 95(B4): 4453-4470.

Li, Y.; Gregory, S. 1974. Diffusion of ions in sea water and in deep-sea sediments. Geochimica et Cosmochimica Acta 38: 703-714.

Lyons, W. B.; Gaudette, H. E.; Smith, G. M. 1979. Pore water sampling in anoxic carbonate sediments: oxidation aftefacts. Nature 277: 48-49.

Martin, J. H.; Gordon, R. M. 1988. Northeast Pacific iron distribution in relation to phytoplankton productivity. Deep-Sea Research 35(2): 177-196.

Martin, H. H.; Knauer, G. A.; Broenkow, W. W. 1985. VERTEX: the lateral transport of manganese in the northeast Pacific. Deep-Sea Research 32(11): 1405-1427.

MBARI. 1997. Bathymetric Maps: Interactive Data Archive. Monterey Bay Aquarium Research Institute, world wide web pages. WWW address: http://www.mbari.org/%7ejoly/IAD/mbay.cont.html.

McManus, J.; Berelson, W. M.; Klinkhammer, G. P.; Kilgore, T. E.; Hammond, D. E. 1994. Remobilization of barium in continental margin sediments. Geochimica et Cosmochimica Acta 58(22): 4899-4907.

Millero, F.; Sotolongo, J. S.; Izaguirre; M. 1987. The oxidation kinetics of Fe(II) in seawater. Geochimica et Cosmochimica Acta 51: 793-801.

Mudroch, A.; Azcue, J. M. 1995. Manual of Aquatic Sediment Sampling. Boca Raton, FL, CRC Press Inc. 219 p.

Murray, J. W. 1987. Mechanisms controlling distribution of trace elements in oceans and lakes. In: Sources and Fates of Aquatic Pollutants. Hites, R. A.; Eisenreich, S. J. eds. Washington, D. C., American Chemical Society. 558 p.

Murray, J. W.; Dillard, J. G. 1979. The oxidation of cobalt(II) adsorbed on manganese dioxide. Geochimica et Cosmochimica Acta 43:781

Obata, H.; Karatani, H.; Matsui, M.; Nakayma E. 1997. Fundamental studies for chemical speciation of iron in seawater with an improved analytical method. Marine Chemistry 56:97-106.

Obata, H.; Karatani, H.; Nakayma, E. 1993. Automated determination of iron in seawater by chelating resin concentration and chemiluminescence detection. Analytical Chemistry 65:1524-1528.

Orians, J. J.; Bruland, K. W. 1986. The biogeochemistry of aluminum in the Pacific Ocean. Earth and Planetary Science Letters 78:397-410.

Orians, J. J.; Bruland, K. W. 1988. The marine geochemistry of dissolved gallium: A comparison with dissolved aluminum. Geochimica et Cosmochimica Acta 52:2955-2962.

Pilskaln, C. H.; Paduan, J. B.; Chavez, F. P.; Anderson, R. Y.; Berelson, W. M. 1996. Carbon export and regeneration in the coastal upwelling system of Monterey Bay, central California. Journal of Marine Research 54:1149-1178.

Reimers, C. E.; Jahnke, R. A.; McCorkle, D. C. 1992. Carbon fluxes and burial rates over the continental slope and rise off central California with implications for the global carbon cycle. Global Biogeochemical Cycles 6(2): 199-224.

Reimers, C. E.; Ruttenberg, K. C.; Canfield, D. E.; Christiansen, M. B.; Martin, J. B. 1996. Porewater pH and authigenic phases formed in the uppermost sediments of the Santa Barbara Basin. Geochimica Cosomochimica Acta 60(21): 4037-4057.

Rutgers van der Loeff, M. M.; Anderson, L. G.; Hall, P. O. J.; Iverfeldt, A.; Josefson, A. B.; Sundby, B.; Westerlund, S. F. G. 1984. The asphyxiation technique: an approach to distinguishing between molecular diffusion and biologically mediated transport at the sediment-water interface. Limnology and Oceanography 29(4): 675-686.

Sakamoto-Arnold, C. M.; Johnson, K. S. 1987. Determination of picomolar levels of cobalt in seawater by flow injection analysis with chemiluminescence detection. Analytical Chemistry, 59: 1789-1794.

Santschi, P. H.; Anderson, R. F.; Fleisher, M. Q.; Bowles, W. 1991. Measurements of diffusive sublayer thicknesses in the ocean by alabaster dissolution, and their implication for the measurements of benthic fluxes. Journal of Geophysical Research 96(C6): 10641-10657.

Sawlan, J. J.; Murray, J. W. 1983. Trace metal remobilization in the interstitial water of red clay and hemipelagic marine sediments. Earth and Planetary Science Letters 64: 213-230.

Schults, D. W.; Ferraro, S. P.; Smith, L. M.; Roberts, F. A.; Poindexter, C. K. 1992. A comparison of methods for collecting interstitial water for trace organic compounds and metals analyses. Water Resources 26(7): 989-995.

Shaw, T. J.; Gieskes, J. M.; Jahnke, R. A. 1990. Early diagenesis in differing depositional environments: the response of transition metals in pore water. Geochimica et Cosmochimica Acta 54: 1233-1246.

Smith Jr., K. L.; Carlucci, A. F.; Jahnke, R. A.; Craven, D. B. 1987. Organic carbon mineralization in the Santa Catalina Basin: benthic boundary layer metabolism. Deep-Sea Research 34(2): 185-211.

Sugai, S. F. 1987. Temporal changes in the sediment geochemistry of two southeast Alaskan fjords. Deep-Sea Research 34(5/6): 913-925.

Sunda, W. G.; Huntsman, S. A. 1983. Effect of competitive interactions between manganese and copper on cellular manganese and growth in estuarine and oceanic species of the diatom Thalassiosira. Limnology and Oceanography 28(5): 924-934.

Sunda, W. G.; Swift, D. G.; Huntsman, S. A. 1991. Low iron requirement for growth in oceanic phytoplankton. Nature 351: 55-57.

Sundby, B.; Anderson, L. G.; Hall, P. O. J.; Iverfeldt, A.; van der Loeff, M. M. R.; Westerlund, S. F. G. 1986. The effect of oxygen on release and uptake of cobalt, manganese, iron, and phosphate at the sediment-water interface. Geochimica et Cosmochimica Acta 50: 1281-1288.

Teasdale, P. R.; Batley, G. E.; Apte, S. C.; Webster, I. T. 1995. Pore water sampling with sediment peepers. Trends in Analytical Chemistry 14(6): 250-256.

Thamdrup, B.; Canfield, D. E. 1996. Pathways of carbon oxidation in continental margin sediments off central Chile. Limnology and Oceanography 41(8): 1629-1650.

Thamdrup, B.; Glud, R. N.; Hansen, J. W. 1994. Manganese oxidation and in situ manganese fluxes from a coastal sediment. Geochimica et Cosmochimica Acta 58(11): 2563-2570.

Townsend, T.; Berelson, W.; Coale, K. 1996. Utilization of benthic chambers and chemical tracers for investigation of bio-irrigation in marine sediments. ASLO '97 Santa Fe, New Mexico.

Uematsu, M.; Tsunogai, S. 1983. Recycling of manganese in the coastal sea, Funka Bay, Japan. Marine Chemistry 13(1):1-14.

Ullman, W. J.; Aller, R. C. 1981. Diffusion coefficients in nearshore marine sediments. Limnology and Oceanography 27(3): 552-556.

von Langen, P. J.; Johnson, K. S.; Coale, K. H.; Elrod, V. A. 1997. Oxidation kinetics of manganese (II) in seawater at nanomolar concentrations. Geochimica et Cosmochimica Acta 61(23): 4945-4954.

Westerlund, S. F. G.; Anderson, L. G.; Hall, P. O. J.; Iverfeldt, A.; Rutgers van der Loeff, M. M.; Sundby, B. 1986. Benthic fluxes of cadmium, copper, nickel, zinc, lead in the coastal environment. Geochimica et Cosmochimica Acta 50: 1289-1296.

Widerlund, A. 1996. Early diagenetic remobilization of copper in near-shore marine sediments: a quantitative pore-water model. Marine Chemistry 54: 41-53.

Zamzow, H. A. 1997. Determination of Cu complexation using flow injection analysis. Master's Thesis, San Jose State University.

Appendix 1. A. Hydrocast data and flux estimates. B. Centrifuged core pore water data and flux estimates. C. Lander data and flux estimates.

Appendix 1a. Hydrocast data and flux estimates. Cruise names and station abbreviations are as in Table 1, except for the previously unpublished data from a 1990 cruise to Santa Monica Basin - PS90. Units for the data are given. Flux is expressed as $\mu mol/m^2/day$ for Mn, Fe and Cu and as $nmol/m^2/day$ for Co. By convention a positive flux is taken as coming out of sediments. Dashes indicate stations where a flux measurement could not be arrived at either due to sample contamination or suspect data.

Cruise	Station	z (m)	O2 (μM)	Mn (nM)	1SD (nM)	Co (pM)	1SD (pM)	Fe (nM)	1SD (nM)	Cu (nM)	1SD (nM)
PS 90	SM	2		4.27							
		50		2.32							
		100		1.75							
		200		1.45							
		400		1.83							
		601		3.08							
		750		5.30							
		800		5.82							
		825		6.80							
		850		7.32							
		875		8.11							
		895		8.26							
	Flux			0.84	0.12						

Cruise	Station	z (m)	O2 (μM)	Mn (nM)	1SD (nM)	Co (pM)	1SD (pM)	Fe (nM)	1SD (nM)	Cu (nM)	1SD (nM)
Teflon '94	TB	0	254.3			133.1	14.4	3.43	0.02	3.61	0.21
		10	253.7			115.6	10.5	2.23	0.09	2.88	0.49
		20	253.3			122.9	4.4	2.07	0.23	3.02	0.43
		40	254.2			117.3	16.5	2.39	0.38	3.05	0.40
		60	254.2			117.1	4.6	2.84	0.30	2.78	0.39
		80	242.4			118.7	5.0	3.13	0.56	2.67	0.29
		100	216.4			118.7	3.6	3.04	0.24	2.73	0.21
		250	109.0			115.7	2.1	4.29	0.75	3.49	0.41
		500	20.7			112.7	5.1	4.12	0.38	3.65	0.40
		750	15.6			86.8	3.1	3.74	0.91	3.84	0.10
		1000	22.6			90.9	10.7	5.68	0.15	4.03	0.00
		1100	26.6			94.6	8.6	6.07	0.26	3.92	0.39
		1100	27.2			100.3	10.5	7.21	0.16	4.10	0.33
		1125	24.2			101.6	16.6	6.62	0.27	4.05	0.37
		1175	24.1			105.9	2.4	7.24	0.48	3.64	
		1200	25.3			97.7	8.4	7.19	0.58	4.05	0.15
		1250	24.5			93.6	7.3	7.86	1.25	4.42	0.37
		1300	24.8			95.6	0.9	7.56	0.58	4.10	0.10
		1350	24.6			100.1	6.6	7.12	0.25	3.82	0.75
		1400	24.0			111.0	9.4	8.21	0.36	4.30	0.22
		1450	24.9			104.8	4.2	8.08	0.03	3.79	0.32
		1475	25.5			109.8	6.2	9.99	0.32	4.11	0.15
		1503	26.6			123.4	2.0	9.64	0.95	4.96	0.72
	Flux			---	---	4.86	1.92	0.67	0.20	0.13	0.10

Cruise	Station	z (m)	O2 (µM)	Mn (nM)	1SD (nM)	Co (pM)	1SD (pM)	Fe (nM)	1SD (nM)	Cu (nM)	1SD (nM)
Teflon '94	PE	0	246.7	1.02	0.07	116.6	4.1	3.40	0.41	2.23	0.34
		10	216.5	0.65	0.19	150.4	23.8	3.69	0.17	2.02	0.05
		20	250.9	0.95	0.02	137.7	7.7	3.80	0.45	2.17	0.21
		40	251.0	0.97	0.06	151.5	18.4	3.79	0.46	2.01	0.07
		60	252.0	0.88	0.17	141.8	16.8	4.02	0.37	1.93	0.09
		80	252.0	0.81	0.09	139.6	14.1	4.09	0.41	2.01	0.12
		100	253.6	0.66	0.38	104.1	26.9	4.37	0.67	1.91	0.02
		150	201.7	0.32	0.18	130.6	12.7	4.71	0.22	1.98	0.15
		250	129.8	0.14	0.05	118.5	18.3	6.48	0.53	2.29	0.08
		500	23.0	0.55	0.06	101.8	10.9	7.04	0.38	1.94	0.16
		750	13.0	0.62	0.19	87.8	10.2	3.37	0.24	2.16	0.32
		1000	17.2	0.65	0.03	106.0	6.7	3.36	0.20	2.19	0.11
		750	23.7	0.42	0.10	78.1	5.7	4.07	0.03	2.63	0.10
		1000	24.8	0.52	0.16	64.2	9.6	4.72	0.53	2.89	0.21
		1500	47.5	0.22	0.06	75.0	8.6	4.16	0.30	3.41	0.16
		2000	80.2	0.11	0.07	69.9	10.9	4.59	0.40	4.16	0.01
		2500	107.4	0.00	0.10	66.9	5.6	4.32	0.25	5.21	0.11
		3000	123.4	0.07	0.05	67.1	2.8	3.48	0.10	5.68	0.04
		3500	128.9	0.12	0.05	66.7	9.6	3.44	0.29	6.10	0.23
		3600	130.5	0.25	0.01	66.6	7.6	3.84	0.36	5.89	0.09
		3650	130.3	0.37	0.44	75.0	7.1	3.82	0.14	5.55	0.18
		3700	131.8	0.23	0.19	63.0	16.2	4.13	0.19	5.69	0.05
		3700	131.7	0.61	0.47	69.9	4.1	4.03	0.14	6.02	0.13
		3711	132.0	0.66	0.21	58.5	6.5	3.62	0.11	5.74	0.14

Cruise	Station	z (m)	O2 (µM)	Mn (nM)	1SD (nM)	Co (pM)	1SD (pM)	Fe (nM)	1SD (nM)	Cu (nM)	1SD (nM)
Teflon '94	CAT	0	258.6	3.08	0.19	219.4	22.7	1.20	0.62	3.42	0.12
		10	265.2	2.65	0.24	182.3	42.5	1.28	0.59	3.90	0.10
		25	255.2	2.02	0.34	189.8	33.7	1.08	0.35	3.86	0.10
		50	221.5	1.60	0.30	163.0	38.2	0.97	0.65	3.44	0.04
		75	197.4	1.38	0.32	197.8	11.0	0.50	0.99	3.55	0.03
		100	170.3	1.08	0.06	215.9	17.1	1.03	0.35	3.41	0.03
		250	81.3	0.81	0.15	146.4	27.6	2.57	0.16	3.09	0.28
		500	19.8	1.16	0.10	143.5	32.9	3.27	0.07	3.35	0.15
		750	14.3	1.49	0.07	176.4	26.1	4.19	0.42	3.37	0.11
		900	18.4	2.22	0.13	162.3	58.2	5.61	0.61	2.75	0.44
		950	18.1	2.82	0.10	171.7	37.7	7.17	0.73	3.40	0.56
		975	18.2	2.93	0.10	182.1	37.6	6.95	0.28	3.31	0.29
		975	18.9	2.83	0.16	180.1	11.1	6.29	0.49	1.71	0.21
		990	18.8	2.69	0.12	220.0	18.9	7.96	0.28	1.74	0.57
		1000	19.8	2.71	0.12	182.2	53.2	8.83	0.17	2.68	0.06
		1025	18.4	2.84	0.11	169.6	32.5	7.04	0.26	2.18	0.12
		1050	18.5	3.23	0.17	177.7	19.7	7.91	0.27	2.11	0.44
		1100	19.3	3.30	0.07	146.3	23.6	8.72	0.04	2.59	0.05
		1150	18.2	3.90	0.14	102.8	17.3	11.25	0.18	2.63	0.19
		1200	19.1	3.92	0.12	118.9	22.2	10.61	0.20	3.29	0.72
		1250	18.8	5.23	0.17	104.9	25.8	13.46	0.10	2.69	0.09
		1300	18.7	6.03	0.11	94.2	7.7	17.92	0.31	2.62	0.20
		1302	20.1	5.94	0.15	135.5	28.2	17.92	0.34	2.56	0.06
		1304	19.2	6.94	0.10	136.2	17.5	14.40	0.18	2.43	0.09
	Flux			1.61	0.26	---	---	4.03	0.54	---	---

Cruise	Station	z (m)	O2 (µM)	Mn (nM)	1SD (nM)	Co (pM)	1SD (pM)	Fe (nM)	1SD (nM)	Cu (nM)	1SD (nM)
Teflon '94	SCI	0	255.7	1.43	0.53	93.4	25.2	5.30	0.79	1.30	0.04
		10	172.2			153.7	39.6	6.47	0.47	1.19	0.03
		25	256.2	2.00	0.07	139.0	4.7	3.20	0.07	0.92	0.08
		50	262.4	5.75	1.26	140.8	8.4	2.85	0.50	0.93	0.08
		75	201.8	3.12	0.39	148.2	0.4	3.19	0.38	0.84	0.10
		100	180.3	2.27	0.51	102.2	33.7	3.66	0.80	1.36	0.11
		250	94.6	1.27	0.43	121.2	14.1	4.77	0.86	0.22	0.13
		500	21.1	0.49	0.38	104.0	3.3	5.31	0.67	1.11	0.11
		750	13.4	1.01	0.32	113.0	22.9	5.45	0.27	1.23	0.08
		1000	24.8	1.03	0.50	85.1	9.3	7.26	0.27	1.46	0.15
		1250	38.2	0.60	0.41	66.0	21.8	7.57	0.25	1.79	0.18
		1500	58.6	0.80	0.14	102.4	3.7	7.03	0.40	2.28	0.01
		1500	51.2	0.41	0.07	52.6	7.2	7.68	0.36	2.83	
		1750	58.8	0.49	0.08	29.9	28.7	11.11	1.08	2.10	0.11
		1775	58.5	0.47	0.04	23.9	32.9	10.66	1.08	2.25	0.31
		1800	58.9	0.63	0.14	35.3	18.1	10.24	0.24	2.40	0.11
		1815	59.9	0.48	0.18	38.7	10.1	9.96	0.09	2.41	0.10
		1825	58.1	0.43	0.12	50.6	4.7	10.11	0.48	1.95	0.01
		1850	59.8	0.64	0.20	55.0	1.6	8.32	0.98	1.91	0.06
		1950	58.6	0.77	0.07	38.4	4.8	6.63	0.61	1.86	0.08
		2000	58.4	1.05	0.11	20.4	28.2	6.37	0.29	1.66	0.06
		2025	58.2	0.82	0.15	26.6	21.9	7.15	0.60	2.53	0.06
		2030	58.2	1.04	0.09	35.1	8.9	7.52	0.60	2.24	0.14
		2035	52.2	1.27	0.12	32.7	14.2	7.31	0.66	1.98	0.08
	Flux			1.09	0.91	---	---	---	---	---	---

Cruise	Station	z (m)	O2 (µM)	Mn (nM)	1SD (nM)	Co (pM)	1SD (pM)	Fe (nM)	1SD (nM)	Cu (nM)	1SD (nM)
Teflon '94	SP	0	265.0	5.02	0.34	264.8	6.8	8.25	0.29	2.69	0.39
		5	268.1	4.89	0.13	253.3	10.8	7.35	0.15	2.96	0.15
		10	264.9	4.84	0.02	210.2	19.2	7.47	0.10	2.28	0.29
		20	262.9	4.77	0.02	248.7	4.3	8.26	0.44	2.51	0.51
		30	250.4	4.05	0.14	242.3	5.6	7.51	0.45	1.88	0.36
		40	191.5	1.82	0.07	231.1	2.3	9.35	0.38	1.28	0.25
		60	175.2	0.36	0.05	227.0	15.8	5.85	0.20	1.19	0.08
		80	155.1	0.52	0.37	209.3	0.1	5.58	0.01	0.99	0.30
		100	143.5	0.58	0.07	189.1	44.0	8.84	0.42	1.13	0.38
		250	75.7	0.61	0.22	191.6	28.4	9.58	0.18	1.50	0.30
		500	22.8	1.58	0.51	156.3	21.8	12.38	0.38	1.30	0.29
		650	11.7	2.86	0.17	116.4	36.2	13.29	0.69	1.79	0.18
		700	9.7	2.27	0.16	213.0	6.6	10.67	0.21	2.85	0.33
		725	9.5	2.64	0.23	188.9	28.9	11.31	0.46	2.27	0.32
		735	8.8	2.34	0.15	190.0	10.8	12.02	0.43	2.93	0.19
		750	9.5	2.62	0.18	225.2	12.9	14.92	0.29	2.99	0.26
		775	8.3	3.03	0.22	196.5	38.4	17.70	0.57	2.71	0.22
		800	8.7	3.00	0.09	207.2	11.2	17.91	0.47	2.30	0.48
		825	9.2	3.12	0.06	203.9	31.7	26.25	0.43	2.10	0.10
		850	9.0	3.45	0.19	188.1	17.4	27.98	0.08	2.51	0.22
		875	8.7	3.23	0.09	220.0	13.8	25.03	0.59	2.42	0.06
		880	8.8	2.86	0.13	203.8	10.1	19.30	0.73	2.07	0.16
		883	8.8	2.84	0.02	207.9	29.5	22.66	0.23	2.55	0.17
		885	8.5	4.31	0.32	191.9	4.4	25.10	1.48	2.38	0.16
	Flux			0.41	0.16	-0.10	2.98	4.30	1.12	-0.13	0.08

Cruise	Station	z (m)	O2 (µM)	Mn (nM)	1SD (nM)	Co (pM)	1SD (pM)	Fe (nM)	1SD (nM)	Cu (nM)	1SD (nM)
Teflon '94	SM	0	264.2	2.91	2.13	221.1	31.3	3.01	0.21	2.59	0.89
		10	263.9	2.16	0.05	202.7	19.2	3.42	0.49	1.90	0.44
		20	268.5	2.06	0.13	228.3	16.1	3.28	0.47	1.76	0.13
		40	238.1	2.13	0.08	212.6	21.5	4.31	0.13	1.01	0.46
		60	191.8	0.28	0.13	190.9	20.1	4.28	0.49	4.11	0.33
		80	167.3	0.19	0.10	184.1	13.7	5.57	0.09	1.27	0.31
		100	149.2	0.13	0.14	179.8	22.5	5.62	0.45	1.54	0.05
		250	79.4	0.35	0.14	185.9	8.2	7.28	0.28	1.08	0.43
		500	19.3	1.63	0.03	161.6	15.7	11.16	0.99	1.58	0.34
		575	12.9	2.53	0.06	173.6	5.2	13.34	0.49	1.27	0.22
		650	12.2	2.89	0.19	164.0	29.2	13.88	0.60	1.29	0.46
		700	10.2	2.91	0.04	170.4	19.8	15.04	0.29	1.50	0.09
		700	9.3	2.94	0.24	212.4	30.8	14.65	1.01	2.37	0.76
		725	8.6	3.84	0.11	211.1	27.6	9.74	0.53	2.16	0.31
		750	9.2	4.23	0.16	228.7	4.7	11.31	0.27	2.35	0.70
		775	7.9	6.07	0.48	219.0	25.5	13.39	1.64	2.02	0.72
		800	6.7	6.91	0.11	220.5	3.4	12.00	0.45	2.08	0.33
		825	9.0	7.72	0.02	234.3	24.0	17.27	0.65	2.70	0.59
		850	5.5					22.36	0.92	3.95	0.74
		875	6.9					23.10	0.12	5.24	0.76
		890	10.2			239.5	13.8			5.14	0.22
		895	9.9			247.7	11.5				
		898	14.9								
		900	10.4			228.1	20.5				
	Flux			3.91	0.89	2.97	1.50	5.65	1.07	1.36	0.35

Cruise	Station	z (m)	O2 (µM)	Mn (nM)	1SD (nM)	Co (pM)	1SD (pM)	Fe (nM)	1SD (nM)	Cu (nM)	1SD (nM)
Teflon '95	SM	3	264.1	7.58	0.18	174.6	10.9				
		20	261.6	7.37	0.51	167.0	11.4				
		30	245.1	7.48	0.15	149.2	4.1				
		50	199.7	4.81	0.21	148.9	7.2				
		75	170.7	6.29	0.05	182.9	7.9				
		100	141.5	3.94	0.23	191.3	8.8				
		200	340.6	2.24	0.01	181.5	13.3				
		300	54.2	1.76	0.24	173.1	9.5				
		500	23.1	3.27	0.04	179.4	18.3				
		700		6.68	0.08	215.4	12.3				
		720	14.7	7.14	0.03	248.9	16.6				
		740	15.6	9.41	0.35	268.3	35.3				
		750	7.6	8.04	0.04	277.0	37.2				
		760	11.1	8.75	0.07	261.9	31.3				
		780	14.2	8.50	0.09	259.4	17.6				
		800	9.0	9.53	0.21	252.0	5.1				
		815	12.9	9.82	0.09	261.8	27.9				
		830	7.7	11.18	0.19	264.5	23.3				
		845	12.2	11.23	0.43	286.4	19.8				
		860	7.3	11.47	0.15	290.8	8.4				
		875	13.9	11.06	0.27	266.4	16.5				
		885	8.7	11.47	0.06	255.7	25.9				
		890	11.5	10.68	0.17	264.6	10.6				
		895	8.9	9.26	0.12	238.6	19.3				
	Flux			1.33	0.17	3.55	2.82				

Cruise	Station	z (m)	O2 (µM)	Mn (nM)	1SD (nM)	Co (pM)	1SD (pM)	Fe (nM)	1SD (nM)	Cu (nM)	1SD (nM)
Teflon '95	TB	3	262.0	7.68	0.65	96.1	20.1	1.09	0.06		
		25	253.7	7.39	1.46	103.0	2.7	1.11	0.06		
		50	241.3	5.03	0.03	160.8	8.8	1.12	0.08		
		75	175.5	4.00	0.35	112.0	6.1	1.31	0.08		
		100	166.5	3.76	0.27	115.3	5.2	1.67	0.07		
		250	80.4	3.34	0.20	106.2	5.9	1.99	0.04		
		500	27.9	3.62	0.16	70.2	2.0	2.10	0.12		
		750	15.2	2.51	0.02	72.6	7.3	2.17	0.07		
		1000	31.7	3.98	0.18	76.2	7.7	2.15	0.09		
		1100	24.7	5.68	0.43	75.8	2.4	2.39	0.06		
		1125	33.5	4.10	0.23	74.4	8.4	2.56	0.07		
		1150	23.8	3.66	0.10	73.0	14.2	2.46	0.08		
		1175	31.9	3.40	0.10	77.4	11.2	2.53	0.10		
		1200	25.4	3.11	0.21	88.6	19.8	2.36	0.13		
		1250	33.3	3.75	0.23	62.6	10.2	2.58	0.05		
		1300	25.5	2.98	0.13	68.3	7.4	2.69	0.07		
		1350	35.6	3.11	0.25	68.2	8.8	2.95	0.09		
		1400	24.7	4.56	0.35	71.2	15.4	3.41	0.16		
		1450	30.1	3.61	0.04	73.1	5.3	3.70	0.06		
		1475	25.7	4.74	0.16	70.4	5.6	4.73	0.14		
		1490	34.9	4.78	0.06	81.4	8.0	4.50	0.05		
		1495	24.3	5.24	0.04	65.5	4.2	4.00	0.13		
		1500	32.2	5.18	0.53	72.6	7.5	4.78	0.15		
		1502	26.3	4.23	0.37	65.1	3.8	4.20	0.00		
	Flux			0.55	0.18	2.27	1.57	0.82	0.20		

Cruise	Station	z (m)	O2 (μM)	Mn (nM)	1SD (nM)	Co (pM)	1SD (pM)	Fe (nM)	1SD (nM)	Cu (nM)	1SD (nM)
Teflon '95	SCI	3	370.4	4.55	0.07	218.9	7.7	0.94	0.01		
		20	270.1	5.25	0.05	197.8	10.5	0.71	0.03		
		50	240.3	5.40	0.08	223.5	20.8	2.06	0.03		
		75	181.2	2.85	0.14	219.4	3.9	1.67	0.01		
		100	138.0	1.47	0.16	197.2	9.0	1.80	0.04		
		250	62.4	1.79	0.02	171.3	8.5	3.88	0.14		
		500	26.3	1.94	0.04	177.4	48.5	1.79	0.06		
		1000	28.4	2.20	0.16	125.7	7.9	2.98	0.09		
		1500	363.5	2.32	0.25	147.6	11.7	1.80	0.10		
		1750	60.3	2.04	0.04	143.7	13.7	1.64	0.21		
		1790	75.0	2.05	0.11	118.0	2.1	0.75	0.06		
		1800	70.2	1.40	0.10	113.4	3.2	1.02	0.03		
		1810	61.1	2.11	0.15	122.1	18.3	1.00	0.07		
		1820	61.7	1.11	0.03	111.8	4.3	1.04	0.03		
		1840	72.2	0.96	0.03	112.4	5.5	0.84	0.08		
		1880	62.7	0.74	0.01	112.1	9.0	1.23	0.05		
		1920		1.19	0.10	126.4	7.0	1.70	0.04		
		1950	75.2	2.01	0.15	127.9	2.6	1.06	0.06		
		1980	62.6	1.89	0.12	120.4	8.9	1.31	0.03		
		2000	69.6	2.07	0.05	102.3	12.3	1.82	0.08		
		2020	64.0	2.21	0.05	125.2	11.1	1.34	0.02		
		2030	64.0	2.24	0.12	147.8	22.0	1.41	0.07		
		2035	65.3	2.24	0.07	130.0	12.1	1.74	0.06		
		2039	336.1	2.27	0.01	133.5	2.4	1.54	0.08		
	Flux			0.98	0.48	20.46	9.99	0.80	0.56		

Cruise	Station	z (m)	O2 (µM)	Mn (nM)	1SD (nM)	Co (pM)	1SD (pM)	Fe (nM)	1SD (nM)	Cu (nM)	1SD (nM)
Teflon '95	PE	3	262.7	4.37	0.19	113.1	3.9	0.80	0.05		
		10	253.2	4.17	0.60	116.2	11.0	0.80	0.02		
		20	265.0	4.84	0.19	107.6	28.0	0.75	0.02		
		40	266.8	4.01	0.07	104.0	27.1	0.72	0.02		
		60	264.1	3.33	0.28	91.8	18.3	0.87	0.03		
		80	214.7	2.68	0.19	120.1	26.5	1.08	0.09		
		100	199.3	1.92	0.25	108.8	9.7	1.43	0.02		
		150	156.3	1.79	0.04	87.7	19.6	1.42	0.02		
		250	111.6	1.58	0.11	99.5	9.0	2.14	0.09		
		500	20.7	2.04	0.03	59.4	20.0	1.80	0.08		
		750	21.2	2.03	0.22	52.1	5.9	1.61	0.04		
		750	24.6		0.09			1.71	0.10		
		1000	25.2	1.94	0.04	70.3	19.0	2.08	0.07		
		1000	30.3	2.13	0.00			2.14	0.22		
		1500	65.2	1.39	0.65	74.3	11.6	1.79	0.04		
		2000	84.9	1.63	0.46	73.0	12.7	1.45	0.08		
		2500	119.7	2.49	0.19	64.7	7.1	1.51	0.05		
		3000	123.1	1.51	0.25	64.2	12.2	1.65	0.07		
		3500	140.5	1.60	0.07	78.2	10.0	1.39	0.11		
		3600	133.7	1.34		76.2	10.7	1.13	0.13		
		3700	143.9	0.65	0.24	87.1	11.6	1.15	0.05		
		3705	138.0	1.70	0.05	81.8	8.8	1.51	0.27		
		3710	142.1	1.20	0.57	88.2	13.9	1.03	0.05		
		3715	137.2	2.22		83.0	1.4	1.14	0.02		

Cruise	Station	z (m)	O2 (µM)	Mn (nM)	1SD (nM)	Co (pM)	1SD (pM)	Fe (nM)	1SD (nM)	Cu (nM)	1SD (nM)
Monterey Bay	TS1	1	255.8	8.45	1.67	369.0	14.0	40.98	7.67	5.44	
		10	249.7	8.35	1.85	361.0	15.0	37.21	1.05	4.12	
		20	248.6	7.74	1.06	347.0	11.0	47.43	6.74	4.49	0.31
		30	146.1	2.76	1.22	224.0	35.0	38.22	2.47	5.08	0.74
		40	140.1	0.92	0.30	140.0	41.0	19.94	4.91	5.65	4.08
		60	140.9	0.03	0.38	189.0	9.0	14.13	2.05	1.96	0.40
		70	154.9	0.00	0.52	147.0	47.0	9.49	0.57	2.62	0.67
		80	191.9	3.16	0.39	218.0	2.0	12.62	2.43	3.79	0.24
		92	101.0	0.77	0.28	266.0	6.0	29.60	3.15	5.54	0.82
		92		1.64	0.16	200.0	58.0	16.81	0.92	5.25	1.37
		92		1.35	0.82	217.0	16.0	19.22	0.25	3.77	1.25
		92		1.39	0.58	192.0	34.0	18.65	2.07	5.34	0.70
Monterey Bay	TS2	0	303.0	10.10	1.41	199.0	17.0			1.87	0.35
		5	284.6	4.85	0.82	207.0	4.0			1.33	0.12
		10	264.0	5.66	1.32	228.0	38.0			1.89	0.41
		20	239.8	6.54	0.72	235.0	8.0			1.76	0.54
		30	231.2	5.14	0.69	223.0	22.0			1.17	0.36
		40	206.9	4.24	0.43	215.0	11.0			2.15	1.18
		50	183.6	3.24	0.38	225.0	13.0			1.21	0.31
		60	172.0	2.57	0.19	185.0	75.0			1.78	0.29
		75	159.1	3.20	0.33	234.0	1.0			2.28	0.27
		85	154.1	4.64	0.21	264.0	7.0			3.85	0.64
		94	135.8	6.79	0.69	363.0	24.0			10.97	0.82
		94	136.6	7.70	0.25	366.0	7.0			12.73	0.21

Cruise	Station	z (m)	O2 (µM)	Mn (nM)	1SD (nM)	Co (pM)	1SD (pM)	Fe (nM)	1SD (nM)	Cu (nM)	1SD (nM)
Monterey Bay	TS3	1	259.9	3.63	0.21	300.0	32.0	8.53	3.62	2.93	0.19
		10	257.6	3.17	0.12	300.0	9.0	8.02	3.51	0.89	0.20
		20	257.1	3.32	0.06	318.0	2.0	13.15	10.09	1.42	0.15
		30	258.2	3.31	0.03	325.0	0.0	10.16	6.19	0.57	0.19
		40	257.3	3.08	0.14	349.0	14.0	13.91	3.29	0.73	0.10
		50	256.6	3.10	0.08	377.0	18.0	17.03	0.39	0.00	1.18
		60	253.0	2.84	0.11	417.0	17.0	17.37	4.66	2.08	2.00
		70	245.0	2.29	0.04	458.0	14.0	21.36	3.71	0.73	0.23
		80	240.7	1.81	0.03	506.0	36.0	33.55	0.15	1.73	1.51
		90	197.0	3.47	0.01	648.0	23.0	110.54	2.86	3.75	0.65
		94	185.4	3.08	0.20	672.0	78.0	111.44	0.22	4.23	0.28
		94	186.6	2.95	0.18	764.0	30.0	108.05	2.62	4.08	0.05
Monterey Bay	TS4	0	215.6	2.22	0.18	177.9	5.0	15.72	0.61	2.26	0.10
		10	285.1	2.41	0.24	149.0	16.5	4.68	0.19	1.37	0.35
		20	279.4	2.88	0.09	144.2	10.6	4.17	0.04	0.82	0.30
		30	266.9	2.55	0.62	129.4	10.5	5.51	0.20	0.73	0.39
		40	230.8	2.60	0.41	178.1	7.3	12.26	0.61	0.94	0.21
		50	187.5	2.17	0.20	187.0	15.4	19.64	1.89	1.60	0.14
		60	169.3	1.84	0.06	199.0	8.1	25.66	0.69	2.00	0.20
		70	153.1	2.95	0.45	180.1	8.0	28.15	0.82	2.09	0.33
		80	136.8	3.20	0.27	170.4	20.0	43.93	2.90	2.99	0.08
		90	94.9	3.05	0.05	182.1	6.7	42.01	0.62	2.92	0.59
		95	130.0	4.71	0.31	198.2	6.1	67.84	0.70	4.16	0.41
		100	130.3	3.27	0.21	187.4	2.2	69.77	1.66	4.21	0.15

Cruise	Station	z (m)	O2 (µM)	Mn (nM)	1SD (nM)	Co (pM)	1SD (pM)	Fe (nM)	1SD (nM)	Cu (nM)	1SD (nM)
Monterey Bay	TS5	1	292.5	9.66	0.15	69.8	6.1	2.02	0.18		
		5	285.2	10.34	0.38	93.5	2.8	1.61	0.12		
		10	278.7	10.08	0.26	79.1	4.0	2.28	0.10		
		20	256.8	9.53	0.58	44.6	2.3	1.81	0.16		
		25	243.1	6.01	0.19	69.5	4.6	2.38	0.22		
		30	230.8	9.29	0.31	93.0	4.2	1.65	0.32		
		40	217.1	7.86	0.20	125.6	5.6	1.98	0.04		
		50	209.3	8.00	0.49	126.9	6.3	1.91	0.24		
		70	199.5	7.35	0.51	117.8	0.6	4.70	0.15		
		80	228.0	6.48	1.33	101.0	1.0	1.82	0.05		
		90	135.7								
		90	158.0								
		92	186.9	5.39	0.36	105.5	2.0	1.62	0.09		
		95	190.6	5.11	0.25	97.9	1.6	2.16	0.15		
		98	152.6								

Appendix 1b. Centrifuged core pore water data and flux estimates. Cruise and station abbreviations are as in Table 1. Sample depth and porosity are determined as described in text. Units for the data are given. Flux is expressed in units of μmol/m^2/day for Mn, Fe, and Cu and in nmol/m^2/day for Co. Dashes indicate stations where a flux measurement could not be arrived at either due to either sample contamination or suspect data.

Cruise	Station	z (cm)	Porosity	Mn (µM)	1SD (µM)	Co (nM)	1SD (nM)	Fe (µM)	1SD (µM)	Cu (µM)	1SD (µM)	NH3 (µM)	NO3 (µM)
Teflon'94	TB	0.25	0.92	0.070	0.001	0.307	0.005	0.056	0.005			5.7	24.7
		0.75	0.90	0.570	0.002	0.815	0.097	0.153	0.008			4.7	5.0
		1.50	0.89	0.826	0.041	0.706	0.140	0.660	0.082			5.7	1.9
		2.50	0.88	0.515	0.013	0.520	0.008	1.711	0.166			9.4	1.4
		3.50	0.87	0.408	0.016	0.481	0.058	1.440	0.101			10.4	1.5
		4.50	0.85	0.396	0.011	0.382	0.036	1.171	0.125			15.6	1.5
		6.00	0.85	0.320	0.024	0.340	0.089					17.5	1.2
		8.00	0.83	0.185	0.001	0.431	0.085	0.807	0.145			20.8	1.6
		10.50	0.76	0.106	0.011	0.289	0.062	0.169	0.030			25.5	0.5
		13.50	0.81	0.126	0.005	0.400	0.005	0.050	0.006			27.8	0.8
		16.50	0.83	0.177	0.003	0.374	0.055	0.085	0.023			20.3	0.3
		20.00	0.81	0.159	0.011	0.379	0.065	0.039	0.005			23.1	0.9
		24.00	0.82	0.157	0.006	0.314	0.003					22.6	1.1
	Flux			1.498	0.253	1.105	0.558	1.861	0.290				
Teflon'94	PE	0.50	0.88	0.007	0.0004	0.13	0.09	0.1458	0.0027	0.190	0.006	5.9	47.1
		1.50	0.84	0.084	0.0023	0.90	0.07	0.0165	0.0013	0.243	0.001	5.1	42.7
		3.00	0.83	0.110	0.0013	0.21	0.08	0.0087	0.0011	0.280	0.005	8.5	27.7
		5.00	0.83			11.24	0.68	0.0896	0.0011	0.374	0.003	11.0	11.6
		7.00	0.87			34.61	1.48	0.0592	0.0013	0.332	0.013	6.4	8.6
		9.00	0.79			68.75	4.43	0.0928	0.0031	0.323	0.059	8.0	7.1
		11.50	0.78			97.13	2.28	0.1080	0.0023	0.232	0.004	7.2	1.0
		14.50	0.77			76.58	0.99	0.1155	0.0005	0.170	0.006	7.2	0.0
	Flux			0.081	0.018	0.181	0.451	0.018	0.003	0.133	0.040		

Cruise	Station	z (cm)	Porosity	Mn (µM)	1SD (µM)	Co (nM)	1SD (nM)	Fe (µM)	1SD (µM)	Cu (µM)	1SD (µM)	NH3 (µM)	NO3 (µM)
Teflon'94	CAT	0.25	0.89	0.06	0.00	1.03	0.15	1.61	0.11			0.0	21.7
		0.75	0.88	2.36	0.01	4.16	0.39	4.71	0.08			1.7	1.4
		1.50	0.86	6.82	0.13	9.53	0.19	25.38	1.00			6.4	0.8
		2.50	0.85	10.18	0.63	10.41	0.12	32.61	0.46			17.4	2.0
		3.50	0.84			10.10	0.23	25.77	2.43			18.2	2.4
		4.50	0.84	9.50	0.09	7.48	0.10					18.2	2.4
		6.00	0.82	9.88	0.12	6.50	0.01	22.91	0.50			19.5	0.8
		8.00	0.82	10.35	0.08	7.20	0.41	23.28	0.11			22.0	0.3
		10.50	0.81	8.30	0.55	3.88	0.32	17.30	1.62			27.1	0.3
		13.50	0.81	8.53	0.11	3.87	0.22	10.35	0.03			26.3	0.3
		16.50	0.80			3.24	0.23	9.04	0.26			25.8	0.2
		19.50	0.80	3.20	0.12	3.01	0.17	4.61	0.29			25.8	0.7
		23.00	0.80	2.94	0.08	2.84	0.11	1.92	0.13			27.5	0.6
	Flux			8.092	2.636	11.394	1.990	36.795	5.408				
Teflon'94	SC I	0.25	0.92	0.06	0.003	1.35	0.19	0.060	0.004			0.3	22.3
		0.75	0.89	0.18	0.004	1.31	0.06	1.639	0.046			3.5	16.5
		1.50	0.88	61.80	5.106	42.79	10.90	0.156	0.030			1.1	6.6
		2.50	0.87	114.17	3.114	90.03	2.65	3.450	0.058			7.6	1.5
		3.50	0.86	139.63	2.303	142.80	2.97	1.077	0.086			10.0	1.2
		4.50	0.86	137.75	3.756			1.651	0.074			19.7	1.3
		6.00	0.86	132.75	9.735	162.08	15.59	11.808	1.261			27.3	0.4
		8.00	0.85	126.03	2.370	162.91	3.64	9.856	0.247			43.9	0.8
		10.00	0.86					11.101	0.254			51.5	0.7
		12.00	0.85	156.71	22.170	132.44	6.85	20.419	0.570			64.4	0.5
		14.50	0.84	143.66	14.126	142.60	3.43	15.597	0.216			75.3	0.1
		18.00	0.85	119.93	2.891	137.21	0.75	14.884	0.056			97.1	0.5
		22.00	0.84	109.66	17.327	146.02	2.12	14.147	0.070			117.7	0.8
		26.00	0.82	97.84	2.442	133.07	3.97	14.298	0.132				
	Flux			0.574	0.002	3.829	3.522	0.917	0.709				

Cruise	Station	z (cm)	Porosity	Mn (μM)	1SD (μM)	Co (nM)	1SD (nM)	Fe (μM)	1SD (μM)	Cu (μM)	1SD (μM)	NH3 (μM)	NO3 (μM)
Teflon'94	SP	0.25	0.91	0.138	0.010	1.87	0.15	0.52	0.02			1.1	9.8
		0.75	0.89	0.163	0.028	2.30	0.16	33.63	1.75			7.5	4.0
		1.50	0.88	0.584	0.049	3.13	0.19	88.29	4.41			21.7	1.1
		2.50	0.86	1.765	0.155	5.45	0.42	115.86	4.76			36.9	1.2
		3.50	0.86	0.623	0.012	3.20	0.24	122.60	0.92			53.4	0.8
		4.50	0.85	0.734	0.027	2.93	0.20	137.84	10.46			81.8	0.6
		6.00	0.84	2.169	0.055	3.27	0.13	144.96	1.76			86.0	0.6
		8.00	0.83	0.974	0.057	2.36	0.03	146.32	5.56			107.1	0.2
		10.00	0.82	0.944	0.045	1.91	0.23	123.72	3.29			129.5	0.5
		12.00	0.81	0.814	0.024	1.94	0.17	124.92	5.05			151.1	0.3
		14.50	0.82	0.970	0.044	1.78	0.21	125.77				188.7	0.5
		18.00	0.81	1.019	0.002	1.72	0.06	108.84	12.38			202.0	0.4
		22.00	0.81	1.180	0.039	1.66	0.10	72.73	1.62			238.3	0.4
		26.00	0.77	1.435	0.030	1.96	0.11	55.57	5.13			269.9	0.4
	Flux			1.745	0.332	0.937	0.642	140.309	15.527				

Cruise	Station	z (cm)	Porosity	Mn (µM)	1SD (µM)	Co (nM)	1SD (nM)	Fe (µM)	1SD (µM)	Cu (µM)	1SD (µM)	NH3 (µM)	NO3 (µM)
Teflon'94	SM	0.25	0.94	0.58	0.08	2.22	0.25	88.2	0.3			8.6	14.0
		0.75	0.90	114.98	9.91	3.37	0.38	183.4	0.1			23.0	3.0
		1.50	0.90	51.61	2.09	3.52	0.60	206.5	1.3			37.3	2.1
		2.50	0.88	25.04	1.37	2.60	0.31	255.7	0.6			28.1	0.2
		3.50	0.88	2.21	0.09	3.18	0.34	248.4	0.1			67.4	1.4
		4.50	0.87			4.02	0.35	219.5	6.0			82.7	0.7
		6.00	0.87	3.16	0.19	3.57	0.59	231.9	4.4			103.1	0.0
		8.00	0.86	1.95	0.15	3.43	0.80	194.4	2.2			124.8	0.1
		10.00	0.86	1.85	0.08	3.08	0.17	145.2	2.8			146.6	0.0
		12.00	0.83			4.37	0.28	211.5	0.6			170.2	0.0
		14.50	0.86	2.67	0.09	4.52	0.77	183.9	3.4			191.0	0.0
		18.00	0.86	3.12	0.02	3.67	0.33	173.5	2.4			221.1	0.2
		22.00	0.85	3.45	0.07	4.95	0.35	184.4	0.6			260.5	0.0
		26.00	0.73	3.53	0.13	5.06	0.66	214.2	2.8			295.6	0.1
		30.00	0.71	19.34	0.37	5.86	0.47	207.3	4.5			338.2	0.3
	Flux			1.590	0.292	0.416	0.151	262.311	71.676				
Teflon '95	SM	0.25	0.94	3.86	0.21	5.16	1.57	142.22	18.80			9.3	12.5
		0.75	0.90	4.91	0.36	4.06	0.15	234.26	15.15			20.7	5.4
		1.50	0.90	4.94	0.23	4.19	0.72	269.88	9.81			35.5	3.1
		2.50	0.89	5.27	0.44	2.78	0.84	254.93	8.38			44.2	3.0
		3.50	0.89	4.74	0.56	3.49	0.17	230.00	8.65			60.8	2.5
		5.00	0.86	4.89	0.48	3.03	0.44	283.62	24.44			74.7	3.2
		7.00	0.88	5.01	0.19	2.79	0.50	290.85	11.19			91.3	2.4
		9.00		3.94	0.16	2.10	0.23	219.92	6.24			108.7	2.4
		11.50	0.86	4.14	0.34	2.49	0.42	252.55	11.33			131.4	2.0
		14.50	0.70	3.15	0.37	2.47	0.83	249.52	9.88			162.7	2.6
		18.00		4.63	0.24	2.61	0.37	243.07	9.86			188.9	1.4
		22.00		2.30	0.64	3.07	0.81	116.14	4.15			218.5	1.7
	Flux			4.13	2.40	4.67	5.97	289.48	110.53				

Cruise	Station	z (cm)	Porosity	Mn (µM)	1SD (µM)	Co (nM)	1SD (nM)	Fe (µM)	1SD (µM)	Cu (µM)	1SD (µM)	NH3 (µM)	NO3 (µM)
Teflon '95	TB	0.25	0.92	0.097	0.000	0.789	1.459	0.02285				-8.10	29.46
		0.75	0.90	0.192	0.006	0.987	0.099	0.03081	0.00031			-9.00	6.95
		1.50	0.89	0.206	0.005	1.221	0.688	0.14221	0.01572			-8.10	1.34
		2.50	0.88	0.268	0.007	1.234	0.714	0.50608	0.02831			-3.80	1.07
		3.50	0.87	0.251	0.002	0.933	0.097	0.51275	0.00746			-2.90	1.08
		5.00		0.248	0.004	0.898	1.294	0.36155	0.00725			-1.10	1.04
		7.00		0.229	0.005	0.991	0.313	0.22662	0.00893			-2.00	0.73
		9.50		0.182	0.004	16.375	17.709	0.13313	0.00590			-2.90	0.91
		12.50		0.177	0.002	11.540	9.790	0.14885	0.00380			-1.10	0.85
		16.00		0.174	0.002	12.537	49.810	0.06189	0.00348			0.60	0.42
		20.00	0.81	0.140	0.003	15.346	8.351	0.02081	0.00216			3.20	1.12
		24.00	0.82	0.149	0.007	14.024	6.760	0.00587	0.00084			40.70	0.41
	Flux			0.63	0.11	1.79	0.74	0.46	0.07				
Teflon '95	SCI	0.25	0.94	0.106	0.011	1.028	1.570	0.03588	0.00133			-3.80	42.43
		0.75	0.92	0.738	0.073	5.495	0.149	0.02295	0.00171			-0.30	27.81
		1.50	0.91	133.830	17.169	101.110	0.717	0.07102	0.00958			1.50	14.11
		2.50	0.89	177.497	8.057	143.173	0.841	0.06815	0.00213			1.50	5.36
		3.50	0.88	225.899	7.452	230.674	0.169	0.08492	0.00481			10.20	2.41
		5.00	0.87	255.686	6.889	282.170	0.438	0.10781	0.00598			22.40	2.59
		7.00	0.87	251.667	15.437	228.196	0.497	1.52022	0.07301			35.50	0.67
		9.00	0.86	208.237	5.003	189.070	0.231	7.90308	0.27238			46.80	1.12
		11.50	0.85	221.380		179.272	0.423	6.43658	0.29596			56.40	0.63
		14.50	0.86	212.137	0.045	190.867	0.825	7.71227	0.12713			76.40	0.61
		18.00		225.625	2.383	208.721	0.371	5.45695	0.13012			94.80	0.65
		22.00		225.267	4.970	207.013	0.606	9.91817	0.59060			128.80	0.58
	Flux			2.60	0.54	10.14	17.81	0.05	0.01				

Cruise	Station	z (cm)	Porosity	Mn (µM)	1SD (µM)	Co (nM)	1SD (nM)	Fe (µM)	1SD (µM)	Cu (µM)	1SD (µM)	NH3 (µM)	NO3 (µM)
Teflon '95	PE	0.50	0.92	0.023	0.003	0.251	0.047	0.00500	0.00001			-9.00	44.16
		1.50	0.91	0.023	0.002	0.524	0.254	0.01500	0.00002			-8.00	38.03
		2.50	0.87	0.029	0.001	0.834	0.620	0.02500	0.00003			-10.70	29.09
		3.50	0.89	4.362	0.202	2.882	0.544	0.03500	0.00004			-13.30	19.80
		5.00	0.84	24.067	1.317	30.015	0.221	0.05000	0.00005			-13.30	11.77
		7.00	0.82	40.593	0.842	49.108	3.547	0.07000	0.00007			-12.50	5.91
		9.50	0.63	61.175	1.150	60.739	11.163	0.09500	0.00010			-10.70	2.51
		12.50	0.78	58.287	0.980	69.258	6.062	0.12500	0.00013			-11.60	0.74
	Flux			0.019	0.010	0.748	0.017	0.02152	0.00007				
Monterey Bay	TS1	0.25	0.57	0.606	0.041	7.37	0.40	0.062	0.016			2.3	10.1
		0.75	0.55	1.081	0.017	10.22	0.62	0.016	0.043			1.3	4.8
		1.50	0.56			8.02	0.48					17.7	4.6
		2.50	0.57	1.185	0.012	7.05	0.07	0.016	0.013			24.5	
		3.50	0.53	0.878	0.016	5.32	0.18	0.057	0.012			25.0	2.0
		5.00	0.53	0.647	0.024	2.11	0.36	0.088	0.023			75.4	2.4
		7.00	0.52	0.568	0.022	1.97	0.07	0.158	0.006			42.2	3.1
		9.00	0.51	0.454	0.013	1.31	0.18	0.102	0.009			34.5	2.2
		11.50	0.52	0.390	0.019	1.44	0.12	0.118	0.010			49.5	1.7
		14.50	0.49	0.330	0.002	0.93	0.05	0.183	0.035			43.6	1.5
		18.00	0.47	0.376	0.019	2.23	0.34	0.322	0.036			52.2	1.8
		22.00	0.45	0.511	0.009	1.73	0.38	0.117	0.038			63.1	
		26.00	0.44									72.2	2.3
	Flux			0.217	0.165	15.058	6.970	-0.011	0.016				

Cruise	Station	z (cm)	Porosity	Mn (µM)	1SD (µM)	Co (nM)	1SD (nM)	Fe (µM)	1SD (µM)	Cu (µM)	1SD (µM)	NH3 (µM)	NO3 (µM)
Monterey Bay	TS2	0.25	0.53	0.426	0.017	5.95	0.15			0.077	0.012	3.7	8.0
		0.75		0.778	0.039	9.39	0.77			0.111	0.002	6.2	3.3
		1.50	0.53	1.061	0.137	5.84	1.17			0.136	0.037	11.0	0.8
		3.00	0.49	1.090	0.068	4.75	0.25			0.175	0.041	12.9	-0.2
		5.00	0.47									16.4	0.1
		7.50	0.50	0.447	0.013	1.89	0.05			0.131	0.031	16.3	-0.4
		11.00	0.51	0.264	0.002	1.52	0.18			0.111	0.022	12.6	0.0
		15.00	0.47	0.289	0.013	1.39	0.10			0.084	0.009	15.0	-1.0
		19.00	0.44	0.327	0.019	1.45	0.08			0.079	0.022	18.8	-0.3
		23.00	0.42	0.297	0.011	1.69	0.24			0.138	0.008	19.3	3.1
	Flux			0.318	0.120	12.798	4.334			0.051	0.014		
Monterey Bay	TS3	0.25	0.66	0.104	0.015	6.13	0.44	0.16	0.01	0.144	0.114	4.0	20.4
		0.75	0.62	0.364	0.006	9.43	0.54	0.18	0.02	0.088	0.052	7.7	6.0
		1.50	0.60	0.419	0.018	6.72	0.14					31.6	2.5
		3.00	0.58	0.456	0.026	6.97	0.64	1.57	0.39	0.239	0.066	65.6	1.1
		5.00		0.596	0.010	4.63	0.23	2.35	0.41	0.207	0.000	88.1	0.4
		7.50	0.57	0.526	0.037	6.74	0.86	2.10	0.25	0.250	0.019	68.5	0.6
		11.00	0.56	0.473	0.014	5.27	0.39	1.77	0.62	0.125	0.004	62.1	28.8
		15.00	0.52	0.821	0.011			1.01	0.03	0.131	0.041	72.2	0.3
		19.00	0.49	0.842	0.017					0.091	0.110	72.2	0.2
	Flux			0.455	0.125	18.85	6.44	0.15	0.08	0.099	0.044		

Cruise	Station	z (cm)	Porosity	Mn (µM)	1SD (µM)	Co (nM)	1SD (nM)	Fe (µM)	1SD (µM)	Cu (µM)	1SD (µM)	NH3 (µM)	NO3 (µM)
Monterey Bay	TS4	0.25	0.63	0.336	0.010	5.28	0.16					19.1	14.3
		0.75	0.60	0.758	0.011	8.74	0.34					19.7	4.1
		1.50	0.57	0.821	0.003	5.85	0.33	0.173	0.003			49.2	2.0
		2.50	0.55	0.858	0.005	3.68	0.46	-0.005	0.010			46.9	1.6
		4.00	0.55	1.164	0.009	2.71	0.44	0.232	0.019			58.3	1.0
		6.00	0.55	1.010	0.036	0.92	0.44					69.1	0.0
		8.50	0.54	0.817	0.004	1.26	0.43	0.530	0.007			78.8	0.7
		11.50	0.50	0.652	0.003	1.01	0.12	1.167	0.061			69.1	1.2
		15.00	0.50	0.840	0.010	14.62	0.38	1.381	0.169			62.8	0.4
		19.00	0.47									73.1	1.2
		23.00										85.6	1.3
	Flux			1.501	0.185	16.986	5.255	0.073	0.022				
Monterey Bay	TS5	0.0	0.64			0.098	0.002	0.0022	0.0002			15.4	8.3
		0.5	0.57			6.195	0.391	0.0173	0.0004			40.7	1.4
		1.5	0.54					0.107	0.003			60.8	0.3
		3.0	0.55			6.335	0.249	0.248	0.027			69.5	0.2
		5.0	0.54			4.492	0.423	0.143	0.014			69.5	0.1
		7.5	0.59			2.152	0.317	0.893	0.026			66.0	0.0
		10.5	0.54			1.490	0.307	0.754	0.031			58.1	0.1
		14.0	0.48			2.805	0.057	11.708	1.138			58.1	0.0
		17.0				1.776	0.065	1.013	0.105				
	Flux					18.825	1.212	0.050	0.027				

Appendix 1c. Lander data and flux estimates. Cruise names are as in Table 1 except for Monterey Bay data that was added from Johnson and others (1992). Station abbreviations are as in Table 1 followed by a lander number. For example TB-7 would be Tanner Basin, lander 7. The Monterey Bay data added have station designation's T1-11 and T2-7. Each lander has three chambers designated blue, red, and yellow with, 6 samples being drawn from each designated 1 thru 6. Chamber height and draw times are as described in the text. Data for Mn, Co, Fe, and Cu has been corrected for dilution and is expressed in the units shown. Flux is expressed in the units of µmol/m²/day for Mn, Fe, and Cu. Dashes are included for the Co flux since the samples are believed to be contaminated as described in the text. Missing data is from an observable malfunctioning chamber or was rejected for reasons such as given in Berelson, and others (1987b).

Cruise	Station/Chamber	Height (cm)	h SE (cm)	Time (hr)	Mn (nM)	Co (nM)	Fe (nM)	Cu (nM)
Teflon '94	TB-4							
	Blue 1	8.0	±1.0	0.50	12.89	0.71	35.31	11.87
	Blue 2			8.50	14.44	9.61	35.82	12.34
	Blue 3			16.50	17.90	15.18	39.80	
	Blue 4			24.00				
	Blue 5			32.00	9.20	24.86	43.24	15.48
	Blue 6			40.00	6.09	29.18	41.69	13.72
	Chamber Flux				-0.39	---	0.38	0.13
	SE Chamber Flux				0.22	---	0.11	0.07
	Red 1	9.1	±1.2	0.50	0.77	0.38	30.16	15.27
	Red 2			8.50	3.19	11.55	28.38	14.02
	Red 3			16.50	2.72	16.74	32.70	12.89
	Red 4			24.00		23.02	35.41	14.65
	Red 5			32.00				
	Red 6			40.00	5.79	31.27	40.06	19.22
	Chamber Flux				0.25	---	0.63	0.23
	SE Chamber Flux				0.07	---	0.15	0.15
	Yellow 1	9.0	±2.0	0.50	1.36	0.97	43.49	18.56
	Yellow 2			8.50	4.38	18.59	66.90	
	Yellow 3			16.50	7.92	29.92	36.57	14.85
	Yellow 4			24.00	11.75	47.29	62.20	17.89
	Yellow 5			32.00		52.24	49.83	14.08
	Yellow 6			40.00	9.91	51.70	36.98	14.31
	Chamber Flux				0.50	---	-0.46	-0.22
	SE Chamber Flux				0.22	---	0.92	0.13
	Avg Lander Flux				0.12	---	0.18	0.05
	SE Avg Lander Flux				0.27	---	0.33	0.14

Cruise	Station/Chamber	Height (cm)	h SE (cm)	Time (hr)	Mn (nM)	Co (nM)	Fe (nM)	Cu (nM)
Teflon '94	TB-7							
	Blue 1	9.5	±2.0	1.0	15.1	0.7	29.4	17.6
	Blue 2			9.0	20.7	1.3	43.8	20.4
	Blue 3			17.0	19.4	1.3	62.4	18.3
	Blue 4			25.0	27.4	1.7	82.2	18.5
	Blue 5			33.0	32.9	1.9	128.2	17.8
	Blue 6			42.0	38.3	2.2	146.3	20.2
	Chamber Flux				1.29	---	6.87	0.05
	SE Chamber Flux				0.31	---	1.58	0.09
	Red 1	9.1	±1.2	1.0	12.7	0.8	16.6	12.4
	Red 2			9.0	11.3	1.0	19.4	12.2
	Red 3			17.0	10.0	1.3	29.9	15.0
	Red 4			25.0	7.9	1.5	24.3	15.5
	Red 5			33.0	7.7	1.6	36.0	12.3
	Red 6			42.0	6.4	3.0	52.8	15.1
	Chamber Flux				-0.34	---	1.74	0.11
	SE Chamber Flux				0.05	---	0.45	0.10
	Yellow 1	10.0	±1.2	1.0	15.8	0.8	21.4	10.9
	Yellow 2			9.0				
	Yellow 3			17.0	12.4	1.2	73.2	20.6
	Yellow 4			25.0	11.9	4.4	64.7	20.1
	Yellow 5			33.0	17.3	18.6	37.5	21.6
	Yellow 6			42.0	14.9	27.9	39.6	15.5
	Chamber Flux				0.04	---	0.50	0.33
	SE Chamber Flux				0.20	---	1.85	0.35
	Avg Lander Flux				0.33	---	3.03	0.16
	SE Avg Lander Flux				0.49	---	1.95	0.09

Cruise	Station/Chamber	Height (cm)	h SE (cm)	Time (hr)	Mn (nM)	Co (nM)	Fe (nM)	Cu (nM)
Teflon '94	PE-4							
	Blue 1	10.7	±1.5	1.0	0.0	0.3	0.0	7.3
	Blue 2			18.0	0.6	3.0	0.0	8.6
	Blue 3			35.0				
	Blue 4			52.0	16.6	8.3	4.5	14.0
	Blue 5			69.0	17.0	9.3	5.0	6.0
	Blue 6			87.0	15.9	10.3	4.6	7.1
	Chamber Flux				0.59	---	0.18	-0.01
	SE Chamber Flux				0.16	---	0.06	0.11
	Red 1	10.0	±1.5	1.0	19.1	0.5	15.6	17.1
	Red 2			18.0	14.5	3.1	6.7	11.4
	Red 3			35.0	14.4	3.1	7.2	16.7
	Red 4			52.0	15.2		6.5	15.3
	Red 5			69.0	14.9	6.0	3.9	16.3
	Red 6			87.0	13.8	8.5	4.5	15.9
	Chamber Flux				-0.10	---	-0.26	0.03
	SE Chamber Flux				0.05	---	0.10	0.08
	Yellow 1	11.1	±2.5	1.0	13.5	1.2	12.0	10.6
	Yellow 2			18.0	15.0	9.1	14.5	10.4
	Yellow 3			35.0	14.0	15.7	12.6	6.9
	Yellow 4			52.0	16.1	9.1	12.0	20.6
	Yellow 5			69.0	16.6	13.9	9.2	16.3
	Yellow 6			87.0	18.3	9.1	7.0	17.6
	Chamber Flux				0.14	---	-0.19	0.30
	SE Chamber Flux				0.04	---	0.07	0.17
	Avg Lander Flux				0.21	---	-0.09	0.11
	SE Avg Lander Flux				0.20	---	0.14	0.10

Cruise	Station/Chamber	Height (cm)	h SE (cm)	Time (hr)	Mn (nM)	Co (nM)	Fe (nM)	Cu (nM)
Teflon '94	PE-7							
	Blue 1	11.2	±1.5	1.0	23.2	0.3	36.0	
	Blue 2			17.0				
	Blue 3			33.0	22.7	1.4	13.2	5.0
	Blue 4			50.0	21.5	2.0	16.5	0.5
	Blue 5			67.0	36.7	2.3	26.1	5.9
	Blue 6			84.0				
	Chamber Flux				0.42	---	-0.47	0.07
	SE Chamber Flux				0.38	---	0.61	0.45
	Red 1	10.6	±1.2	1.0	7.3	0.1	43.5	
	Red 2			17.0	15.8	0.4	41.4	1.4
	Red 3			33.0	23.2	0.3	33.5	3.8
	Red 4			50.0	26.3	0.1	31.9	9.1
	Red 5			67.0	35.2	0.3	33.3	11.6
	Red 6			84.0				
	Chamber Flux				1.02	---	-0.46	0.55
	SE Chamber Flux				0.14	---	0.15	0.09
	Yellow 1	11.8	±1.5	1.0	4.9	0.1	27.2	3.1
	Yellow 2			17.0	2.4	0.5	27.5	5.9
	Yellow 3			33.0	3.4	0.8	16.8	8.4
	Yellow 4			50.0	1.5	1.5	17.9	10.4
	Yellow 5			67.0	2.7	1.8	28.1	14.4
	Yellow 6			84.0	2.9	3.3	31.8	17.7
	Chamber Flux				-0.05	---	0.13	0.49
	SE Chamber Flux				0.04	---	0.27	0.07
	Avg Lander Flux				0.46	---	-0.27	0.37
	SE Avg Lander Flux				0.31	---	0.20	0.15

Cruise	Station/Chamber	Height (cm)	h SE (cm)	Time (hr)	Mn (nM)	Co (nM)	Fe (nM)	Cu (nM)
Teflon '94	CAT-4A							
	Blue 1	11.0	±1.5	0.5	17.6	0.5	58.1	23.2
	Blue 2			6.0	13.9	1.8		30.3
	Blue 3			12.0				
	Blue 4			18.0	31.0	8.0	99.3	30.3
	Blue 5			24.5	31.4	7.9	78.7	35.0
	Blue 6			31.3		9.6	86.7	38.2
	Chamber Flux				1.97	---	2.33	1.10
	SE Chamber Flux				0.71	---	1.83	0.29
	Red 1	11.7	±1.5	0.5		0.5	43.9	20.0
	Red 2			6.0	16.8	1.7		24.7
	Red 3			12.0	23.1	2.6	52.0	18.8
	Red 4			18.0	40.8	4.0	58.9	15.7
	Red 5			24.5				
	Red 6			31.3	30.9	5.6	47.3	11.1
	Chamber Flux				1.62	---	0.37	-1.05
	SE Chamber Flux				1.53	---	0.97	0.36
	Yellow 1	11.3	±2.0	0.5	2.8	0.6	43.4	34.6
	Yellow 2			6.0	29.2	2.2		38.5
	Yellow 3			12.0	40.9	2.3	39.8	40.3
	Yellow 4			18.0	27.5	3.5	46.5	34.4
	Yellow 5			24.5				
	Yellow 6			31.3	35.4	6.2		33.2
	Chamber Flux				2.07	---	0.30	-0.30
	SE Chamber Flux				1.56	---	0.98	0.36
	Avg Lander Flux				1.89	---	1.00	-0.08
	SE Avg Lander Flux				0.13	---	0.67	0.63

Cruise	Station/Chamber	Height (cm)	h SE (cm)	Time (hr)	Mn (nM)	Co (nM)	Fe (nM)	Cu (nM)
Teflon '94	CAT-4B							
	Red 1	9.3	±1.2	0.5	18.1	0.4	68.8	17.1
	Red 2			6.0	24.8	1.9	80.8	14.0
	Red 3			13.0	29.6	3.8	82.6	15.7
	Red 4			20.0		5.2	110.6	17.9
	Red 5			27.0		6.5	66.6	16.8
	Red 6			34.0		7.1	98.4	16.4
	Chamber Flux				2.03	---	1.23	0.07
	SE Chamber Flux				0.42	---	1.38	0.11
	Yellow 1	10.8	±2.4	0.5	16.8	0.9	40.3	
	Yellow 2			6.0	20.0	3.5	42.5	11.4
	Yellow 3			13.0	21.4	5.7	44.5	11.2
	Yellow 4			20.0		5.8	40.0	11.2
	Yellow 5			27.0		7.8	46.4	11.8
	Yellow 6			34.0		8.5	58.6	
	Chamber Flux				0.93	---	1.08	0.05
	SE Chamber Flux				0.35	---	0.51	0.05
	Avg Lander Flux				1.48	---	1.15	0.06
	SE Avg Lander Flux				0.55	---	0.07	0.01

Cruise	Station/Chamber	Height (cm)	h SE (cm)	Time (hr)	Mn (nM)	Co (nM)	Fe (nM)	Cu (nM)
Teflon '94	SCI-7							
	Blue 1	9.3	±1.2	0.5	22.9	0.2		24.2
	Blue 2			10.5	25.5		23.8	27.3
	Blue 3			20.5	28.1	0.3	19.9	24.4
	Blue 4			30.5	32.1	0.2	22.0	25.1
	Blue 5			40.5	42.1	0.2	28.0	24.4
	Blue 6			50.5				
	Chamber Flux				1.00	---	0.33	-0.04
	SE Chamber Flux				0.23	---	0.36	0.10
	Red 1	8.4	±1.0	0.5		0.3	30.7	19.4
	Red 2			10.5		0.4	29.4	24.3
	Red 3			20.5		0.7	31.2	22.2
	Red 4			30.5		0.8	33.0	26.5
	Red 5			40.5		0.7	33.5	22.8
	Red 6			50.5		0.9	34.0	25.0
	Chamber Flux					---	0.18	0.16
	SE Chamber Flux					---	0.05	0.11
	Yellow 1	10.2	±1.5	0.5				
	Yellow 2			10.5	18.7	0.6	30.8	24.8
	Yellow 3			20.5	14.6	0.6	25.5	15.4
	Yellow 4			30.5	15.3	0.8	32.4	
	Yellow 5			40.5	18.0	0.9	37.6	19.3
	Yellow 6			50.5	25.5	0.8	32.2	14.5
	Chamber Flux				0.41	---	0.37	-0.41
	SE Chamber Flux				0.31	---	0.33	0.34
	Avg Lander Flux				0.71	---	0.29	-0.10
	SE Avg Lander Flux				0.29	---	0.06	0.17

Cruise	Station/Chamber	Height (cm)	h SE (cm)	Time (hr)	Mn (nM)	Co (nM)	Fe (nM)	Cu (nM)
Teflon '94	SP-7							
	Blue 1	9.5	±2.0	0.5	12.5	2.1	28.8	0.0
	Blue 2			6.0	19.9	5.6	117.0	5.9
	Blue 3			13.0	33.4	7.9	140.4	8.6
	Blue 4			21.0	34.4	9.7		5.7
	Blue 5			30.0	57.8	9.7		8.4
	Blue 6			39.0				
	Chamber Flux				3.26	---	19.79	0.48
	SE Chamber Flux				0.84	---	9.19	0.29
	Red 1	9.4	±1.4	0.5	22.8	1.8	36.3	6.0
	Red 2			6.0		2.2	72.3	6.0
	Red 3			13.0	34.8	2.5	153.6	17.0
	Red 4			21.0	35.1	3.0	205.4	13.2
	Red 5			30.0	66.7	3.4		16.0
	Red 6			39.0				
	Chamber Flux				3.03	---	19.37	0.81
	SE Chamber Flux				1.16	---	3.33	0.38
	Yellow 1	9.6	±1.5	0.5	9.0	0.7	25.3	7.0
	Yellow 2			6.0	13.1	0.6	47.9	8.4
	Yellow 3			13.0	21.2	0.6	50.6	10.7
	Yellow 4			21.0	21.6	0.8	65.4	10.6
	Yellow 5			30.0	29.9	0.9		19.2
	Yellow 6			39.0				
	Chamber Flux				1.56	---	4.05	0.85
	SE Chamber Flux				0.32	---	1.20	0.26
	Avg Lander Flux				2.62	---	14.40	0.71
	SE Avg Lander Flux				0.53	---	5.18	0.12

Cruise	Station/Chamber	Height (cm)	h SE (cm)	Time (hr)	Mn (nM)	Co (nM)	Fe (nM)	Cu (nM)
Teflon '94	SM-7							
	Red 1	8.2	±1.0	0.5	5.3	0.7	111.5	9.0
	Red 2			8.5				
	Red 3			19.5	19.9	1.0	200.7	18.1
	Red 4			30.5	14.7	1.0	272.2	13.8
	Red 5			41.5	17.3	1.0	275.6	12.9
	Red 6			52.5	30.0	1.2	311.4	10.4
	Chamber Flux				0.75	---	7.57	0.01
	SE Chamber Flux				0.28	---	1.41	0.20
	Yellow 1	8.3	±1.0	0.5	12.4	1.1		17.9
	Yellow 2			8.5	29.9	1.5	284.9	19.3
	Yellow 3			19.5	23.0	1.7	351.8	30.1
	Yellow 4			30.5	26.8	2.0	429.6	36.1
	Yellow 5			41.5	36.5	2.4	492.5	39.5
	Yellow 6			52.5		2.3	694.4	52.0
	Chamber Flux				0.84	---	17.38	1.28
	SE Chamber Flux				0.41	---	3.43	0.19
	Avg Lander Flux				0.79	---	12.47	0.64
	SE Avg Lander Flux				0.05	---	4.91	0.64

Cruise	Station/Chamber	Height (cm)	h SE (cm)	Time (hr)	Mn (nM)	Co (nM)	Fe (nM)	Cu (nM)
Teflon '95	SM							
	Blue 1	8.3	±0.8	0.5	65.2	0.7	47.5	
	Blue 2			4.0		1.3	225.5	
	Blue 3			10.0	77.7	3.8	258.2	
	Blue 4			16.0	71.4	6.5	226.9	
	Blue 5			24.0	70.2	2.6		
	Blue 6			34.5	84.0	17.0		
	Chamber Flux				0.80	---	19.36	
	SE Chamber Flux				0.46	---	14.42	
	Red 1	8.9	±0.9	0.5	5.2	0.2	48.0	
	Red 2			4.0	78.1	0.6	127.3	
	Red 3			10.0	73.9	1.4	158.4	
	Red 4			16.0	98.7	5.4	221.2	
	Red 5			24.0	79.5	4.6		
	Red 6			34.5	74.1	5.8		
	Chamber Flux				2.67	---	21.81	
	SE Chamber Flux				2.35	---	4.62	
	Yellow 1	9.2	±1.3	0.5	54.4	1.6	114.7	
	Yellow 2			4.0	72.4	6.1	277.3	
	Yellow 3			10.0	79.2	7.8	260.6	
	Yellow 4			16.0	83.5	8.4	325.5	
	Yellow 5			24.0	82.4	11.2	365.8	
	Yellow 6			34.5	102.8	11.1	350.6	
	Chamber Flux				2.51	---	12.74	
	SE Chamber Flux				0.65	---	5.04	
	Avg Lander Flux				1.99	---	17.97	
	SE Avg Lander Flux				0.60	---	2.71	

Cruise	Station/Chamber	Height (cm)	h SE (cm)	Time (hr)	Mn (nM)	Co (nM)	Fe (nM)	Cu (nM)
Teflon '95	TB							
	Blue 1	8.4	±0.9	0.5	38.8	1.0	10.0	
	Blue 2			6.0	68.4	2.2	24.5	
	Blue 3			14.0	69.0	3.4	27.9	
	Blue 4			23.0	75.9	4.0	32.0	
	Blue 5			35.0	57.5	5.4	29.5	
	Blue 6			47.5	68.4	7.5	31.8	
	Chamber Flux				0.59	---	0.70	
	SE Chamber Flux				0.69	---	0.32	
	Red 1	8.6	±1.0	0.5	27.2	0.0	10.5	
	Red 2			6.0	40.4	1.3	7.8	
	Red 3			14.0	47.1	1.6	16.2	
	Red 4			23.0	59.6	2.2	21.1	
	Red 5			35.0	42.0	5.0	43.9	
	Red 6			47.5	64.4	5.4	24.5	
	Chamber Flux				1.19	---	1.11	
	SE Chamber Flux				0.53	---	0.52	
	Yellow 1	9.1	±1.0	0.5	38.2	0.2	15.9	
	Yellow 2			6.0	46.2	1.7	8.6	
	Yellow 3			14.0		3.6	25.2	
	Yellow 4			23.0				
	Yellow 5			35.0	104.9	6.6	25.8	
	Yellow 6			47.5	101.1	6.5	33.4	
	Chamber Flux				3.28	---	0.90	
	SE Chamber Flux				0.74	---	0.33	
	Avg Lander Flux				1.69	---	0.90	
	SE Avg Lander Flux				0.82	---	0.12	

Cruise	Station/Chamber	Height (cm)	h SE (cm)	Time (hr)	Mn (nM)	Co (nM)	Fe (nM)	Cu (nM)
Teflon '95	SCI							
	Blue 1	9.3	±0.9	1.0		1.6	8.0	
	Blue 2			8.0		10.0	10.0	
	Blue 3			16.0				
	Blue 4			29.0				
	Blue 5			44.0		8.0	10.1	
	Blue 6			59.0		8.4	8.8	
	Chamber Flux					---	0.02	
	SE Chamber Flux					---	0.06	
	Red 1	8.7	±0.8	1.0	32.6	0.9	8.6	
	Red 2			8.0	51.8	7.0	9.8	
	Red 3			16.0				
	Red 4			29.0				
	Red 5			44.0	90.8	12.6	11.1	
	Red 6			59.0	106.7	11.4	13.5	
	Chamber Flux				2.53	---	0.15	
	SE Chamber Flux				0.33	---	0.04	
	Yellow 1	9.0	±0.9	1.0	36.7	3.6		
	Yellow 2			8.0	64.3		5.5	
	Yellow 3			16.0				
	Yellow 4			29.0				
	Yellow 5			44.0	89.4	9.5	7.3	
	Yellow 6			59.0	78.3	4.8	7.3	
	Chamber Flux				1.46	---	0.08	
	SE Chamber Flux				0.71	---	0.02	
	Avg Lander Flux				1.99	---	0.08	
	SE Avg Lander Flux				0.54	---	0.04	

Cruise	Station/Chamber	Height (cm)	h SE (cm)	Time (hr)	Mn (nM)	Co (nM)	Fe (nM)	Cu (nM)
Teflon '95	PE							
	Blue 1	11.7	±0.9	1.0	25.6	0.5	19.9	
	Blue 2			13.0	37.9	2.7	19.1	
	Blue 3			31.0		3.6		
	Blue 4			46.0	26.5			
	Blue 5			62.0	32.1	2.6	32.2	
	Blue 6			81.0	35.3	2.7		
	Chamber Flux				0.12	---	0.62	
	SE Chamber Flux				0.25	---	0.16	
	Red 1	12.3	±1.5	1.0	28.3	0.6		
	Red 2			13.0	35.4	1.0		
	Red 3			31.0	31.3	1.1		
	Red 4			46.0	42.2	1.3	23.0	
	Red 5			62.0		2.9	20.1	
	Red 6			81.0		3.8	18.5	
	Chamber Flux				0.70	---	-0.37	
	SE Chamber Flux				0.40	---	0.09	
	Yellow 1	13.8	±1.3	1.0	22.4	1.7	18.4	
	Yellow 2			13.0	25.6	2.3	18.7	
	Yellow 3			31.0	21.4	3.6	17.2	
	Yellow 4			46.0	25.1	7.0	19.1	
	Yellow 5			62.0	21.1	6.9	16.8	
	Yellow 6			81.0	25.1	5.2		
	Chamber Flux				0.02	---	-0.06	
	SE Chamber Flux				0.11	---	0.07	
	Avg Lander Flux				0.28	---	0.06	
	SE Avg Lander Flux				0.21	---	0.29	

Cruise	Station/Chamber	Height (cm)	h SE (cm)	Time (hr)	Mn (nM)	Co (nM)	Fe (nM)	Cu (nM)
Monterey Bay	T1-11							
	Red 1	8.6	1	1	10.00	0.29	5.20	16.90
	Red 2			13	82.29	2.83	60.61	19.06
	Red 3			25	162.20	2.79	19.99	22.82
	Red 4			36	171.47	2.61	45.51	
	Red 5			48				
	Red 6			59				
	Chamber Flux				10.01	---	1.41	0.51
	SE Chamber Flux				2.20	---	2.19	0.10
	Yellow 1	8.6	1	1	19.00	0.52	58.00	26.50
	Yellow 2			13	95.34	1.83	69.25	27.99
	Yellow 3			25	160.15	3.34	70.82	34.63
	Yellow 4			36	149.37	4.12		70.56
	Yellow 5			48				
	Yellow 6			59				
	Chamber Flux				8.11	---	1.10	2.42
	SE Chamber Flux				2.61	---	0.50	1.08
	Avg Lander Flux				9.06	---	1.26	1.46
	SE Avg Lander Flux				0.95	---	0.16	0.95

Cruise	Station/Chamber	Height (cm)	h SE (cm)	Time (hr)	Mn (nM)	Co (nM)	Fe (nM)	Cu (nM)
Monterey Bay	T2-7							
	Blue 1	11.3	0.5	1	9.36	0.75	21.71	3.12
	Blue 2			6	21.23	1.53	27.08	3.61
	Blue 3			11	38.94	2.44	32.61	5.23
	Blue 4			15	51.28	2.57	44.39	6.23
	Blue 5			19	60.63	2.70	49.93	8.76
	Blue 6			23	70.03	3.19	130.58	10.69
	Chamber Flux				7.71	---	10.77	0.95
	SE Chamber Flux				0.44	---	3.99	0.13
	Red 1	10.4	0.6	1				
	Red 2			6				
	Red 3			11	36.38	1.41		14.29
	Red 4			15	43.45	3.07		16.96
	Red 5			19				
	Red 6			23	70.88	4.07		25.49
	Chamber Flux				7.37	---		2.38
	SE Chamber Flux				1.11	---		0.28
	Yellow 1	11	0.6	1	11.22	0.59	1.36	6.62
	Yellow 2			6	16.58	1.65	4.34	8.42
	Yellow 3			11	16.34	2.87	6.90	7.08
	Yellow 4			15	22.57	3.23	10.26	8.97
	Yellow 5			19	29.66	3.98	17.71	11.07
	Yellow 6			23	37.15	3.69	31.40	14.95
	Chamber Flux				2.97	---	3.28	0.86
	SE Chamber Flux				0.48	---	0.72	0.25
	Avg Lander Flux				6.02	---	3.84	1.40
	SE Avg Lander Flux				1.53	---	0.56	0.49

Cruise	Station/Chamber		Height (cm)	h SE (cm)	Time (hr)	Mn (nM)	Co (nM)	Fe (nM)	Cu (nM)
Monterey Bay	TS1-4								
		Blue 1	12.7	±1.0	0.5	28.9			
		Blue 2			2.0	51.7	24.5	32.2	
		Blue 3			4.0	67.8	41.4	36.2	
		Blue 4			6.5	80.9	57.7	41.9	
		Blue 5			10.0	114.4	60.9	50.3	
		Blue 6			13.0	134.9	71.7	79.1	
		Chamber Flux				24.84	---	11.97	
		SE Chamber Flux				2.38	---	2.80	
		Red 1	10.5	±1.0	0.5	9.3		37.7	
		Red 2			2.0	28.5		61.2	
		Red 3			4.0	43.6		51.3	
		Red 4			6.5	62.7		67.3	
		Red 5			10.0	107.0		72.0	
		Red 6			13.0	132.8		68.5	
		Chamber Flux				24.81		5.37	
		SE Chamber Flux				2.55		2.15	
		Avg Lander Flux				24.82	---	8.67	
		SE Avg Lander Flux				0.02	---	3.30	
Monterey Bay	TS1-7								
		Blue 1	11.6	±1.0	0.5	48.4	1.3		46.7
		Blue 2			2.0	57.4	2.0	14.7	79.4
		Blue 3			4.0	59.1	1.8	15.6	75.7
		Blue 4			6.5	63.4	1.9	18.1	78.6
		Blue 5			10.0	64.4	1.9	20.2	93.9
		Blue 6			13.0	66.9	2.1	30.6	76.5
		Chamber Flux				3.47	---	3.68	5.41
		SE Chamber Flux				0.89	---	0.94	3.60
		Avg Lander Flux				3.47	---	3.68	5.41
		SE Avg Lander Flux				0.89	---	0.94	3.60

Cruise	Station/Chamber	Height (cm)	h SE (cm)	Time (hr)	Mn (nM)	Co (nM)	Fe (nM)	Cu (nM)
Monterey Bay	TS2-4							
	Blue 1	12.7	±1.0	0.5	21.2	3.5	68.5	24.7
	Blue 2			4.0	43.8	32.0	66.3	31.0
	Blue 3			7.5	58.5	53.6	52.7	49.6
	Blue 4			11.0	72.7	58.5	69.2	23.8
	Blue 5			14.5	89.8	69.5	61.2	26.2
	Blue 6			18.0				
	Chamber Flux				14.5	---	-1.0	-0.4
	SE Chamber Flux				1.4	---	2.1	3.4
	Red 1	11.5	±1.0	0.5	22.8		31.5	33.5
	Red 2			4.0	56.7		47.9	34.5
	Red 3			7.5	74.1		49.2	27.5
	Red 4			11.0	82.2		80.9	48.0
	Red 5			14.5	102.8		87.8	29.3
	Red 6			18.0				
	Chamber Flux				14.6	---	11.5	0.4
	SE Chamber Flux				2.3	---	2.1	2.3
	Yellow 1	13.1	±1.0	0.5	28.1	1.3	94.7	36.4
	Yellow 2			4.0	40.2	5.5	80.9	32.5
	Yellow 3			7.5	48.9	10.7	87.3	32.4
	Yellow 4			11.0	63.3	14.7	81.5	44.0
	Yellow 5			14.5	71.7	19.4	81.7	47.3
	Yellow 6			18.0				
	Chamber Flux				9.92	---	-2.28	2.99
	SE Chamber Flux				0.87	---	1.43	1.43
	Avg Lander Flux				13.01	---	3.85	1.01
	SE Avg Lander Flux				1.54	---	3.82	1.02

Cruise	Station/Chamber	Height (cm)	h SE (cm)	Time (hr)	Mn (nM)	Co (nM)	Fe (nM)	Cu (nM)
Monterey Bay	TS2-7							
	Blue 1	10.6	±1.0	0.5	11.4	1.8	41.8	47.1
	Blue 2			4.0	16.4	5.2	51.4	39.4
	Blue 3			7.5	25.2	6.6	53.5	36.9
	Blue 4			11.0	29.7	9.6		
	Blue 5			14.5	33.7	10.7	77.3	38.5
	Blue 6			17.8	44.6	11.1	74.3	34.0
	Chamber Flux				4.64	---	5.24	-1.39
	SE Chamber Flux				0.56	---	0.96	0.59
	Red 1	11.0	±1.0	0.5	3.0	1.2		51.3
	Red 2			4.0	17.1	3.3		37.5
	Red 3			7.5	27.9	4.9	50.2	38.2
	Red 4			11.0	30.5	5.3	52.3	44.6
	Red 5			14.5	65.2		91.0	43.0
	Red 6			17.8	73.2	8.9	77.3	34.0
	Chamber Flux				10.80	---	9.25	-1.38
	SE Chamber Flux				1.71	---	5.19	1.06
	Yellow 1	10.7	±1.0	0.5	2.7	2.8	69.0	23.7
	Yellow 2			4.0	17.0	5.7	56.4	23.7
	Yellow 3			7.5	38.5	7.7	68.4	30.0
	Yellow 4			11.0	42.5	10.1	76.2	34.5
	Yellow 5			14.5	68.0	11.6	66.8	35.9
	Yellow 6			17.8	84.6	11.6	97.0	42.2
	Chamber Flux				11.94	---	3.76	2.82
	SE Chamber Flux				1.40	---	1.97	0.40
	Avg Lander Flux				9.13	---	6.09	1.30
	SE Avg Lander Flux				2.27	---	1.64	1.03

Cruise	Station/Chamber	Height (cm)	h SE (cm)	Time (hr)	Mn (nM)	Co (nM)	Fe (nM)	Cu (nM)
Monterey Bay	TS3-4							
	Blue 1	12.1	±2.0	0.5	49.8	6.7	39.6	1.46
	Blue 2			4.0	50.8	6.7	39.6	0.03
	Blue 3			7.5	54.6	7.0	42.3	0.75
	Blue 4			11.0	60.9	7.7	43.0	2.10
	Blue 5			14.5	70.1	9.3	46.7	0.44
	Blue 6			18.0	71.8	11.3		1.14
	Chamber Flux				4.13	---	1.46	0.02
	SE Chamber Flux				0.85	---	0.38	0.16
	Yellow 1	10.3	±2.0	0.5	24.1	1.6	12.8	
	Yellow 2			4.0	27.3	4.8	20.7	
	Yellow 3			7.5	31.8	6.3		
	Yellow 4			11.0	29.5	7.0	27.6	
	Yellow 5			14.5	35.9	8.0	27.3	
	Yellow 6			18.0	37.8	9.4	33.8	
	Chamber Flux				1.86	---	2.62	
	SE Chamber Flux				0.48	---	0.65	
	Avg Lander Flux				3.00	---	2.04	0.02
	SE Avg Lander Flux				1.14	---	0.58	0.16

Cruise	Station/Chamber	Height (cm)	h SE (cm)	Time (hr)	Mn (nM)	Co (nM)	Fe (nM)	Cu (nM)
Monterey Bay	TS4-4							
	Blue 1	12.3	±1.5	0.5	10.1	2.5	41.1	24.3
	Blue 2			2.5	36.7	8.6	53.0	22.7
	Blue 3			5.5	35.9	12.5	54.9	24.5
	Blue 4			8.5	38.9	18.1		
	Blue 5			11.5	43.0	24.7	58.0	22.3
	Blue 6			14.5	50.0	32.1	74.7	20.5
	Chamber Flux				6.30	---	5.48	-0.65
	SE Chamber Flux				2.16	---	1.59	0.29
	Red 1	11.5	±1.5	0.5	33.2	1.8	50.9	13.8
	Red 2			2.5	32.4	5.5	56.1	23.7
	Red 3			5.5				
	Red 4			8.5	43.3	16.4	64.6	25.0
	Red 5			11.5	45.3	19.0	70.0	27.6
	Red 6			14.5	49.9	21.6	104.4	25.0
	Chamber Flux				3.53	---	8.65	1.88
	SE Chamber Flux				0.59	---	2.90	0.98
	Yellow 1	14.0	±2.0	0.5	31.7	2.6	37.9	7.3
	Yellow 2			2.5	29.4	10.6	55.4	20.7
	Yellow 3			5.5	41.4	20.7	42.5	18.8
	Yellow 4			8.5	41.5	30.3	42.8	17.0
	Yellow 5			11.5	45.7	37.4	70.1	23.7
	Yellow 6			14.5	49.5	43.4	54.6	17.5
	Chamber Flux				4.65	---	4.21	1.81
	SE Chamber Flux				1.04	---	3.14	1.51
	Avg Lander Flux				4.83	---	6.11	1.01
	SE Avg Lander Flux				0.80	---	1.32	0.83

Cruise	Station/Chamber	Height (cm)	h SE (cm)	Time (hr)	Mn (nM)	Co (nM)	Fe (nM)	Cu (nM)
Monterey Bay	TS4-7							
	Blue 1	12.6	±1.5	0.5				
	Blue 2			3.0	13.3	1.9	26.0	20.4
	Blue 3			8.0	21.5	4.0	29.2	18.2
	Blue 4			12.5	35.5	6.6	34.2	18.3
	Blue 5			17.0	47.6	7.4	58.4	17.6
	Blue 6			22.5	54.1	9.6	112.1	19.9
	Chamber Flux				6.75	---	12.84	-0.09
	SE Chamber Flux				0.99	---	3.96	0.27
	Red 1	11.8	±1.5	0.5		2.2	12.2	12.4
	Red 2			3.0	2.5	4.1	14.6	12.2
	Red 3			8.0	23.0	11.5	18.9	14.9
	Red 4			12.5	25.8	12.6		15.4
	Red 5			17.0		21.9	28.0	12.2
	Red 6			22.5	29.4	19.6	61.6	14.8
	Chamber Flux				3.40	---	5.55	0.23
	SE Chamber Flux				1.71	---	1.66	0.23
	Yellow 1	13.9	±2.0	0.5	13.6	1.0	31.6	10.9
	Yellow 2			3.0	27.1	4.2	35.1	15.4
	Yellow 3			8.0	38.8	6.7	34.1	20.5
	Yellow 4			12.5	24.6	7.0	35.7	19.9
	Yellow 5			17.0	26.1	10.7	38.9	21.3
	Yellow 6			22.5	33.3	14.9	41.1	15.2
	Chamber Flux				1.59	---	1.29	0.73
	SE Chamber Flux				1.51	---	0.29	0.73
	Avg Lander Flux				4.04	---	6.56	0.29
	SE Avg Lander Flux				1.41	---	3.37	0.24

Cruise	Station/Chamber	Height (cm)	h SE (cm)	Time (hr)	Mn (nM)	Co (nM)	Fe (nM)	Cu (nM)
Monterey Bay	TS5-7							
	Blue 1	12.3	±1.2	0.5		1.8		
	Blue 2			2.5	37.1	10.0	13.0	
	Blue 3			4.5	56.8	14.1	16.5	
	Blue 4			6.5	82.2	17.4	19.8	
	Blue 5			11.5	106.4	20.2	28.5	
	Blue 6			16.5	104.7	20.2	28.7	
	Chamber Flux				14.22	---	3.50	
	SE Chamber Flux				4.14	---	0.75	
	Red 1	11.9	±1.0	0.5	60.2	1.2	8.7	
	Red 2			2.5	80.7	2.9	13.3	
	Red 3			4.5	80.1	10.2	14.9	
	Red 4			6.5	90.9	14.9		
	Red 5			11.5	114.1	20.6	18.7	
	Red 6			16.5	137.0	25.7	87.8	
	Chamber Flux				12.97	---	11.95	
	SE Chamber Flux				1.44	---	4.52	
	Yellow 1	12.2	±1.8	0.5	86.9		9.4	
	Yellow 2			2.5	169.1			
	Yellow 3			4.5	147.4		18.7	
	Yellow 4			6.5	191.5		25.4	
	Yellow 5			11.5	233.0		28.0	
	Yellow 6			16.5	232.1		112.2	
	Chamber Flux				23.88		16.91	
	SE Chamber Flux				7.37		6.23	
	Avg Lander Flux				17.02	---	10.79	
	SE Avg Lander Flux				3.45	---	3.91	

Appendix 2. Flux estimates for each station by year. Multiple chambers from landers are averaged together. Cruise and station abbreviations are as in Table 1 except hydrocast data from Pt Sur '90 (Appendix 1a) and the first two years of Monterey Bay data (Appendix 1c). Flux is expressed in units of µmol/m^2/day for Mn, Fe, and Cu and in nmol/m^2/day for Co. Dashes indicate stations where a flux measurement could not be arrived at either due to either sample contamination or suspect data.

Cruise	Flux From	Station	Mn	Mn SE	Co	Co SE	Fe	Fe SE	Cu	Cu SE
Pt Sur '90	Hydrocast	SM	0.84	0.12						
Teflon '94	Landers	SP	2.62	0.53	—	—	14.40	5.18	0.712	0.118
		SM	0.79	0.05	—	—	12.47	4.91	0.643	0.638
		CAT	1.73	0.21	—	—	1.06	0.37	-0.027	0.346
		TB	0.23	0.25	—	—	1.61	1.09	0.105	0.077
		SCI	0.71	0.29	—	—	0.29	0.06	-0.097	0.167
		PE	0.34	0.18	—	—	-0.18	0.12	0.236	0.099
	Centrifuged Core Pore Waters	SP	1.74	0.33	0.94	0.64	140.31	15.53		
		SM	1.59	0.29	0.42	0.15	262.31	71.68		
		CAT	8.09	2.64	11.39	1.99	36.79	5.41		
		TB	1.50	0.25	1.11	0.56	1.86	0.29		
		SCI	0.574	0.002	3.83	3.52	0.92	0.71		
		PE	0.08	0.02	0.18	0.45	0.02	0.00	0.133	0.040
	Hydrocasts	SP	0.41	0.16	-0.10	-2.98	4.30	1.12	-0.126	-0.078
		SM	3.91	0.89	2.97	1.50	5.65	1.07	1.357	0.354
		CAT	1.61	0.26	—	—	4.03	0.54	—	—
		TB	—	—	4.86	1.92	0.67	0.20	0.126	0.103
		SCI	1.09	0.91	—	—	—	—	—	—
Teflon '95	Landers	SM	1.99	0.60	—	—	17.97	2.71		
		TB	1.69	0.82	—	—	0.90	0.12		
		SCI	1.99	0.54	—	—	0.08	0.04		
		PE	0.28	0.21	—	—	0.06	0.29		
	Centrifuged Core Pore Waters	SM	4.13	2.40	4.67	5.97	289.48	110.53		
		TB	0.63	0.11	1.79	0.74	0.46	0.07		
		SCI	2.60	0.54	10.14	17.81	0.05	0.01		
		PE	0.019	0.010	0.748	0.017	0.02152	0.00007		
	Hydrocasts	SM	1.33	0.17	3.55	2.82				
		TB	0.55	0.18	2.27	1.57	0.82	0.20		
		SCI	0.98	0.48	20.46	9.99	0.80	0.56		
Monterey Bay	Landers	T1-11	9.06	0.95	—	—	1.26	0.16	1.46	0.95
		T2-7	6.02	1.53	—	—	3.84	0.56	1.40	0.49
		TS1	17.71	7.12	—	—	7.01	2.53	3.657	1.757
		TS2	11.07	1.50	—	—	4.97	1.93	1.150	0.649
		TS3	3.00	1.14	—	—	2.04	0.58	0.024	0.164
		TS4	4.44	0.75	—	—	6.34	1.62	0.650	0.419
		TS5	17.02	3.45	—	—	10.79	3.91		
	Centrifuged Core Pore Waters	TS1	0.22	0.17	15.06	6.97	-0.01	0.02		
		TS2	0.32	0.12	12.80	4.33			0.05	0.01
		TS3	0.46	0.13	18.85	6.44	0.152	0.075	0.10	0.04
		TS4	1.50	0.18	16.99	5.25	0.07	0.02		
		TS5			18.82	1.21	0.05	0.03		